

**İMMOBİLİZE METAL AFFİNİTE KROMATOĞRAFİSİ (İMAK)
İLE SİTOKROM C SAFLAŞTIRILMASI**

**CYTOCHROME C PURIFICATION WITH IMMOBILIZED
METAL AFFINITY (IMAC) CHROMATOGRAPHY**

Deniz TÜRKMEN

A THESIS OF MASTER OF SCIENCE

Prepared in the Chemistry Department
According to the Regulations of
The Institute for Graduate Studies in Pure
and Applied Sciences of Hacettepe University

ANKARA

2005

Graduate School of Natural and Applied Sciences,

This is to certify that we have read this thesis and that our opinion it is fully adequate in scope and quality, a thesis for degree of Master of Science in Chemistry.

Head :
(Supervisor) Prof. Dr. Adil DENİZLİ

Member :
Prof. Dr. Serap ŞENEL

Member :
Prof. Dr. Emir Baki DENKBAŞ

Member :
Assoc. Prof. Dr. Rıdvan SAY

Member :
Assoc. Prof. Dr. Hakan AYHAN

APPROVAL

This thesis has been certified as a thesis for the Degree of Master by the above Examining Committee on/..../2005

..../..../2005

Prof.Dr. Ahmet R. ÖZDURAL
Director of Graduate School of
Natural and Applied Sciences

İMMOBİLİZE METAL AFİNİTE KROMATOĞRAFİSİ (İMAK) İLE SİTOKROM C SAFLAŞTIRILMASI

DENİZ TÜRKMEN

ÖZ

İmmobilize metal iyon afinite kromatografisi (İMAK) terapötik proteinlerin, peptidlerin, nükleik asitlerin, hormonların ve enzimlerin saflaştırılması için yaygın olarak kullanılan bir analitik ayırma yöntemidir. Birçok geçiş metal iyonu elektronca zengin bileşiklerle kararlı kompleksler oluştururlar ve O, N ve S içeren moleküllerle iyon dipol etkileşimleriyle koordinasyon bağı kurarlar. Birinci sıra geçiş metal iyonları (Zn^{2+} , Ni^{2+} , Cu^{2+} ve Fe^{3+}) iminodiasetik asit, nitriloasetik asit ve tris(karboksimetil)etilen-diamin gibi bileşikler üzerinden kompleksleştirilerek İMAK sorbenti elde edilebilir. İMAK'de şelatlanmış metal iyonuna göre afiniteleri temeline göre ayırma sağlanır. Bu çalışmada, İMAK ile sitokrom c saflaştırılması için metal şelat oluşturucu ligand olarak poli(etilen imin) (PEI) içeren manyetik poli(hidroksietil metakrilat) (m-PHEMA) küreler hazırlanmıştır. Sitokrom c mitokondriyal solunum zincirinin heme içeren bir elektron taşıyıcısıdır. PEI'in primer imin grupları metal iyonları ile şelat oluşturucu özelliğe sahiptir. Ortalama 100-140 μm boy aralığındaki m-PHEMA mikroküreler magnetit partikülleri (Fe_3O_4) varlığında süspansiyon polimerizasyonu ile üretilmiştir. Manyetik kürelerin spesifik yüzey alanı ve ortalama gözenek çapı sırası ile 50 m^2/g ve 819 nm'dir. PHEMA yapısındaki ester grupları NaH varlığında PEI ile reaksiyona sokularak imin gruplarına dönüştürülmüştür. PEI yüklemesi 102 mg PEI/g polimer olarak bulunmuştur. Daha sonra, küreler üzerine Cu^{2+} iyonları şelatlanmıştır (0-793 $\mu mol Cu^{2+}/g$ polimer). Sulu çözeltilerden İMAK sorbente sitokrom c adsorpsiyonu farklı koşullarda incelenmiştir. m-PHEMA/PEI kürelere sitokrom c adsorpsiyonu 4.61 mg/g'dır. Cu^{2+} takılması adsorpsiyonu önemli derecede artırmıştır. 320 $\mu mol/g Cu^{2+}$ taşıyan polimerlerin maksimum sitokrom c adsorpsiyon kapasitesi pH 11.0 karbonat tamponunda 30.1 mg/g olarak belirlenmiştir. Sıcaklık ve iyonik şiddetin artmasıyla adsorpsiyon kapasitesi azalmıştır. Kesikli deneylerde belirlenen optimum koşullarda MSFB sisteminde adsorpsiyon deneyleri yürütülmüştür. Adsorpsiyon kapasitesi akış hızınının 0.5 ml/dk'dan 4 ml/dk'ya çıkarılması ile 26.87 mg/g'dan 5.36 mg/g değerine düşmüştür.

Adsorpsiyon kapasitesinde önemli bir azalma olmaksızın sitokrom c molekülleri on kez tersinir olarak adsorbe-desorbe edilebilmektedir. Elde edilen manyetik şelat oluşturuvcu küreler uzun süreli depolama kapasitesine sahiptir.

Anahtar kelimeler: İMAK, manyetik küreler, PHEMA, sitokrom c adsorpsiyonu, MSFB

Danışman: Prof. Dr. Adil DENİZLİ, Hacettepe Üniversitesi
Kimya Bölümü, Biyokimya Anabilim Dalı

CYTOCHROME C PURIFICATION WITH IMMOBILIZED METAL AFFINITY CHROMATOGRAPHY (IMAC)

DENİZ TÜRKMEN

ABSTRACT

Immobilized metal ion affinity chromatography (IMAC) has become a widespread analytical and preparative separation method for therapeutic proteins, peptides, nucleic acids, hormones, and enzymes. Many transition metals can form stable complexes with electron rich compounds and may coordinate molecules containing O, N, and S by ion dipole interactions. Metal ion ligands are first-row transition metal ions (Zn^{2+} , Ni^{2+} , Cu^{2+} , and Fe^{3+}) incorporated by iminodiacetic acid, nitrilotriacetic acid, and tris(carboxymethyl)ethylene-diamine. In this study, we propose preparation of magnetic poly(hydroxyethyl methacrylate) (m-PHEMA) beads containing poly(ethylene imine) PEI as a metal-chelating ligand for use in the IMAC for cytochrome c purification. Cytochrome c is a heme containing electron carrier of the mitochondrial respiratory chain. The primary imine groups of PEI have a chelating property with transition metal ions. Magnetic beads (m-PHEMA) with an average diameter of 100-140 μm were produced by suspension polymerization in the presence of magnetite particles (i.e. Fe_3O_4). Specific surface area and average pore size of the magnetic beads was found to be 50 m^2/g and 819 nm, respectively. Ester groups in the PHEMA structure were converted to imine groups by reacting with PEI in the presence of NaH. PEI loading was found to be 102 mg PEI/g polymer. Then, Cu^{2+} ions were chelated on these beads (0-793 $\mu mol Cu^{2+}/g$ polymer). Then, cytochrome c adsorption on the metal chelating beads from aqueous solutions containing different amounts of cytochrome c, at different buffers and pH levels were performed. The cytochrome c adsorption on the m-PHEMA/PEI beads was 4.61 mg/g. Cu^{2+} complexation increased the cytochrome c adsorption significantly. The maximum cytochrome c adsorption capacity of the Cu^{2+} -chelated beads (carrying 320 $\mu mol Cu^{2+}$ per g of polymer) was found to be 30.1 mg/g at pH 11.0 in carbonate buffer. Cytochrome c adsorption decreased with increasing temperature and ionic strength. Cytochrome c adsorption experiments were performed in a magnetically stabilized fluidized bed (MSFB) system at optimum conditions determined from the batch experiments.

The adsorption capacity decreased significantly from 26.78 mg/g to 5.36 mg/g polymer with the increase of the flow-rate from 0.5 ml/min to 4.0 ml/min. Cytochrome c molecules could be reversibly adsorbed and desorbed ten times with the magnetic adsorbents without noticeable loss in their cytochrome c adsorption capacity. The resulting magnetic chelator beads possess excellent long term storage stability.

Keywords: IMAC, magnetic beads, PHEMA, cytochrome c adsorption, MSFB

Advisor: Prof. Dr. Adil DENİZLİ, Hacettepe University
Department of Chemistry, Biochemistry Division.

ACKNOWLEDGMENT

I am very greatly obliged and indepted to Prof Dr. Adil Denizli, my supervisor, for his valuable guidance, professional advice, constrictive criticism and suggestion during my research.

Special thanks to Prof. Dr.Süleyman Patır, Assoc. Prof Dr. Abdulkerim Karabakan, and Prof. Dr. Mustafa Korkmaz (Physical Engineering Department) for their suggestions and help throughout my Master Science Study.

Special thanks to Dr. Handan Yavuz and Research Asistant Lokman Uzun for their friendship and help.

I wish to thank all my friends, Dr. Mehmet Odabaşı, Dr. Sinan Akgöl, Müge Andaç, Bora Garipcan, Serpil Özkara, Müfrettin Sarı, Evrim Banu Altıntaş, Fatma Yılmaz, Nilay Bereli, Melike Karataş, Gözde Baydemir, Sinem Mirel, Veyis Karakoç, Nilgün Başar, Esin Evrim Özyapı, İlker Koç, Seçil Utku, Başak Şaşmaz, Erkut Yılmaz for their help in laboratory, for their collaborating assisting and providing me a pleasant atmosphere to work in.

I am especially grateful to Murat Gelenoğlu and Melike Özkaya for their kindly help during my study.

Also I would like to thank all colleagues in Chemistry Department.

Finally;

I am very much indebted to my parent for their support and encouragement during my M Sc. studies.

Deniz Türkmen

INDEX

ÖZ	i
ABSTRACT	iii
ACKNOWLEDGMENT	v
INDEX	vi
FIGURE LEGENDS.....	ix
TABLE LEGENDS.....	xi
1. INTRODUCTION.....	1
2. GENERAL INFORMATION	3
2.1. Bioaffinity Chromatography.....	3
2.1.1. General Aspect of Bioaffinity Chromatography	3
2.2. Magnetically Stabilized Fluidized Bed Systems (MSFB).....	7
2.3. Immobilized Metal Affinity Chromatography.....	10
2.3.1. Immobilized Metal Ion Affinity Chromatography: Utilization of Differences In Protein–Metal Ion Affinity	12
2.3.1.1. Principles and Procedures	12
2.3.2. Commonly Used Metal Ions.....	12
2.3.3. Factors Contributing to Protein–Metal Binding.....	14
2.3.4. Metal Chelators and Chelating Polymeric Matrices.....	16
2.3.5. Chelate Structure and Metal Ions.....	19
2.3.6. Mobile Phase: pH, Buffers and Ionic Strength	19
2.3.7. Purification by Immobilized Metal Ion Affinity Chromatography	21
2.3.8. Purification of Proteins Fused with Poly-Histidine Tags and Other Engineered Metal-Binding Sites.....	24
2.3.9. Purification of Naturally Occurring Metal-Binding Proteins.....	25
2.3.10. Immobilized Metal Ion Affinity Chromatography: Up-Scaling and Industrial Use	26
2.3.11. Use of Immobilized Metal Ion Affinity Chromatography in Conjunction with Other Chromatographic Techniques.....	28
2.3.12. Metal affinity tags: advantages and applications.....	28
2.3.13. Metal affinity tagging: pitfalls and limitations	31
2.3.14. Immobilized metal ion affinity chromatography and protein refolding: matrix-assisted refolding	32
2.3.15. Poly(ethylenimine)	35

2.4. Cytochromes c	36
2.4.1. Structure	37
3. EXPERIMENTAL	39
3.1. Materials	39
3.2. Preparation of Magnetic Poly(HEMA) Beads	39
3.3. Characterization of m-PHEMA Beads	42
3.3.1. Swelling Test	42
3.3.2. Surface Area and Porosity Measurements	42
3.3.3. Screen Analysis	42
3.3.4. Surface Morphology	42
3.3.5. FTIR Studies	43
3.3.6. Analysis of Magnetism	43
3.4. Poly(ethylene imine) (PEI) immobilization	43
3.5. Incorporation of Cu ²⁺ ions	44
3.6. Cytochrome c Adsorption-Desorption Studies	44
3.6.1. Adsorption of Cytochrome c from Aqueous Solutions in Batch Mode ...	44
3.6.2. Adsorption of Cytochrome c From Aqueous Solutions in Magnetically Stabilized Fluidized Bed (MSFB)	45
3.7. Desorption and Repeated Use	47
4. RESULTS AND DISCUSSION	49
4.1. Characterization of Beads	49
4.1.1. PEI Immobilized onto m-PHEMA Beads	49
4.1.2. Swelling Properties	50
4.1.3. Surface Area Measurements	50
4.1.4. Surface Morphology	51
4.1.5. Cu ²⁺ Loading onto m-PHEMA/PEI Beads	53
4.1.6. Analysis of Magnetism	55
4.2. Adsorption of Cytochrome C from Aqueous Solutions	57
4.2.1. Effect of pH	57
4.2.2. Adsorption Time	59
4.2.3. Adsorption Isotherms	60
4.2.4. Adsorption Kinetics Modeling	64
4.2.5. Effect of Temperature	67
4.2.6. Effect of Ionic Strength	68

4.2.7. Effect of Cu ²⁺ Loading	69
4.2.8. Cytochrome C adsorption in continuous MSFB system	70
4.3. Comparison with Related Literature.....	71
4.4. Regeneration of the Beads	72
5. CONCLUSION	74
REFERENCES.....	77
CIRRUCULUM VITAE.....	87

FIGURE LEGENDS

Figure 2.1.	Schematic Representation Of The Main Steps In Affinity Chromatoraphy.	6
Figure 2.2.	Comparison of the stable and unstable states of the fluidized beds. (A): Unstabilized, (B): Magnetically stabilized.	9
Figure 2.3.	Schematic representation of magnetically stabilized fluidized bed system.	10
Figure 2.4.	Diagram of the mechanisms involved in protein adsorption and desorption in IMAC.	13
Figure 2.5.	Structures of two commonly used chelating resins charged with Ni(II) ions: Ni(II)–IDA and Ni(II)–NTA.....	16
Figure 2.6.	Structures of newly designed chelating groups for IMAC.....	18
Figure 2.7.	Schematic representation of matrix-assisted refolding on an IMAC support.	34
Figure 2.8.	Matrix-assisted refolding mechanism consisting of refolding and elution steps.....	34
Figure 2.9.	Structure of Polyethyleneimine	36
Figure 2.10.	The Crystal Structures Of Mitochondrial Cytochrome <i>c</i>	37
Figure 2.11.	Different Cytochrome <i>c</i> 's Amino Acid Chains	38
Figure 3.1.	Schematic representation of cleaning procedure for polymeric beads..	41
Figure 3.2.	Schematic representation of magnetically stabilized fluidized bed. system. A; Bobbin, B; Column with jacket, C; Water circulation system on fixed temperature, D; Peristaltic pump, E; AC Power supply, F; Sample, G; Reservoir, H; Magnetic stirrer.	47
Figure 4.1.	FTIR spectra of m-PHEMA and m-PHEMA/PEI beads.....	49
Figure 4.2.	Network formation of HEMA and EGDMA monomers.....	50
Figure 4.3.	SEM micrographs of m-PHEMA/PEI beads.	52
Figure 4.4.	Optical microscope photographs of m-PHEMA/PEI beads.	53
Figure 4.5.	m-PHEMA/PEI beads before and after incubation with Cu ²⁺ solution..	54
Figure 4.6.	Proposed structure of m-PHEMA/PEI-Cu ²⁺ complexes in aqueous solutions.....	54
Figure 4.7.	ESR spectrum of m-PHEMA beads.	56
Figure 4.8.	ESR spectrum of Cu(II) Loaded m-PHEMA/PEI beads.....	57

Figure 4.9. Effect of pH on cytochrome c adsorption. V: 10 ml; m _{polymer} : 30 mg; C _{cytochrome c} : 0.2 mg/ml; T: 25 ° C; Cu ²⁺ loading: 302 μmol/ g polymer...	58
Figure 4.10. Effect of buffer type on cytochrome c adsorption. V: 10 ml; m _{polymer} : 30 mg; C _{cytochrome c} : 0.2 mg/ml; T: 25 ° C; Cu ²⁺ loading: 302 μmol/ g polymer	59
Figure 4.11. Cytochrome C adsorption rates. . pH:11.0 Carbonate buffer; V: 20 ml; m _{polymer} : 60 mg; T: 25 ° C; Cu ²⁺ loading: 302 μmol/ g polymer.....	60
Figure 4.12. Effect of cytochrome c concentration. pH:11.0 Carbonate buffer; V: 20 ml; m _{polymer} : 60 mg; T: 25 ° C; Cu ²⁺ loading: 302 μmol/ g polymer	61
Figure 4.13. Langmuir adsorption isotherm of m-PHEMA/PEI/Cu ²⁺ beads.....	63
Figure 4.14. Freundlich adsorption isotherm of m-PHEMA/PEI/Cu ²⁺ beads.	63
Figure 4.15. First order kinetics of cytochrome c adsorption onto m-PHEMA/PEI/Cu ²⁺ beads.	66
Figure 4.16. Second order kinetics of cytochrome c adsorption onto m-PHEMA/PEI/Cu ²⁺ beads.	66
Figure 4.17. Effect of temperature on cytochrome c adsorption. pH:11.0 Carbonate buffer; V: 10 ml; m _{polymer} : 30 mg; C _{cytochrome c} : 0.2 mg/ml; Cu ²⁺ loading: 302 μmol/ g polymer	68
Figure 4.18. Effect of temperature on cytochrome c adsorption. pH:11.0 Carbonate buffer; V: 10 ml; m _{polymer} : 30 mg; C _{cytochrome c} : 0.2 mg/ml; T: 25 ° C; Cu ²⁺ loading: 302 μmol/ g polymer.....	69
Figure 4.19. Effect of Cu ²⁺ loading onto cytochrome c adsorption. pH:11.0 Carbonate buffer; V: 10 ml; m _{polymer} : 30 mg; C _{cytochrome c} : 0.2 mg/ml; T: 25 ° C.....	70
Figure 4.20. Effect of flow rate on cytochrome c adsorption. pH:11.0 Carbonate buffer; V: 40 ml; m _{polymer} : 30 mg; C _{cytochrome c} : 0.2 mg/ml; T: 25 ° C; Cu ²⁺ loading: 302 μmol/ g polymer.....	71
Figure 4.21. Reusability of m-PHEMA/PEI/Cu ²⁺ beads. pH:11.0 Carbonate buffer; V: 10 ml; m _{polymer} : 30 mg; m _{cytochrome c} : 0.2 mg/ml; T: 25 ° C; Cu ²⁺ loading: 302 μmol/ g polymer	73

TABLE LEGENDS

Table 2.1. Examples of Biological Interactions Used in Affinity Chromatography.....	4
Table 2.2. Subcategories of Affinity Chromatography	5
Table 2.3. Protein metal affinity prediction based on accessible histidine and tryptophan residues on the protein surface.....	15
Table 2.4. Individual contributions of amino acids involved in protein retention	15
Table 2.5. Commercially available chromatographic resins for IMAC.....	20
Table 2.6. Comparisons between IMAC and standard affinity chromatography.....	22
Table 3.1. Recipe and the polymerization conditions for the preparation of m-PHEMA beads.....	40
Table 4.1. Kinetic constants of Langmuir and Freundlich isotherms.....	64
Table 4.2. First and second order kinetic constants	67

1. INTRODUCTION

Immobilized metal ion affinity chromatography (IMAC) has become a widespread analytical and preparative separation method for therapeutic proteins, peptides, nucleic acids, hormones, and enzymes [1-8]. Many transition metals can form stable complexes with electron rich compounds and may coordinate molecules containing O, N, and S by ion dipole interactions. Metal ion ligands are first-row transition metal ions (Zn^{2+} , Ni^{2+} , Cu^{2+} , and Fe^{3+}) incorporated by iminodiacetic acid, nitrilotriacetic acid, and tris(carboxymethyl)ethylene-diamine.

IMAC introduces a new approach for selectively interacting materials on the basis of their affinities for chelated metal ions. The separation is based on the interaction of a Lewis acid (electron pair acceptor), i.e., a chelated metal ion, with an electron donor atom (N, O, and S) on the surface of the protein [9-16]. Proteins are assumed to interact mainly through the imidazole group of histidine and, to a lesser extent, the indoyl group of tryptophan and the thiol group of cysteine. Cooperation between neighboring amino acid side chains and local conformations play important roles in protein binding. Aromatic amino acids and the amino terminal of the peptides also have some contributions [17]. The low cost of metals and the reuse of adsorbents for hundred of times without any detectable loss of metal-chelating properties are the attractive features of metal affinity separation.

Polyethyleneimine (PEI) is one of the polycations reported to have a positive effect on enzyme activity and stability [18]. The polymer has been found to be rather versatile, with a number of interesting applications. PEI immobilized on a rigid inorganic matrix of high porosity is ideal for use in columns or in suspension (without magnetic stirrers). It binds polyanions, such as nucleic acids, very strongly. Suggested applications include chromatography of proteins, nucleotides and nucleic acids. It also effectively binds metal ions such as Ni^{2+} , Pd^{2+} , Pt^{2+} , Co^{2+} and Cu^{2+} .

There has been several separation approaches performed under magnetic field [19]. The most well known technique is the magnetically stabilized fluidized bed. Magnetically stabilized fluidized bed exhibits combination of the best characteristics of both packed and fluidized bed. These include the efficient fluid-

solid mass transfer properties, elimination of particle mixing, low pressure drop, high feed-stream solid tolerances, good fluid-solid contact, elimination of clogging and continuous countercurrent operation [20]. Especially, when dealing with highly viscous mediums contact with the magnetic adsorbent in a magnetically stabilized fluidized bed is desirable because of high convective transport rates. Recently, there has been increased interest in the use of magnetic adsorbents in biomolecule coupling and nucleic acid purification [21]. Magnetic adsorbents can be produced using inorganic materials or polymers. High mechanical resistance, insolubility and excellent shelf life make inorganic materials ideal as adsorbent. The main disadvantage of inorganic supports is their limited functional groups for ligand coupling. Magnetic adsorbents can be porous or non-porous [22]. They are more commonly manufactured from polymers since they have a variety of surface functional groups which can be tailored to use in different applications [23-29].

In this study, we propose preparation of magnetic poly(hydroxyethyl methacrylate) (m-PHEMA) beads containing poly(ethyleneimine) PEI as a metal-chelating ligand for use in the IMAC for cytochrome c purification. Cytochrome c is a heme containing electron carrier of the mitochondrial respiratory chain. The primary imine groups of PEI have a chelating property with transition metal ions. m-PHEMA beads were synthesized by suspension polymerization in the presence of magnetite particles (i.e. Fe_3O_4). Ester groups in the PHEMA structure were converted to imine groups by reacting with PEI in the presence of NaH. Then, Cu^{2+} ions were chelated on these beads. m-PHEMA/PEI beads were characterized by swelling tests, FTIR, ESR, SEM, mercury porosimeter, and optical microscope photographs. Then, cytochrome c adsorption on the metal chelating beads from aqueous solutions containing different amounts of cytochrome c, at different buffers and pH levels were performed. Effects of temperature and ionic strength of the medium were also investigated. Then, cytochrome c adsorption experiments were performed in a magnetically stabilized fluidized bed (MSFB) system at optimum conditions determined from the batch experiments. Desorption of cytochrome c and reusability of these magnetic metal-chelate affinity adsorbents were also tested.

2. GENERAL INFORMATION

2.1. Bioaffinity Chromatography

2.1.1. General Aspect of Bioaffinity Chromatography

Affinity sorption is already a well established method for identification, purification and separation of complex biomolecules. This may be achieved by a number of traditional techniques such as gel permeation chromatography, high performance liquid chromatography, chromatofocusing, electrophoresis, centrifugation, etc., in that the process relies on the differences in the physical properties (e.g., size, charge and hydrophobicity) of molecules to be treated. In contrast, affinity sorption techniques exploit the unique property of extremely specific biological recognition [30]. This is due to the complementarity of surface geometry and special arrangement of the ligand and the binding site of the biomolecule. All biological processes depend on specific interactions between molecules. These interactions might occur between a protein and low molecular weight substances (e.g., between substrates or regulatory compounds and enzymes; between biomformative molecules-hormones, transmitters, etc., and receptors, and so on), but biospecific interactions occur even more often between two or several biopolymers, particularly proteins. Affinity chromatography enables the separation of almost any biomolecule on the basis of its biological function or individual chemical structure. Examples can be found from all areas of structural and physiological biochemistry, such as in multimolecular assemblies, effector-receptor interactions, DNA-protein interactions, and antigen-antibody binding.

Affinity chromatography owes its name to the exploitation of these various biological affinities for adsorption to a solid phase [31-33]. One of the members of the pair in the interaction, the ligand, is immobilized on the solid phase, whereas the other, the counterligand (most often a protein), is adsorbed from the extract that is passing through the column. Examples of such affinity systems are listed in Table 2.1.

Affinity sorption requires that the compound to be isolated is capable of reversibly binding (i.e., sorption-elution) to a sorbent which consists of a complementary substance (i.e., the so-called ligand) immobilized on a suitable insoluble support, i.e., the so-called carrier.

Table 2.1. Examples of Biological Interactions Used in Affinity Chromatography.

Ligand	Counter ligand
Antibody	Antigen, virus, cell
Inhibitor	Enzyme (ligands are often substrate analogs or cofactor analogs)
Lectin	Polysaccharide, glycoprotein, cell surface receptor, membrane protein, cell
Nucleic acid	Nucleic acid binding protein (enzyme or histone)
Hormone, vitamin	Receptor, carrier protein
Sugar	Lectin, enzyme, or other sugar-binding protein

The term affinity chromatography has been given quite different connotations by different authors. Sometimes it is very broad, including all kinds of adsorption chromatographies based on nontraditional ligands, in the extreme all chromatographies except ion exchange. Often it is meant to include immobilized metal ion affinity chromatography (IMAC), covalent chromatography, hydrophobic interaction chromatography, and so on. In other cases it refers only to ligands based on biologically functional pairs, such as enzyme-inhibitor complexes. The term not only to include functional pairs but also the so-called biomimetic ligands, particularly dyes whose binding apparently often occurs to active sites of functional enzymes, although dye molecules themselves of course do not exist in the functional context of the cell. Thus chromatography based on the formation of specific complexes such as enzyme-substrate, enzyme-inhibitor, etc., i.e. on biological recognition, is termed bioaffinity or biospecific chromatography and the respective interaction-biospecific adsorption or bioaffinity [34]. The original term "affinity chromatography" acquired a broader meaning also including hydrophobic chromatography, covalent chromatography, metal-chelate chromatography, chromatography on synthetic ligands, etc., i.e. chromatography procedures based on different, less specific types of interaction. The broad scope of the various applications of affinity has generated the development of subspecialty techniques, many of which are now recognized by their own nomenclature. Table 2.2.

summarizes some of these techniques. As can be seen from Table 2.2. some of these subcategories have become accepted useful techniques [35].

Table 2.2. Subcategories of Affinity Chromatography

Affinity Chromatography	1. Hydrophobic Chromatography
	2. Immunoaffinity Chromatography
	3. Covalent AC
	4. Metal-Chelate AC
	5. Moleculaar Imprinting Affinity
	6. Membrane-Based AC
	7. Affinity Tails Chromatography
	8. Lectin Affinity
	9. Dye-Ligand AC
	10. Reseptor Affinity
	11. Weak AC
	12. Perfusion AC
	13. Thiophilic Chromatography
	14. High Performance AC
	15. Affinity Density Pertubation
	16. Library-Derived Affinity
	17. Affinity Partitioning
	18. Affinity Electrophoresis
	19. Affinity Capillary Electrophoresis
	20. Centrifuged AC
	21. Affinity Repulsion Chromatography

Schematic representantion of bioaffinity is shown in Figure 2.1. Affinity chromatography demonstrated in this figure is based on the simple principle that every biomolecule usually recognize another natural or artificial molecule. A wide variety of ligands may be covalently attached to an inert support matrix, and subsequently packed into a chromatographic column.

In such a system, only the protein molecules which selectively bind to the immobilized ligand will be retained on the column. Washing the column with a suitable buffer will flush out all unbound molecules. There are several techniques permit to desorb the product to be purified from the immobilized ligand.

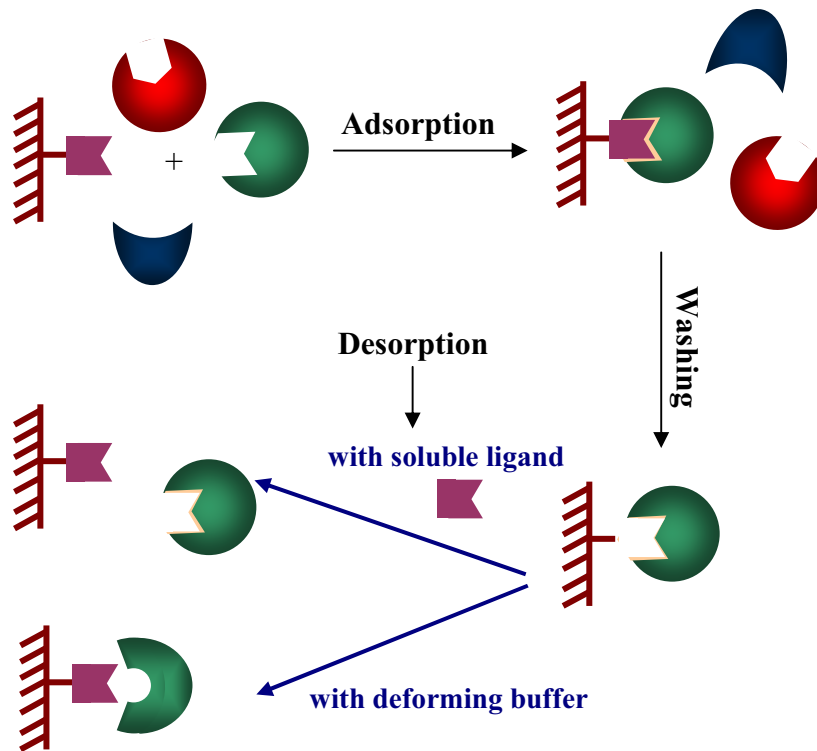


Figure 2.1. Schematic Representation Of The Main Steps In Affinity Chromatography.

Because affinity chromatography proper relies on the functional properties, active and inactive forms can often be separated. This is however, not unique to affinity methods. Covalent chromatography can do the same thing when the activity depends on a functional thiol group in the protein. By affinity elution, ion-exchange chromatography is also able to separate according to functional properties. These are, however, exceptions to what is a rule for the affinity methods.

Affinity chromatography has proved to be of great value also in the fractionation of nucleic acids, where complementary base sequences can be used as ligands, and in the separation of cells, where cell surface receptors are the basis of the affinity. Its main use has, however, been in the context of protein purification.

A field that has been so successful that it is often treated separately is affinity based on antigen-antibody interactions, called immunosorption. Sometimes this is the only available route to the purification of a protein and is especially attractive when there is a suitable monoclonal antibody at hand.

Very often the use of affinity chromatography requires that the investigator synthesizes the adsorbent. The methods for doing this, which are described later, are well worked out and are also easily adopted for those not skilled in synthetic organic chemistry. To further simplify the task, activated gel matrices ready for the reaction with a ligand are commercially available. The immobilization of a ligand can, in the best cases, be a very simple affair. In addition, immobilizations are just as easy for proteins as for small molecules.

A property that needs special consideration is the association strength between ligand and counterligand. If it is too weak there will be no adsorption, whereas if it is too strong it will be difficult to elute the protein adsorbed. It is always important to find conditions, such as pH, salt concentration, or inclusion of, for example, detergent or other substances, that promote the dissociation of the complex without destroying the active protein at the same time. It is often here that the major difficulties with affinity methods are encountered. Ligands can be extremely selective, but they may also be only group specific. The latter type includes glycoprotein-lectin interactions, several dye-enzyme interactions, and interactions with immobilized cofactors. However, these interactions have also proved to be extremely helpful in solving many separation problems. Good examples are ligands that are group selective against immunoglobulins (e.g., staphylococcal protein A or streptococcal protein G)[33].

2.2. Magnetically Stabilized Fluidized Bed Systems (MSFB)

The separation and purification of a product from a typical biochemical reactor can require extensive capital, space and operation costs; in some cases, these recovery steps may even be the substantial fraction of the product's cost [36]. Optimal separation processes should be versatile to reduce capital costs, able to handle large process volumes due to the dilute nature of the feed, and efficient to reduce operating costs. Additionally, the separation unit should be able to operated either batch-wise or continuously and, since a typical biochemical reactor output contains cells or cell debris, the unit should be able to handle suspended solids.

Conventional techniques for product recovery typically include a filtration or centrifugation step to remove any suspended solids followed by a batch separation operation and, if necessary, additional purification steps. The separation and purification techniques are performed predominantly in chromatography and adsorption (ion-exchange, affinity, etc.) packed columns, although for some products liquid-liquid extraction is also feasible. Although extremely versatile, packed column separations are limited to a batch-wise operation and are not generally capable of handling cells or cell debris.

Attempts have been made to circumvent these limitations. Several separation systems operate in either a semicontinuous or continuous mode and have been developed to process aqueous feed streams [37-40]. Although these systems eliminate the problems of batch-wise operation, the presence of solids mixing in some of the devices results in uneven residence times and solids attrition. In devices where true packed columns are used [41] complex piping/valve systems or rotary motion is necessary. These packed-column devices can perform continuous separations but are still unable to handle solids-laden fermentation broths.

The magnetically stabilized fluidized bed (MSFB) is a continuous column separation device able to handle suspended solids. The MSFB is a fluidized bed of magnetically susceptible particles that are stabilized by a uniform magnetic field. The stabilization of the particles results in a bed that has the dispersion and mass transfer properties of a packed-bed while retaining the solids-phase fluidity of a fluidized bed. Figure 2.2. shows the stable and unstable states of the fluidized beds [42-49].

Other properties of the bed include little or no power consumption (if permanent magnets are used), a low and constant operating pressure drop regardless of particle size or liquid flow rate, and the ability to handle suspended solids.

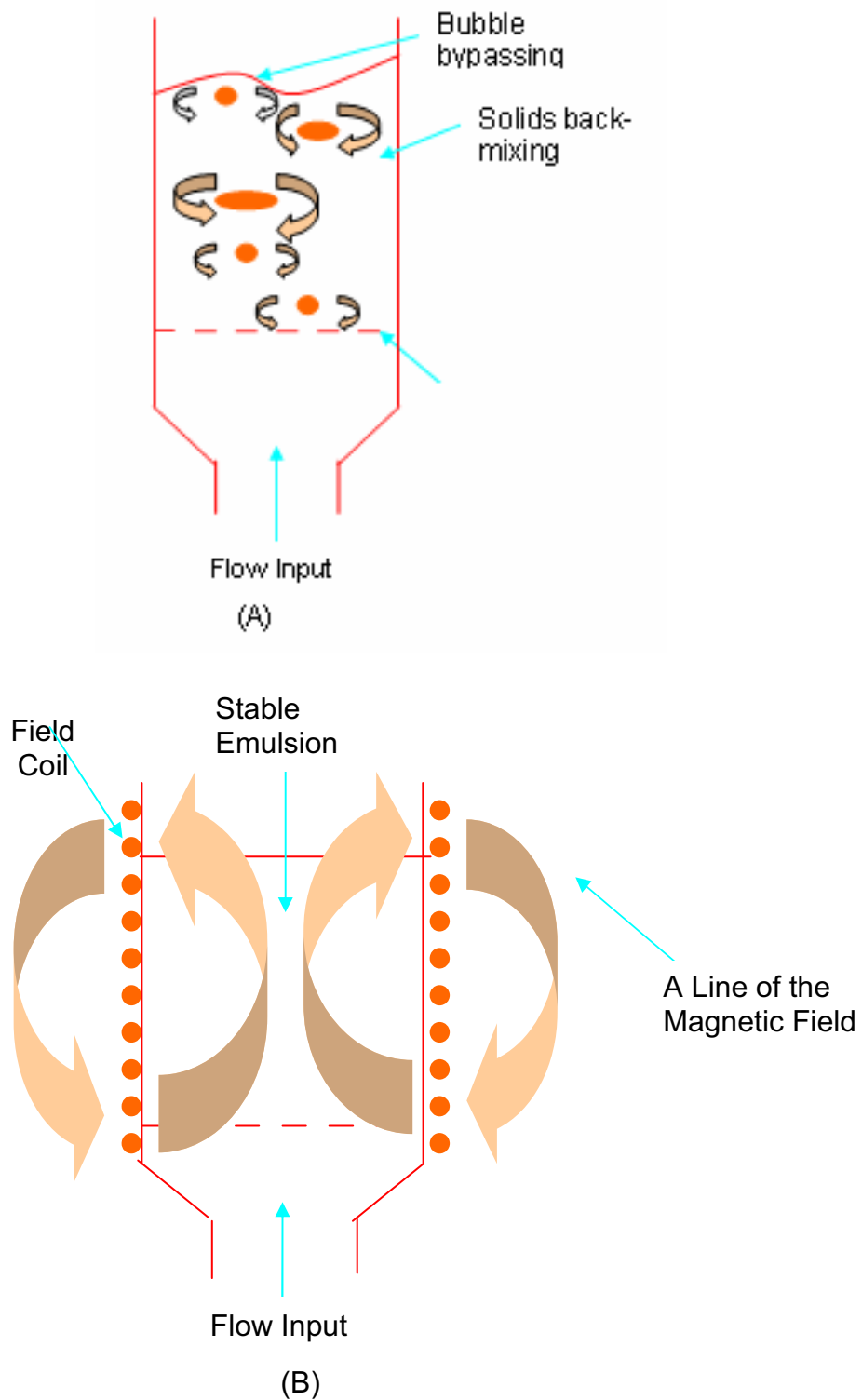


Figure 2.2. Comparison of the stable and unstable states of the fluidized beds. (A): Unstabilized, (B): Magnetically stabilized.

These properties of the bed allow continuous separation to be performed by moving both fluid phases (the liquid and the solids) countercurrent to each other.

The motion of the phases is plug flow which allows many theoretical stages to be obtained in a single column. Most applications of the MSFB have involved gas fluidized beds, but more recent applications of stabilized beds can be found in biotechnology and include continuous protein recovery from aqueous streams continuous cell filtration from fermentation broth. And other applications.

Although the liquid MSFBs used in the previously mentioned biochemical applications have many advantages over conventional techniques, they require that the support material be both magnetically susceptible and biologically active. For example, for affinity adsorption of proteins from an aqueous solution a support was specifically designed to be both capable of binding affinity ligands and magnetically susceptible. The lack of such commercially available magnetic supports necessitates the development of special supports for each application, thereby limiting the versatility of the MSFB. Figure 2.3. show the typical apparatus of a magnetically stabilized fluidized bed system.

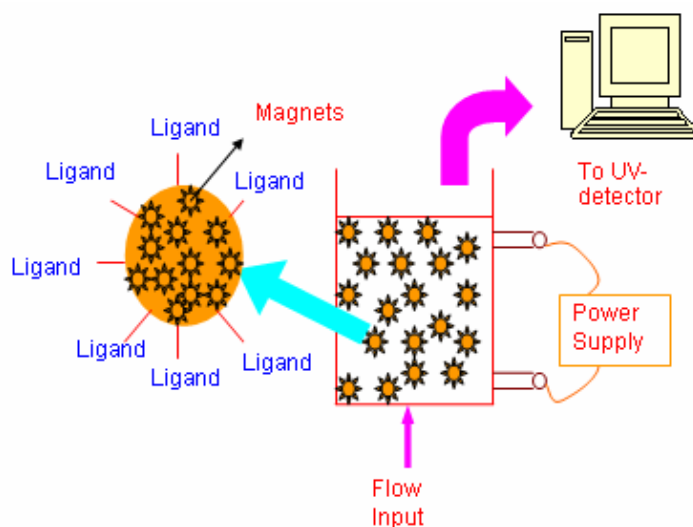


Figure 2.3. Schematic representation of magnetically stabilized fluidized bed system.

2.3. Immobilized Metal Affinity Chromatography

In the mid 1970s, Porath et al. [50] introduced a new type of chromatography which was first designated "metal chelate chromatography", but was later termed "immobilized metal (ion) affinity chromatography" (IMAC). While the basis of this

method was not new [51], Porath et al. [50] focused on its use for the separation and isolation of proteins. The technique is based on differences in the affinity of proteins for metal ions bound to a metal-chelating substance which is immobilized on a chromatographic support (resin) [52]. This "bio-affinity" feature soon caught attention of biochemists and biologists who employed IMAC and enhanced it to suit their particular applications. The best known improvement is the application of histidine tags for separation of recombinant polypeptides [53-63], which consists of the insertion of a short tail of histidine residues on either the N- or C-terminus of a protein or peptide [64]. The use of such histidine and other metal affinity tags in IMAC [68-73] proved to be a powerful tool for protein recovery, especially when high production and maximum yield of the proteins of interest were essential [74]. Consequently, IMAC emerged as one of the major preparative methodologies used for protein purification, ranging from bench [53-63] to pilot/industrial scale [65-81].

Many reviews on IMAC have been published so far [82-90] some of them dealt with new IMAC applications and even introduced new possible territories where IMAC could be exploited. In light of the new IMAC applications this review tried to go deeper into this new dimension of IMAC based techniques and their implications in life sciences. Whereas many of the recently devised metal affinity-based methodologies in protein chemistry are based on IMAC, a number of them are not. The latter range from protein purity analysis [91] and protein refolding through matrix-assisted refolding [92] to more complex procedures such as the Biacore analysis of His-tagged proteins using a chelating sensor chip [93] and use of a metal-chelating microscopy tip for single molecule force measurement by atomic force microscopy [94]. This wide range of applications can also be observed within the IMAC realm, where this type of chromatography can be employed not just for protein or peptide purification, but also for separation of His₆-tagged oligonucleotides [95], inactivation of viruses [96] and endotoxin removal from protein preparations [97]. It would be safe to state that although IMAC comprises a vast area of the metal affinity applications field, it is not the only methodology based on metal-protein interactions. Many other methods make use of the same principle and hence play an important role in this developing area of protein biochemistry.

2.3.1. Immobilized Metal Ion Affinity Chromatography: Utilization of Differences in Protein–Metal Ion Affinity

2.3.1.1. Principles and Procedures

Binding of proteins (or peptides) to metal ions is based on interaction between an electron-donating group present on a protein surface and a metal ion presenting one or more accessible coordination sites. In IMAC, use is made of a sorbent, or matrix, to which metal-chelating groups are covalently attached (Figure 2.4.). When metal ions are added (loaded), the multidentate chelators and metal ions form complexes in which the metal ions are secured for subsequent interaction with the compounds to be resolved. To this end, the metal ions in the complexes must have free coordination sites in order that solvent or solute molecules can bind to them. Following interaction of proteins and metal ions, the bound proteins can be released using a displacer (e.g. imidazole). The strength of the metal–protein bond varies from protein to protein, and in many cases this differential can be exploited to yield effective separation and isolation of specific proteins [52].

2.3.2. Commonly Used Metal Ions

Differences in affinity of proteins for a metal can be explained, at least in part, by the principles of hard and soft acids and bases (HSAB) as described by Pearson [98]. This theory states that when two atoms form a bond, one atom acts as a Lewis acid and the other as a Lewis base. The strength of the bond is governed by the intrinsic "hardness" or "softness" ratings of the atoms involved. The HSAB dictates that bonds between atoms with a similar rating, e.g. a hard acid combined with a hard base, are the strongest. Following the HSAB concept, metal ions such as K^+ , Ca^{2+} , Mg^{2+} and Fe^{3+} are classified as hard Lewis acids, whereas monovalent metal ions such as Ag^+ and Cu^+ are categorized as soft Lewis acids. The transition metal ions, Co^{2+} , Zn^{2+} , Cu^{2+} and Ni^{2+} , are considered "borderline acids.

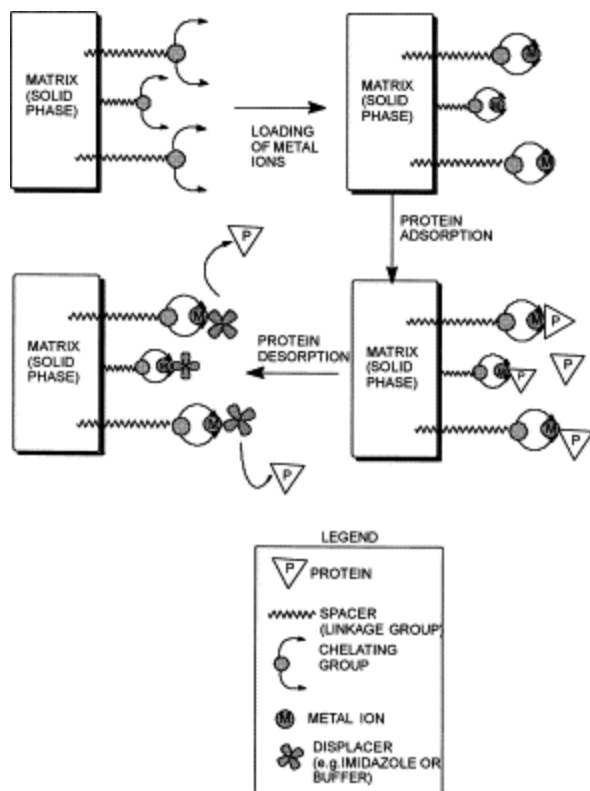


Figure 2.4. Diagram of the mechanisms involved in protein adsorption and desorption in IMAC.

These metal ions are most often employed in IMAC, in particular Ni(II), which provides a coordination number of six, electrochemical stability under chromatographic conditions, borderline polarizability and redox stability. The chelated metal ions show variations in affinity toward proteins, which can be predicted using HSAB. The latter postulates that there are three major types of ligands. Those containing oxygen (e.g. carboxylate), aliphatic nitrogen (e.g. asparagine and glutamine) and phosphor (e.g. phosphorylated amino acids) are classified as hard Lewis bases. Ligands containing sulfur (e.g. cysteine) are classified as soft bases, those containing aromatic nitrogen (e.g. histidine and tryptophan) are considered borderline bases. The borderline acids, containing Co^{2+} , Zn^{2+} , Cu^{2+} and Ni^{2+} , coordinate favorably with aromatic nitrogen atoms (borderline bases) and also with sulfur atoms (soft bases) [83]. The retention strength of the borderline metal cations, as chelated by iminodiacetate (IDA), follows the order $\text{Cu(II)} > \text{Ni(II)} > \text{Zn(II)} \sim \text{Co(II)}$. It may be noted that use of chelated metal ions displaying the highest protein retention does not necessarily translate

into the best protein separation, since very high retention could also lead to increased adsorption of impurities [82].

2.3.3. Factors Contributing To Protein–Metal Binding

As indicated by several studies, histidine is the amino acid with the strongest affinity for metal ions [52, 82, 87,99-106]. It is widely accepted that histidine, and also tryptophan and cysteine residues, as a result of strong interactions with metal ions, are key players in the binding of proteins in IMAC [50]. These three amino acids have much stronger retentions, for example, than glutamate and aspartate residues, which show essentially no retention [105 and 106]. Yip et al. [99] have correlated the retentions of a large number of synthetic, biologically active peptides on Ni(II), Zn(II) and Cu(II) chelated in IDA, with their amino acid profiles in order to evaluate the adsorption properties of amino acids involved in the retention of the peptides. Other investigations revealed that the retention behavior of proteins is largely governed by exposed histidine residues on the protein surface [101 and 107].

Cysteine also displays strong metal affinity, although to a somewhat lesser extent than histidine [82,78 and 108]. The metal affinity of these two amino acids can be largely attributed to their functional groups, in particular the imidazole and thiol groups, of histidine and cysteine, respectively. In the case of histidine, other functional groups, such as carboxyl and α -amino groups, also play a role in the metal-binding process [109 and 110]. Other amino acids may also have substantial metal affinity, including tryptophan, phenylalanine and tyrosine acting directly via their aromatic side chains [82] and arginine, lysine, asparagine, glutamine and methionine, acting indirectly via individual or combined effects on histidine accessibility [82 and 111]. Although the retention of proteins or peptides is primarily due to the metal affinities of their individual amino acids, other factors also contribute profoundly toward their metal affinity, including their amino acid sequences, folding, and surface properties. In view of the latter, the retention behavior of proteins in IMAC is not easily predictable [82].

In interactions between immobilized Cu(II), Ni(II), Co(II) or Zn(II) ions and amino acid residues on protein surfaces, imidazolyl, thiol and indolyl functional groups

are the main targets for the metal ions. Carboxyl and phosphate functional groups are the main targets for hard metal ions such as Fe(III) and Mg(II). A well-accepted concept is that the spatial distribution of histidine residues over a protein surface and their accessibility would influence the retention behavior of the protein molecule [82]. Several high metal affinity peptides have been described in the literature [112 and 113] as well as non-contiguous metal-binding motifs such as those found in prolactin [114-119], and growth hormone [114,120-122]. It is notable that the possession of a metal-binding motif is not always a guarantee for successful IMAC, since there are a number of enzymes with metal affinity that bind to the chelating matrix via a site that is not the metal-binding catalytic site [52 and 82]. Some metal-binding sections of a protein, even when exposed, may contribute very little to the net retention strength of the protein in IMAC [82].

When the amino acid composition of a protein, or peptide, of interest is known, the rule presented in Table 2.3. can be used to predict what kind of metal ions will lead to its retention in IMAC [52]. The retention strengths of the main amino acids involved in protein adsorption in IMAC are shown in Table 2.4. [82].

Table 2.3. Protein metal affinity prediction based on accessible histidine and tryptophan residues on the protein surface

Occurrence of accessible histidine or tryptophan residues on protein surface	Metal ions providing retention
No His/Trp	–
1 His	Cu(II)
>1 His	Cu(II), Ni(II)
His clusters	Cu(II), Ni(II), Zn(II), Co(II)
Several Trp, no His	Cu(II)

Table 2.4. Individual contributions of amino acids involved in protein retention

Functional group	Retention strength
Histidine	++++
Cysteine ^a	++++
Aspartic acid, glutamic acid	–
Lysine, arginine	+
Tryptophan, tyrosine, phenylalanine	+
N-Terminus	++

2.3.4. Metal Chelators And Chelating Polymeric Matrices

The majority of the chelating groups used in IMAC are multidentate chelating compounds providing the strength of the complex formed by the protein, metal ion and chelating group. The composition of the eluent buffer employed varies greatly when one is seeking optimal conditions for a given protein separation, and in many cases, is the main factor of the specificity reached in some IMAC based purification protocols. These chelating substances are attached on the sorbent surface via spacers (linkage groups) which can vary in length and composition. The final structure formed after the metal ion is chelated by the chelating group must allow some free coordination sites in the metal ion for the adsorption or binding of proteins or solvent molecules. Differences in the number of free coordination sites may in part explain why some chelating substances (IDA, Iminodiacetic acid; NTA, Nitrilotriacetic acid, etc.) display different selectivities and adsorption activities towards a given target protein. In the three-dentate IDA, the metal will bind to the nitrogen atom and the two carboxylate oxygens, leaving three sites for protein or solvent molecules (using Ni^{2+}). Likewise the tetradentate NTA is supposed to bind the metal ion with an extra carboxylate oxygen; this could give it a superior metal chelating strength, but on the other hand a weaker protein retention power [52]. Another feature of the tetradentate chelator would be a minor risk of metal leaching [123]. Figure 2.5. shows a model of the most commonly used chelators, IDA and NTA bound to Ni (II) atoms.

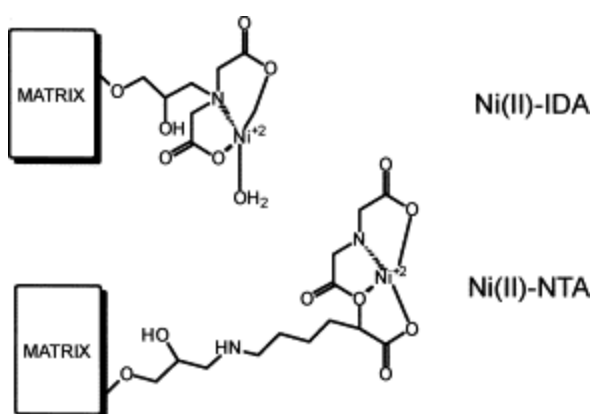


Figure 2.5. Structures of two commonly used chelating resins charged with Ni(II) ions: Ni(II)-IDA and Ni(II)-NTA.

IDA is the standard, most commonly used metal-chelating ligand for immobilization of metal ions in IMAC supports [87 and 124]. Many other chelators (adsorbents) employed in IMAC have been designed over the past decades, each having their own advantages and limitations. They are predominantly carboxymethylated amines such as tetraethylene pentamine (TEPA) or carboxymethylated aspartic acid (CM-ASP) [87]. Another extensively used IMAC chelator would be NTA, quite recently developed by Hochuli et al. [125]. The development of new, potential chelating agents for metal affinity is not limited to a particular functional group, and new classes of compounds will likely be employed as metal-anchoring molecules for IMAC in the near future. Several compounds, not chemically related to carboxymethylated amines, are used quite commonly: e.g. dye-resistant yellow 2KT [126], O-phosphoserine (OPS) and 8-hydroxyquinoline (8-HQ) [127]. Selecting the proper combination of chelator and metal ion is important, since the chelating resin can adversely affect protein retention. Lehr et al. [128] observed that apart from the metal employed, the chelating resin can have an important effect on protein retention, and suggested that, by using a different resin, protein retention can be altered as a result of interactions between the protein–metal complex and the chelating resin used. They succeeded in purifying histidine-tagged proteins from copper-containing medium in a single step using a chelating Sepharose matrix. This was probably due to favorable interaction between protein–copper complexes and the resin. In contrast, Ni–NTA resin displayed poor protein retention strength, likely a result of interference by the copper ions from the medium. There are a number of reports in the literature describing how the chelating matrix can influence protein purification [127,129-132]. One particular interesting case of "metal ion transfer" underscores the need for a cautious selection of the resin for IMAC: some proteins or solutes used in an IMAC run are able to disrupt the chelator–metal ion complex and can strip off the metal ion from the matrix; as a consequence they are not adsorbed by the column [133]. Figure 2.6. displays the chemical structures of some more recently developed IMAC chelator groups.

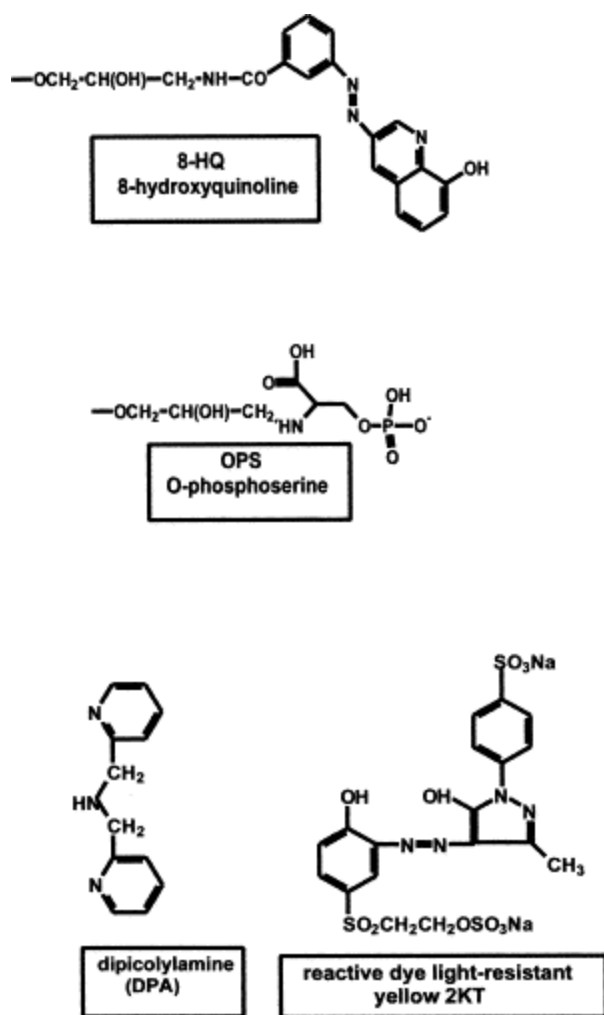


Figure 2.6. Structures of newly designed chelating groups for IMAC.

The first IMAC supports were manufactured by immobilization of chelating agents on the surface of a relatively inert, appropriately activated polymeric surface (e.g. agarose). Usually IDA was covalently coupled to the selected resin [134]. Many other IMAC supports have been developed in the last decades, each with their individual advantages and limitations [52]. A number of commercially available IMAC resins are presented in Table 2.5.

The polymeric support has to meet some physico-chemical characteristics in order to be suitable for IMAC, the ideal support would:

- (i) Be easy to derivatize;
- (ii) Not exhibit non-specific adsorption;
- (iii) Display good physical, mechanical and chemical stability;

- (iv) Possess high porosity to provide easy ligand accessibility;
- (v) Allow use of high flow-rates;
- (vi) Be stable to eluents including, for instance, denaturing compounds;
- (vii) Permit regeneration of columns without degeneration of the matrix;
- (viii) Provide a stable gel bed with no shrinking or swelling during the chromatographic run.

2.3.5. Chelate Structure and Metal Ions

As already mentioned, the number of linkages between a metal ion and an immobilized metal chelator governs the total affinity of the chelator–metal ion complex for proteins or peptides [83]. The chelator should have a strong affinity for the metal ion (to prevent, for example, the metal ion transfer effect) [133], but should also allow some free coordination sites to enable binding of the protein to the metal ion [82]. It appears that the stability of the chelator–metal ion structure depends on the type of metal ion and the composition of the eluent buffer used [52]. A number of chelate characteristics can influence the selectivity of metal–protein binding: complex coordination geometry, charge, steric bulk and chirality [82].

2.3.6. Mobile Phase: pH, Buffers And Ionic Strength

The selectivity of IMAC for a protein also depends on the composition of the mobile phase. Increasing the ionic strength of buffers can lead to suppression of secondary, electrostatically undesirable interactions while augmenting protein binding to the chelate complexes, since decreasing the salt concentration can even result in a poorer protein adsorption [82 and 87]. Sodium chloride (at 0.1–1.0 *M*) is commonly included in IMAC buffers to suppress ionic interactions between sample and matrix, as well as between proteins [52]. The effect of electrolytes on protein retention is related to the affinity of the metal ion for its solvated water molecules. Weakening of the forces between the metal ions and water molecules by increasing the ionic strength of the buffers, favors the protein adsorption processes. The use of high pH values (7 or 8) and high ionic strength makes IMAC different from other ion-exchange chromatography. IMAC best resembles hydrophobic interaction chromatography (HIC) because of the use of high salt concentration buffers [87].

Table 2.5. Commercially available chromatographic resins for IMAC.

Manufacturer	Designation	Support description	Metal/chelating group
Chemicell, Germany	Berlin, ChromaCELL-metal	Cellulose	Ni ²⁺ , Co ²⁺ ,
Iontosorb, Czech Republic www.iontosorb.cz/iontos00.htm	Iontosorb OXI Iontosorb SALICYL Iontosorb DETA Iontosorb DTTA	Cellulose beads Cellulose beads Cellulose beads Cellulose beads	Cu ²⁺ or Zn ²⁺ phosphonic acid group 8-Hydroxyquinoline immobilized Salicylic acid Diethylenetriamine Diethylenetriamine- tetraacetic acid
Amersham Biosciences (former Pharmacia Biotech. Uppsala, Sweden)	Chelating Sepharose Fast Flow Chelating Superose HiTrap Chelating	Cross-linked agarose Cross-linked agarose Highly cross-linked agarose, prepacked columns	IDA IDA IDA
Pierce, Rockford, IL, USA	Immobilized iminodiacetic acid gel Immobilized iminodiacetic acid gel	Cross-linked agarose TSK HW-65F	IDA IDA
Sigma, St. Louis, MO, USA	Iminodiacetic acid-agarose Iminodiacetic acid-epoxy activated Sepharose 6B TSKgel Chelate-5PWb	Agarose Cross-linked agarose Polymer resin	IDA IDA IDA
Tosoh, Japan Qiagen, Chatsworth, USA	Ni-NTA agarose Ni-NTA superflow Ni-NTA magnetic agarose beads Ni-NTA spin column ProBond Resin	Cross-linked agarose Highly cross-linked agarose Cross-linked agarose beads containing magnetic parti- cles Silica particles Agarose	Ni ²⁺ -NTA Ni ²⁺ -NTA Ni ²⁺ -NTA Ni ²⁺ -NTA
Invitrogen, CA, USA Merck, Darmstadt, Ger- many	Fractogel EMD IMAC	Polymer support with poly- mers branching from the poly- mer backbone	IDA IDA
Chtotech Laboratories Applied Biosystems (former PerSeptive Biosys- tems) Affiland, Belgium	Talon resin Talon superflow resin Talon cell thru Talon spin columns Poros MC Iminodiacetic acid-agarose PDC PMIB	Cross-linked agarose Cross-linked agarose Cross-linked agarose Silica Hydrophilized polystyrene-divinyl- benzene particles Cross-linked agarose	Co ²⁺ -tetradentate chelator ² IDA IDA
Serva Electrophoresis, Ger- many www.serva.de	Serdolit/CheLite/CHE Serdolit/CheLite/P	Macroporous polystyrene- based resin Macroporous polystyrene- based resin	Pentadentate chelator ² Pentadentate chelator ² IDA Aminomethylphosphonic acid group

If desirable, one could easily elute the target protein by applying a continuous decreasing pH gradient rather than an increasing imidazole gradient. Some elution protocols involving the simultaneous use of both imidazole addition and pH decreasing gradient in order to achieve a better chromatographic resolution are also described [135 and 136]. Alternatively, the protein can be eluted by a chelating compound such as EDTA, but the elution will elute all proteins retained along with the metal ion used, thus diminishing the resolution and selectivity [52].

Adsorption of protein in IMAC is carried out at a given pH at which the electron donor groups on the protein surface are partially unprotonated. It is common practice to induce protein adsorption on the IMAC support under a weakly alkaline pH in the presence of high ionic strength buffers. Phosphate and acetate buffers are most commonly used in IMAC. The role of the pH is fairly complex in the elution and adsorption of proteins, because it influences a number of properties, including the nucleophilic behavior of the buffer components, the electron-donor acceptor properties of the solutes and metal stability. The pH range 6–8 favors retention of histidine and cysteine residues; at a more alkaline range, coordinations with amino functional groups are favored, thus decreasing selectivity [87].

2.3.7. Purification by Immobilized Metal Ion Affinity Chromatography

IMAC is primarily based on affinity adsorption and therefore possesses advantages as well as disadvantages associated with this type of separation technology. Notably, the main feature of affinity chromatography is the specificity of the interaction between the protein of interest and the ligand (e.g. chelated metal ion, antibody, dye etc.). However, when compared to other types of affinity chromatography, in particular immunoaffinity chromatography, IMAC exhibits some noteworthy advantages, as described in Table 2.6. and discussed below [82].

Table 2.6. Comparisons between IMAC and standard affinity chromatography.

Feature	Metal affinity	"Bio-specific/bio-affinity"
Ligand stability	High	Low
Protein loading	High	Low
Elution conditions	Mild	Often extreme
Ligand recovery after column regeneration	Complete	Generally incomplete
Selectivity	Low-medium	High
Cost	Low	High

Purification of proteins by IMAC is based on their affinity for metal ions. Many proteins, however, lack metal affinity, a disadvantage which in the case of recombinant proteins can be overcome by using an oligohistidine tag inserted at their N- or C-terminus [125], where it likely is freely exposed on the protein surface [107]. Using this technology, large amounts of recombinant protein can be recovered, most often in a single chromatographic step. Contamination by *E. coli* proteins is usually low since such proteins in general lack metal affinity, although some *E. coli* proteins which show metal affinity, e.g. superoxide dismutase, could interfere with the purification process [107].

Since there is no need for extreme pHs in the mobile phase, elution conditions are usually mild. High imidazole and salt concentrations, however, could create a problem, in particular if the isolated protein is required for structural analysis (e.g. crystallography).

The most outstanding features of the use of histidine tail tags are the highly selective binding between the tag and the chelated metal ion and the relatively low interference of other compounds during a purification run [107]. IMAC has some unique, attractive characteristics:

- (i) IMAC often allows single step purification [137];
- (ii) The protein loading capacity is relatively high when compared with other affinity chromatographic techniques (0.1–10 μM /ml gel) [82 and 137];
- (iii) The metal ions can be easily removed from the resin with a strong chelating agent such as EDTA or EGTA. Different metal ions can therefore be tested, using

the same chelating resin, to determine the best ligand for separation of a protein of interest;

(iv) IMAC up-scaling is fairly easy and reproducible, also for industrial applications [137];

(v) IMAC is useful for concentrating dilute protein solutions [137];

(vi) IMAC is compatible with a number of buffers containing high ionic force or chaotropic components [137];

(vii) IMAC in general does not adversely affect the structure of proteins. A few cases have been reported in which metalloenzymes their essential metal ion had stripped off. A case has also been reported where a protein was damaged by IMAC on a Cu(II)–IDA column, but the damage was triggered by reducing agents which caused oxidative proteolysis catalysed by Cu(II) [138];

(viii) Upon passage through a non-charged IMAC column, solutions become transiently sterile since all metal ions essential for bacterial growth are removed by chelation [137];

(ix) An IMAC resin can be regenerated several hundreds of times without loss of chromatographic characteristics [103]. IMAC gels are also extremely sturdy provided that pH values below 4 are not used [137].

Some potential IMAC disadvantages are:

(i) Metal ion transfer (MIT) phenomena leading to protein loss [123, 133, 137 and 139] and low protein yields are not the only concerns about this subject. Another problem would be if the target protein retains the capturing metal ion within its structure. In this case the trapped ion could hinder or even abolish the protein's bioactivity, but MIT could also be carried out to charge a given protein with a desired metal [133 and 139]. The metal ion sequestered by the protein could also be hazardous if the protein is intended for therapeutics since some metals commonly used in IMAC are considered carcinogens. Metal ions Co(II) or Ni(II), widely used in IMAC, are known carcinogenic agents, although they are considered weak mutagens when compared with arsenic or hexavalent chromium. Nickel has been linked to the anomalous expression of a very large number of genes related to cancer induction [140]. One could strip off the undesired metal from the protein using a metal-free chelating column packed with a strong

chelating adsorbent such as TED [tris(carboxymethyl)ethylenediamine] [89 and 141].

(ii) Metal ion leakage from the resin leading to metal ion contamination of the final product, a problem which would be especially important in the use of IMAC for the preparation of therapeutics [91]. Apart from the obvious threat of metal contamination of the final product, a major problem would be the shelf life of the therapeutic protein since metal ions are known to trigger not only oxidative reactions as catalysts [137, 138, 142 and 143] but also disrupt stabilization of lyophilized protein preparations [143], although metallic ions have also been used as additives along with sugars to enhance protein stability upon lyophilization [143-145]. Some authors, aware of the stabilizing effects of metal ions on proteins, have proposed their use to enhance protein stability [126]. In cases when the metal is a destabilizing factor, chelating agents can be added for stability improvement [146]. Protein samples tainted with metals should also raise some concern, since metal displacement can occur during an IMAC step [89 and 147], and metal toxicity is undesirable when it comes to therapeutic proteins, but purification protocols usually have multiple steps after IMAC and this subsequent polishing generally yields a metal free final preparation [91]. In case one would like to rest assured that all metal traces were banished, one could rely on the same post treatment recommended for MIT prone samples and carry out an IMAC with an uncharged TED column to capture the contaminating metal ions from the protein mixture [89 and 141]. Another elegant way to circumvent the metal leaching problem is to use either chelating or metal immobilizing supports with strong ion binding constants that prevent such metal loss [148].

(iii) Use of oxidative and catalytic conditions during a run, when the immobilized metal ions are prone to undergo redox reactions [137, 138 and 142].

2.3.8. Purification of Proteins Fused With Poly-Histidine Tags and Other Engineered Metal-Binding Sites

A reliable and easy way to obtain a highly purified recombinant protein is to synthesize the protein fused to a metal affinity site and then purify it using IMAC [149]. The use of a poly-histidine tag as a metal affinity site, applied at the C- or N-terminus of the protein to be purified, proved to be a highly effective approach, usually enabling purification of the protein by IMAC in a one-step procedure [128,

150-154]. Consequently, this methodology has been widely used for protein recovery and purification. Proteins such as human glutathione S-transferase P1-1 [155], murine interleukin 12 [128], cytochrome *b5* [69], green fluorescent protein [152], chicken lactate dehydrogenase [150], mitochondrial ADP/ATP carrier protein [93], HTLV-I surface envelope glycoprotein fragment [154], and many others, have been successfully purified making use of poly-histidine tagging. High affinity for metal ions can also be achieved using other metal-binding peptide tags or via engineering of metal affinity sites on protein structures [102, 156 and 157]. Such tags/sites were devised to suit specific demands not met by regular histidine tags. Pasquinelli et al. [158] identified several fusion tags that shifted the elution of the target protein to the low background region of the Zn(II)–IDA elution profile, thus facilitating purification under mild conditions. Gaberc-Porekar et al. [159] developed a new histidine tag which enabled the purification of a multimeric protein (TNF- α). Enzelberger et al. [88] indicated the need for newly designed metal affinity tags, offering more choices of selectivity; a new affinity tag (His–Asn–Arg–Tyr–Gly–Cys–Gly–Cys–Cys) was produced which exhibited a stronger metal-binding capacity and higher yields when compared to the regular hexa-histidine tag. Schmidt et al. [160] engineered a Zn(II)-binding site from the active center of human carbonic anhydrase II into a retinol-binding protein, giving it selectivity for Zn(II) when compared to Cu(II) and Ni(II), an advantage which cannot be obtained with regular oligo-histidine tags which exhibited a less rigid conformation when compared with the engineered zinc-binding site. The design of synthetic tags with an affinity for Cu(II) ions higher than that of hexa-histidine tags has also been described [161].

2.3.9. Purification of Naturally Occurring Metal-Binding Proteins

In general, histidine residues in proteins are relatively rare, amounting to about 2% of the amino acid content of globular proteins; in addition, only half of them are exposed on protein surfaces [102]. In view of this, only a low number of naturally occurring proteins would present some metal affinity and hence be potentially suitable for purification by this type of chromatography. Natural possession of metal affinity by a protein poses a great advantage for its purification, since there is no need for inclusion of an affinity tag or metal-binding scaffold engineering. As previously mentioned, these naturally occurring metal affinity domains have

selectivity for certain metals, a characteristic not shared by hexa-histidine tags which are able to bind to most divalent metal ions, thereby increasing the selectivity of the separation obtained via IMAC [162]. Many proteins showing metal affinity have been successfully purified by IMAC without prior modification, including growth hormone and prolactin [134, 135, 162-164], two pituitary protein hormones with zinc affinity domains. Prolactin also exhibits a relatively high affinity for Ni(II), and Ni(II)-based IMAC of prolactin proved to be superior to other chromatographic techniques previously utilized [165]. Anguenot et al. [166] have described the purification of tomato sucrose synthase isoforms by Fe(III)-IMAC; Boden et al. [167] reported a one-step IMAC purification for goat immunoglobulins. Other proteins such as human protein C [95], calcium-binding proteins [168], recombinant human interferon γ [91] and pore-forming protein (perforin) [169] have also been purified or fractionated by IMAC without prior modification. It may be noted that the ability of a protein to bind a metal ion in solution is not necessarily a guarantee that it can be purified by IMAC. Thus it was found for many metalloenzymes that the sites, which bind metals for catalytic function, were not available for use in IMAC, turning this potential binding site useless with regard to application of this type of separation technology [52].

2.3.10. Immobilized Metal Ion Affinity Chromatography: Up-Scaling and Industrial Use

Metal affinity chromatography has compelling properties encouraging its application in large scale protein processing. Among the major advantages of the use of IMAC for protein purification at an industrial scale is the ease with which its bench level protocols can be scaled up and the high reproducibility of this technology [137]. A potential drawback of IMAC, however, would be metal ion leakage from its resins leading to metal contamination of the final product [107 and 137]. This shortcoming could be circumvented by the use of an additional chelating gel column to capture the metal ion contaminants [107]. This extra step, besides the additional costs to the process, would bring other concerns such as environmental problems associated with the disposal of the metal residues [107]. An alternative to regular IMAC, which basically is packed-bed chromatography, is "expanded bed adsorption" (EBA) chromatography. This technique allows separation of soluble target proteins in whole mammalian cell culture broth from

the crude extract in a single step, by adsorption to chelator–metal ion complexes on resin particles packed in a column (e.g. metal affinity adsorption). By applying an upward flow of the broth the sorbent gel is expanded, creating a void space between the sorbent resin beads which allows cell debris, whole cells and other matter to flow through the EBA column as the protein is adsorbed [170 and 171]. Thus the adsorption of the protein of interest to the adsorbent gel in a "fluidized" bed eliminates the need for an extra step for particle removal. During elution of the protein, the liquid flow is reversed, leading to packing of the resin bed. Chromatography using fluidized beds can be scaled up and there are several reports describing applications of expanded bed adsorption chromatography in large-scale protein separation [172-176]. Use of EBA for purification of His-tagged proteins [177-179] and for non-modified protein [180] has been reported. Streamline expanded bed adsorption is a technique based on fluidized bed chromatography, in which the expanded bed has been stabilized; this renders features to the method of regular packed bed chromatography, in terms of adsorption and flow-rates, but still allows processing of unclarified extracts [174]. Another protein separation system, based on metal affinity of proteins and often used in industrial scale methodologies, is the "aqueous two-phase system," also known as "affinity partitioning of protein" [82]. This methodology is based on the partitioning of proteins of a given mixture between two aqueous phases, one of them a PEG-based metal chelate phase which selectively pulls metal-binding proteins into this phase. The affinity partitioning of proteins and peptides which makes use of metal-chelating polymers is termed "immobilized metal affinity partitioning" (IMAP) and has been described in several studies on protein isolation [126, 181-184]. Another non-chromatographic purification approach, described by O'Brien et al. [185], is based on the use of magnetic chelator particles charged with Cu(II) ions for the recovery of His-tagged proteins, e.g. T4 lysozyme. As indicated by the authors, the high recovery yield and the avoidance of a clarification step are major advantages of this method when compared to standard IMAC. As pointed out in a comprehensive review by Wong et al. [87], many parameters, including pH, buffer ionic force, flow-rate and protein structure are major players in large-scale IMAC. A better understanding of their roles could lead to improvements in the up-scaling of IMAC and in its industrial application. Other important chromatographic parameters, including adsorption rate constants, mass

transfer coefficients and equilibrium parameters also need attention [87]. To date, there are only a few reports on the use of IMAC for purification of proteins to be used in clinical therapy [186]. This is likely due to concern over potential metal ion leakage interfering with the very stringent purity requirements of therapeutics [159], although data are available showing that metal ion tainting of IMAC-purified products is not likely to occur [91].

2.3.11. Use of Immobilized Metal Ion Affinity Chromatography in Conjunction with Other Chromatographic Techniques

IMAC is frequently carried out with high ionic strength running buffers. As such, IMAC could supplement other chromatographic procedures where a high salt concentration is needed or does not interfere with the separation, such as HIC [83]. Another possible combination described in the literature is the development of a new class of chromatographic methods termed "adsorptive size exclusion," where size exclusion chromatography is combined with adsorption chromatography such as IMAC or HIC [174]. Use of sequential IMAC columns, charged with different metal ions, would make it possible to retain a variety of target proteins on the basis of their particular metal affinity characteristics [83]. Another methodology devised to improve resolution is the use of IMAC followed by affinity chromatography employing anti-His-tag monoclonal antibodies [187].

2.3.12. Metal affinity tags: advantages and applications

Applications of metal affinity tags as well as other tags, e.g. based on avidin affinity, such as the biotin acceptor peptide [188], have proven highly advantageous to protein purification:

(i) Identification of fusion proteins, incorporating a metal affinity peptide tag (e.g. hexa-histidine), has become possible with the use of antibodies directed against the tag in e.g. an immunodetection assay [79]. It allowed step-by-step monitoring of a fusion protein, by western blots or enzyme-linked immunosorbent assay (ELISA), during procedures aimed at optimizing the expression of the protein [189]. McMahan and Burgess [190] synthesized a bifunctional compound for the detection of nitrocellulose-bound his-tagged proteins. It has a biotin as one functional group and a Ni(II)-charged nitrilotriacetic acid as the other. Following binding of the latter to a histidine tag, the biotin group can be detected using a

streptavidin–horseradish peroxidase conjugate; its emitted chemiluminescence can be detected using X-ray film. Using this technique, as little as 0.11 pmol of polyhistidine-tagged *Escherichia coli* RNA polymerase σ^{70} subunit could be detected on nitrocellulose membranes [190]. Similarly, Ni–NTA–alkaline phosphatase conjugate (commercially available from Qiagen, Hilden, Germany) was used to analyze polyhistidyl peptides on bacterial surfaces [191]. Another labeling system used for visualization of his-tagged protein structures was developed by Buchel et al. [192] and is based on the use of Ni(II)–NTA gold clusters for imaging via electron microscopy.

(ii) Obviously, the major advantage of metal affinity or other affinity tags is that they speed up the purification process. The expressed fusion protein can be rapidly purified using a chelating resin, charged with the metal ion of choice, which captures and retains the engineered protein; the purification can usually be carried out in a single step operation [128, 150, 153, 154 and 189]. The specific interaction between the target protein and the support is highly critical when the protein of interest is present in crude extract at low levels due, for example, to poor expression. There are some examples where the use of affinity tags enables the purification of poorly expressed proteins without the need of upstream regulation, since protein expression control adjustments are more cumbersome than downstream processing set-ups. Another advantage is that the metal affinity tag can most of the times be used for a variety of proteins, eliminating the necessity of elaborating individual downstream processes [189].

(iii) Metal affinity tags can be used to immobilize proteins on a surface, as required for certain assays. This approach would permit rapid screening of bioactivity or affinity towards a given analyte [189]. Nieba et al. [93] demonstrated that His tags can be used not only to facilitate purification and detection of proteins but also to ease kinetic studies through biosensor analysis. It would also be useful for immobilization of enzymes, since it has been found that such bio-affinity based immobilization procedures often yield preparations exhibiting high catalytic activity and enhanced stability against denaturation. Bio-affinity immobilization is reversible (facilitating reuse of the support matrix), orients the enzymes favorably and permits immobilization of target enzymes from crude extracts or cell lysates [193]. The same orientation or immobilization methodology can be applied to the manufacturing of affinity columns [194] and to other processes where molecule

orientation or anchoring is required, such as in atomic force microscopy [94], surface plasmon resonance (Biacore detection technology) and the scintillation proximity format [93 and 194]. The importance of site-specific immobilization of proteins is accentuated by the problems encountered with random immobilization of enzymes: i.e. structural deformations, inability to control and predict structure–function relationships and impaired catalytic activity [195].

(iv) The use of metal affinity tags can in many instances circumvent problems resulting from incorrect protein expression. In *E. coli* expression systems, for example, truncated forms of the target protein can be produced due to errors such as internal initiation of translation or premature terminations of protein synthesis. Since these truncated forms share many common physico-chemical characteristics with the non-modified molecule, they can lead to contamination of the final product. Inserting a metal affinity tag at a terminus of the molecule of interest could enhance isolation of only the correctly expressed proteins. To which terminus the tag would have to be added would depend on the type of truncation encountered [189].

(v) Affinity tags can be helpful in other ways than facilitating protein screening. A number of authors have reported improvements in protein stability, and protein expression levels following insertion of a metal affinity tag [87 and 196]. Supattapone et al. [197] have reported increased resistance of histidine-tagged PrP proteins against protease activity, resulting from a protease-resistant conformation of the tagged proteins. The protein stabilization induced by insertion of histidine or other metal affinity tags could be a result of disruption of the natural protein turnover as controlled by the N-terminus of the protein, since the N-end rule states that insertion of an N-terminal histidine before a destabilizing amino acid would increase the in vivo half life of the protein [198]. However, it is possible that the protein stabilization is in fact related to the increased speed of the purification process rather than to a change induced by insertion of the metal tag [107]. Fusion proteins can have their affinity tags removed when required, usually via enzymatic cleavage by a site-specific protease [71, 151 and 199], although in many instances the histidine tail does not impair activity or folding of the protein [155, 200-203]. Metal-binding tags can be combined with other affinity tags in the same target molecule. This dual affinity approach can bring many advantages, including increased protein stability, higher purity due to increased selectivity and

the option of employing different methodologies for detection, quantification, immobilization and adsorption of the target fusion protein [199].

2.3.13. Metal affinity tagging: pitfalls and limitations

Although use of metal-binding tags has exceptional advantages, it is not free of problems and in many cases other approaches may have to be considered. It is worth emphasizing, however, that the limitations associated with the tag insertion approach have not blocked its increasing application, as can be validated by the growing number of manuscripts published on the subject [189]. As use of tag technology escalated over the past few years, some important limitations have been spotted. A major problem arises if the attached peptide tag disrupts protein bioactivity or function by altering the folding of the protein [189 and 199]. This apparently is the case when a polyhistidine tag is introduced in **L**-lactate dehydrogenase at the C-terminus. The resulting fusion protein has decreased bioactivity when compared both to the wild-type enzyme or the N-terminally tagged variant [204]. Interference with antigen-binding property was also detected in histidine tag-containing antibodies where again the C-terminal position of the histidine tag adversely affected the binding properties of the construct [205]. Problems associated with functionality have also been reported. Histidine tags were found to modify the interaction of a DNA-binding protein with DNA [206]. Another case concerning a DNA-binding protein [protein pi(30.5)], showed that insertion of histidine tails induced dimerization of the fused proteins [74]. Insertion of metal-binding tags can also lead to unstable or degraded proteins [207], or interfere with both the expression and assembly of a protein complex, e.g. the PsaK1 [208]. Ni(II)-induced oligomerization was observed in proteins containing 10-mer histidine tags [209]. Whereas a new metal affinity tag (heli_{wt}-tag) has a higher metal-binding strength than the frequently used his₆-tag, the much higher imidazole concentrations, required for eluting a heli_{wt}-tagged protein, can lead to protein denaturation [68]. Following a decision to adopt tag technology in the purification of proteins, careful evaluation of the fusion protein design is required for each individual protein. The more information on the structure and folding of the protein or peptide of interest can be obtained, the more successful the use of the tag will be; ideally, the tag would produce minimal changes in the activity or structure of the protein. In the tag selection process, details such as the type of metal affinity

tag, the terminus at which the tag will be inserted and the structure of the protein should be given utmost attention to ensure a successful application [189].

Other problems, associated with the use of metal affinity tags, may arise when the target protein is generated for studies of its properties that could be affected by the tag, including structural, physiological and pharmacological features. In such a case, removal of the tag following purification of the protein would be essential. In general, however, there is no need for removal of histidine tags [151 and 189]. Removal of the tag can be achieved by chemical cleavage or by enzymatic action. Chemical cleavage has several drawbacks such as harshness of the conditions used and the generation of toxic byproducts [151]. Enzymatic cleavage via endoproteases that recognize specific amino acid sequences within the protein, has distinct advantages over the chemical method, including greater specificity and less harsh conditions. However, enzymatic cleavage can be incorrect due to cleavage of internal, non-canonical cleavage sites and may not always be effective, as found for the his-tag removal from human prolactin by factor Xa, which was only partially successful. The latter was presumably a result of poor accessible cleavage sites displayed by the protein [151 and 200].

2.3.14. Immobilized metal ion affinity chromatography and protein refolding: matrix-assisted refolding

Production of recombinant proteins in bacteria in the form of cytoplasmic inclusion bodies is associated with serious problems with regard to the proper structure and function of the proteins resulting from protein misfolding. The latter is especially a problem when the proteins are composed of multiple subunits, have several disulfide bridges, or contain prosthetic groups. In the inclusion bodies, the protein is present in an insoluble form, with reduced disulfide bonds and no or impaired bioactivity. This worst scenario of misfolded proteins in particular occurs if the bacterial synthesis of the protein is not supported by chaperones assisting in the folding of the protein. However, even when use is made of protein folding aid devices in the production of the protein (co-expression of chaperones, optimization of growth conditions), a refolding step is usually needed for maximum recovery of the desired protein in the native form [210 and 211]. In many cases, however, the folding step is ineffective, resulting in poor recovery and high operation costs

[211]. Recently, a reliable technique, based on affinity tagging and designated "matrix-assisted refolding," has been developed for the production of soluble and functional proteins from inclusion bodies (Figure 2.7. and Figure 2.8.). Briefly, following production of the tagged protein in inclusion bodies, it is solubilized, denatured and then immobilized on a charged chelating resin [e.g. Ni(II)–NTA]. The subsequent renaturation step can be carried out by applying a linear gradient spanning denaturing to renaturing conditions or by iterative refolding, a technique based on repeated cycles of renaturation and denaturation with a decreasing concentration of the denaturing agent in each consecutive cycle. After the final renaturation, the target protein is eluted in its native and soluble form [92 and 126]. Successful renaturation of a β -glucosidase, Zm-p60.r, was accomplished through IMAC-based, matrix-assisted refolding: the only refolding protocol that so far has produced a correctly folded Zm-p60.r protein [92]. Matrix-assisted refolding on a Ni(II)–NTA column of a mammalian prion protein has yielded a stable and aggregate-free protein preparation [212]. Other refolding protocols, employing Ni(II)–NTA as the matrix support, have been used for the renaturation of human matrix metalloproteinase-7 [213], a DNA helicase [214], a recombinant fragment of the Willebrand factor [215] and human pulmonary surfactant protein B [216]. The IMAC-based, matrix-assisted protocol for protein refolding has distinct advantages over standard refolding techniques:

- (i) Matrix-assisted refolding of some proteins was successful in contrast to other techniques [86];
- (ii) Protein immobilization on the matrix prevents non-specific protein–protein interactions, thus precluding undesirable aggregate formation. This is particularly important when the denaturing agent is removed [86 and 217];
- (iii) The immobilized protein has a decreased probability of misfolding due to its limited spatial range of motion when docked to the polymeric support [215];
- (iv) Functional or quantitative assays can be carried out on the refolded immobilized proteins prior to the elution step [216];
- (v) Matrix-assisted refolding allows gradual renaturation of the desired protein [217]; it usually gives high recovery yields of soluble, functional protein [215];
- (vi) The technique is rather simple; special skills, equipment or reagents are not required;

(vii) The immobilization of the protein via metal affinity interactions is reversible. As such, it allows use of unbound protein molecules in an assay in the event that the matrix support would interfere with the assay.

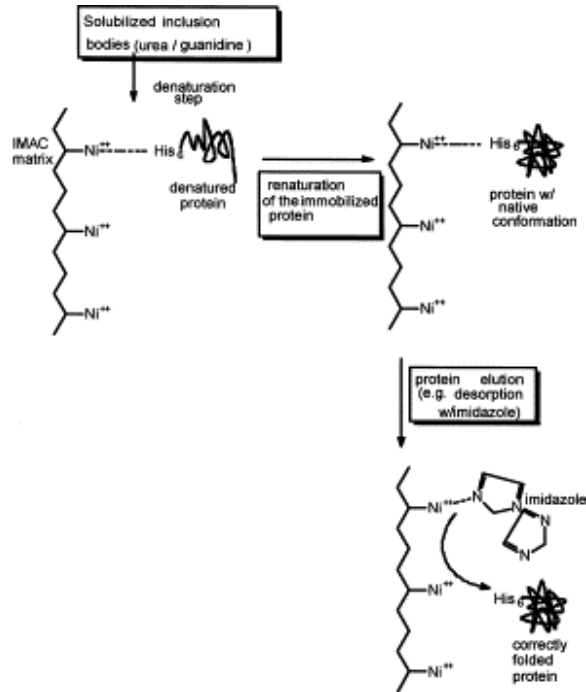


Figure 2.7. Schematic representation of matrix-assisted refolding on an IMAC support.

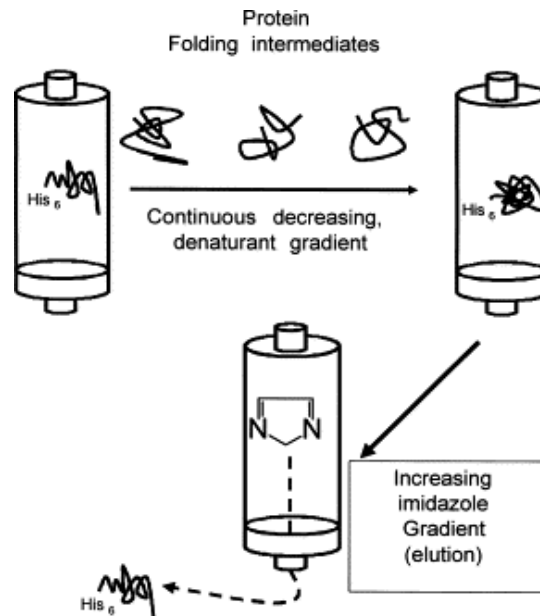


Figure 2.8. Matrix-assisted refolding mechanism consisting of refolding and elution steps.

2.3.15. Poly(ethylene imine)

Polyethylene imine (PEI) is one of the polycations reported to have a positive effect on enzyme activity and stability [18]. The polymer has been found to be rather versatile, with a number of interesting applications. Its application as synthetic enzyme is well known [218,18]. PEI finds use for precipitation of nucleic acids [219] and as flocculating agent for cell debris [219] during purification of proteins from crude feedstocks. The polymer has been shown to be effective for immobilisation of biocatalysts to solid supports by adsorption [220, 221]. It has also been used as a soluble carrier for enzymes and affinity ligands, the polymer recovery being achieved by precipitation. Furthermore, membrane-destabilising effect of PEI has been reported both for prokaryotic [222] and eukaryotic cell types, making it an effective permeabilizer and an antimicrobial agent.

PEI immobilized on a rigid inorganic matrix of high porosity is ideal for use in columns or in suspension (without magnetic stirrers). It binds polyanions, such as nucleic acids, very strongly. Suggested applications include chromatography of proteins, nucleotides and nucleic acids. It also effectively binds metal ions such as Ni^{2+} , Pd^{2+} , Pt^{2+} , Co^{2+} and Cu^{2+} .

Polyethyleneimine is formed by polymerising ethyleneimine to give a highly branched hydrophilic three-dimensional matrix. About 25% of the resultant amines are primary, 50% secondary and 25% tertiary (Figure 2.9.).

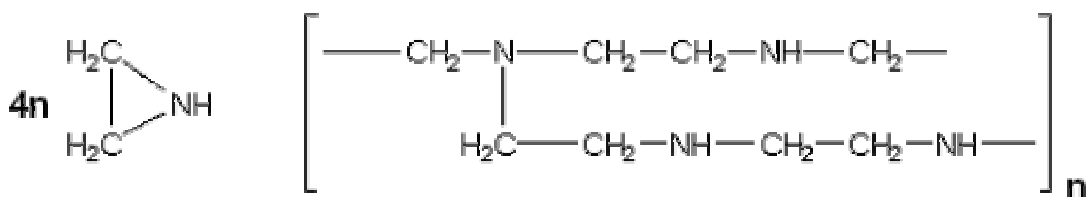


Figure 2.9. Structure of Polyethyleneimine

2.4. Cytochromes c

Cytochromes *c* (cyt *c*) can be defined as electrontransfer proteins having one or several haem *c* groups, bound to the protein by one or, more commonly two, thioether bonds involving sulphhydryl groups of cysteine residues. The fifth haem iron ligand is always provided by a histidine residue. Cyt *c* possess a wide range of properties and function in a large number of different redox processes [223-224]. Ambler [225] recognised four classes of cyt *c*:

- **Class I** includes the lowspin soluble cyt *c* of mitochondria and bacteria, with the haemattachment site towards the Nterminus, and the sixth ligand provided by a methionine residue about 40 residues further on towards the Cterminus. The proteins contain three conserved "core" helices which form a "basket" around the haem group with one haem edge exposed to the solvent.
- **Class II** includes the highspin cyt *c'* and a number of lowspin cytochromes, e.g. cyt *c*556. The haemattachment site is close to the Cterminus. The protein fold comprises a four~~h~~ helix bundle [226].
- **Class III** comprises the low redox potential multiplehaem cytochromes: cyt *c*₇ (trahaem), *c*₃ (tetrahaem), and highmolecularweight cyt *c* (HMC; hexadeca~~h~~haem), with only 30-40 residues per haem group. The haem *c* groups, all bisHis coordinated, are structurally and functionally nonequivalent and present different redox potentials in the range 0 to -400 mV [227].
- **Class IV** was originally created to hold the complex proteins that have other prosthetic groups as well as haem *c*, e.g. flavocytochrome *c* and cytochromes *cd*. Alternatively, Moore and Pettigrew [225] have suggested that **Class IV** cyt *c* are tetrahaem proteins containing both bisHis and HisMet coordinated haems, with a 3D structure exemplified by that of the photosynthetic reaction centre (PRC) cyt *c*, and form a structurally homogeneous fami

2.4.1. Structure

Mitochondrial cytochromes *c* are the most extensively studied electron-transfer proteins. For example, the cytochrome *c* amino acid sequences have been determined for organisms including humans, chimps, rhesus monkeys, spider monkeys, horses, donkeys, zebras, cows, pigs, sheep, camels, great whales, elephant seals, dogs, hippos, bats, rabbits, bull frogs, starfish and fruit flies. Cytochrome *c* is easily separated from its mitochondrial environment because of its solubility in water. Furthermore, cytochrome *c* is weakly associated with the inner membrane space. Cytochrome *c* is readily available in pure and native form, although it is expensive. The crystal structures of mitochondrial cytochrome *c* from several sources have been determined to atomic resolution (Figure 2.10.). The interpretation of the physiochemical properties of cytochrome *c* is facilitated by the knowledge of conformation [228].

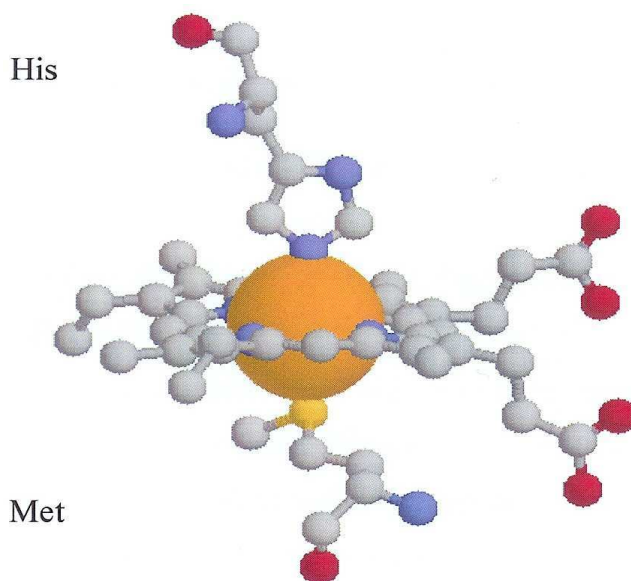


Figure 2.10. The Crystal Structures Of Mitochondrial Cytochrome *c*.

Cytochrome *c* (MW 12, 400) consists of a single polypeptide chain of 104 amino acid residues and covalently attached to a heme group. Cytochrome *c* has 19 positively charged lysine residues, plus two arginines also positively charged, but only 12 acidic residues (aspartic or glutamic acids). Cytochrome *c* is very basic with an isoelectric point near pH 10. Isoelectric point is the pH at which the number of positive charges and the number of negative charges of a compound are equal [229].

There is no difference between the cytochrome c's of human and chimp. Human cytochrome c differs from a rhesus monkey's by just one amino acid, and from an erythrocebus patas monkey's by a different one [230]. But, humans differ from whales at ten different cytochrome c sites, at 15 for turtles, and so on (Figure 2.11.). There is a "Message" in these proteins: species thought to be closely related turn out to have proteins that are *also* closely related. If human cytochrome sequences were completely different from those of the apes, or even all other creatures, evolution would have collapsed overnight. Instead, the molecules were in perfect accord with evolutionary expectations - independent and compelling confirmation.

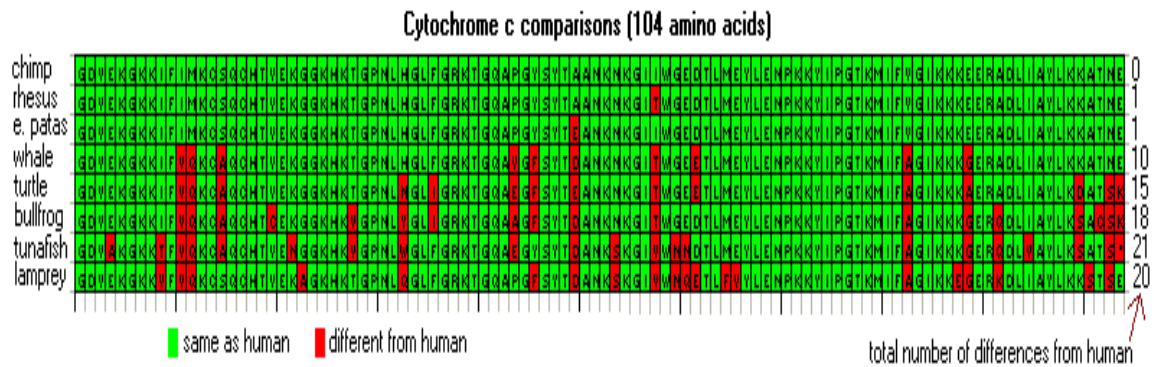


Figure 2.11. Different Cytochrome c's Amino Acid Chains

3. EXPERIMENTAL

3.1. Materials

Horse Heart Cytochrome c (from horse heart, Mr: 12.384, pl: 10.6), morpholinopropane sulfonic acid (MOPS), poly(ethyleneimine) (PEI; MW: 25.000, branched), morpholinoethane sulfonic acid (MES) and 2-hydroxyethyl methacrylate (HEMA) were supplied by Sigma (St Louis, USA). The monomer, ethylene glycol dimethacrylate (EGDMA) was obtained from Fluka A.G. (Buchs, Switzerland), distilled under reduced pressure in the presence of hydroquinone inhibitor and stored at 4°C until use. Benzoyl peroxide (BPO) was obtained from Fluka (Switzerland). Poly(vinyl alcohol) (PVAL; MW: 100.000, 98% hydrolyzed) and magnetite (Fe_3O_4 ; < 5 μm) were supplied from Aldrich Chem. Co. (USA). All other chemicals were of reagent grade and were purchased from Merck AG (Darmstadt, Germany). All water used in the adsorption experiments was purified using a Barnstead (Dubuque, IA) ROpure LP[®] reverse osmosis unit with a high flow cellulose acetate membrane (Barnstead D2731) followed by a Barnstead D3804 NANOpure[®] organic/colloid removal and ion exchange packed-bed system. The resulting purified water (deionized water) has a specific conductivity of 18 ms.

3.2. Preparation of Magnetic PHEMA Beads

Magnetic PHEMA (m-PHEMA) beads were prepared by a radical suspension polymerization technique [231]. Polymerization was carried out in an aqueous dispersion medium containing (polyvinyl alcohol) (PVAL) which was used as a stabilizer. Toluene and EGDMA was included in the recipe as the diluent (as a pore former) and cross-linker, respectively. The monomer phase containing HEMA, EGDMA, toluene, magnetite particles and benzoylperoxide (BPO) was added to the dispersion medium within a laboratory type reactor (i.e., a two neck flask with a volume of 500 ml) provided with a blade type stirrer. In order to produce spherical adsorbents of about 100-140 μm in diameter and with a narrow size distribution, the HEMA/EGDMA ratio, the monomer phase/dispersion phase ratio, the amounts of EGDMA and BPO, and the agitation speed were optimized and the optimum polymerization conditions and the recipe were given in Table 3.1.

Table 3.1. Recipe and the polymerization conditions for the preparation of m-PHEMA beads.

<u>Aqueous Dispersion Phase</u>	<u>Organic Phase</u>
Distilled water: 50 ml	HEMA: 4.0 ml
PVAL: 0.2 g	EGDMA: 8.0 ml
	Toluene: 12 ml
	BPO: 0.06 g
	Fe ₃ O ₄ : 0.5 g
<u>Polymerization Conditions</u>	
Reactor volume: 500 ml	
Stirring Rate: 600 rpm	
Temperature and Time: first at 65°C for 4 h, and then at 90°C for 2	

After cooling, the adsorbents were separated from the polymerization medium by filtration, and the residuals (e.g., monomer, toluene, etc.) were removed by a cleaning procedure [231]. Briefly, adsorbents were transferred into a reservoir, and washing solutions (i.e., a dilute HCl solution and a water-ethanol mixture) were recirculated through the system which includes also an activated carbon column, until to be assured that the adsorbents are clean (Figure 3.1). Purity of the adsorbents were followed by observing the change of optical densities of the samples taken from the liquid phase in the recirculation system, and also from the DSC thermograms of the adsorbents obtained by using a differential scanning microcalorimeter (Mettler, Switzerland). Optical density of uncleaned adsorbent was 2.86. But after cleaning operation, these values were reduced to 0.06. In addition, when the thermogram of uncleaned adsorbent was recorded, it has a peak around 60°C. This peak might be originated from initiator. But after application of this cleaning procedure, no peak was observed on this thermogram between 30-100°C. When not in use, the resulting adsorbents were kept under refrigeration in 0.02% NaN₃ solution for preventing of microbial contamination.

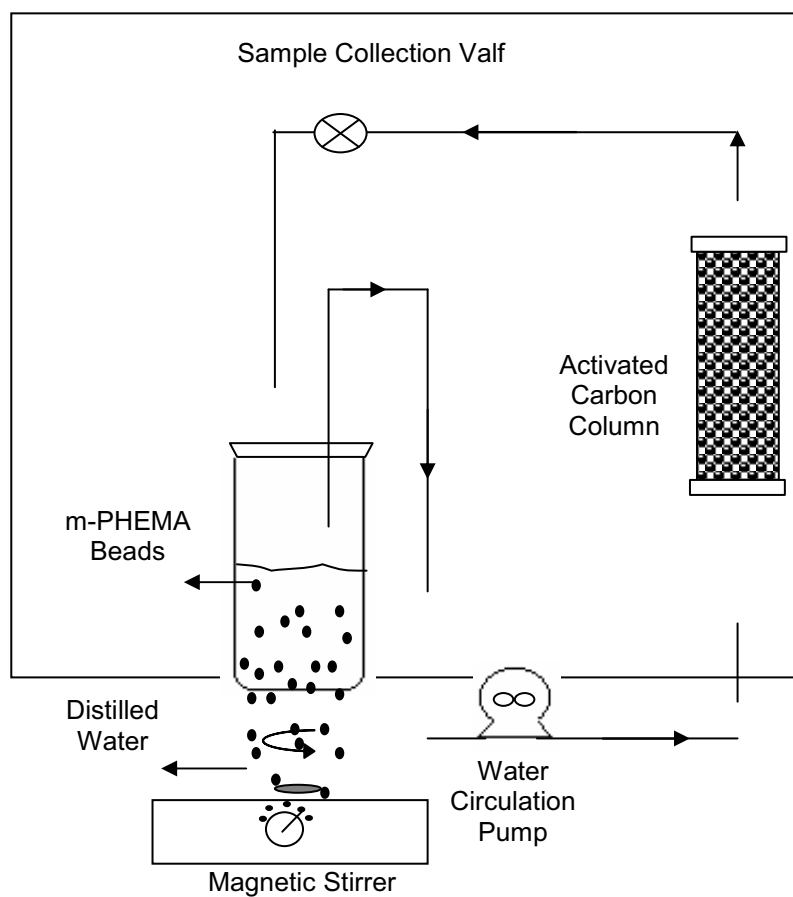


Figure 3.1. Schematic representation of cleaning procedure for polymeric beads.

3.3. Characterization of m-Poly(M-PHEMA) Beads

3.3.1. Swelling Test

Swelling ratio of the m-PHEMA beads was determined in distilled water. The experiment was conducted as follows: initially dry polymer sample was carefully weighed before being placed in a 50 mL vial containing distilled water. The vial was put into an isothermal water bath with a fixed temperature ($25 \pm 0.5^\circ\text{C}$) for 2 h. The polymer sample was taken out from the water by centrifugation periodically, and weighed. The water content of the swollen beads calculated by using the following expression:

$$\text{Swelling ratio \%} = [(W_s - W_o) / W_o] \times 100 \quad (3.1)$$

where W_o and W_s are the weights of polymer before and after swelling, respectively.

3.3.2. Surface Area and Porosity Measurements

Pore volumes and average pore diameter greater than 20\AA were determined by mercury porosimeter up to 2000 kg/cm^2 using a Carlo Erba model 200 (Italy). The surface area of the polymer sample was measured with a surface area apparatus (BET method).

3.3.3. Screen Analysis

The average size and size distribution of the m-PHEMA beads were determined by screen analysis performed by using Retsch Standard Sieves (Model AS200, Retsch GmbH & Co, KG, Haan, Germany).

3.3.4. Surface Morphology

The surface morphology of the polymeric beads was examined using scanning electron microscopy (SEM) and optical microscope. The samples were initially dried in air at 25°C for seven days before being analyzed. A fragment of the dried bead was mounted on a SEM sample mount and was sputter coated for 2 minutes. The sample was then mounted in a scanning electron microscope (Model: Raster Elektronen Microscopy, Leitz-AMR-1000, Germany). The surface of the sample was then scanned at the desired magnification to study the

morphology of the m-PHEMA beads. Optical microscope photographs were taken by Olympus System Microscope (CH 40 Series, Japan).

3.3.5. FTIR Studies

FTIR spectra of the m-PHEMA and m-PHEMA/PEI beads were obtained by using a FTIR spectrophotometer (FTIR 8000 Series, Shimadzu, Japan). The dry beads (about 0.1 g) was thoroughly mixed with KBr (0.1 g, IR Grade, Merck, Germany), and pressed into a pellet and the FTIR spectrum was then recorded.

3.3.6. Analysis of Magnetism

The magnetism degree of the m-PHEMA beads was measured in a magnetic field by using a vibrating-sample magnetometer (Princeton Applied Research, USA). The presence of magnetite particles in the polymeric structure was investigated with electron spin resonance (ESR) spectrophotometer (EL 9, Varian).

3.4. Poly(ethylene imine) (PEI) immobilization

Following procedure was applied for covalent attachment of PEI onto the m-PHEMA beads. After removal of water in the PEI solution with benzene, 10 g of PEI was dissolved in tetrahydrofuran (THF). NaH (3.0 g) was added into this solution. A 10 g of dry beads was weighed and transferred into this solution mixture. This reaction medium was boiled in Dean-Stark apparatus at reflux for 24 h. At the end of this reaction period, the PEI-immobilized beads were removed by filtration and washed with methanol several times and then dried in vacuum at room temperature for 24 h [232].

The free amine content of PEI immobilized m-PHEMA beads were determined by potentiometric titration. For this purpose, PEI immobilized m-PHEMA beads (1.0 g) were treated with 0.10 M standard HCl solution (100 ml) for 6 h with 120 rpm shaking rate. After consumption of HCl by free amine groups of m-PHEMA/PEI beads, the final HCl concentration in the aqueous medium was determined by a potentiometric titration with 0.1 M NaOH solution.

3.5. Incorporation of Cu²⁺ ions

Chelates of Cu²⁺ ions with m-PHEMA/PEI beads were prepared as follows: 1.0 g of the beads was mixed with 100 ml of aqueous solutions containing 100 ppm Cu²⁺ ions, at constant pH of 4.1 (adjusted with HCl and NaOH), which was the optimum pH for Cu²⁺ chelate formation at room temperature. A 1000 ppm atomic absorption standard solution (containing 10% HNO₃) was used as the source of Cu²⁺ ions. The flask was stirred magnetically at 100 rpm for 1 h (sufficient to attain equilibrium). The concentration of the Cu²⁺ ions in the resulting solution was determined with a graphite furnace atomic absorption spectrometer (AA800, Perkin-Elmer, Bodenseewerk, Germany). The amount of adsorbed Cu²⁺ ions was calculated by using the concentrations of the Cu²⁺ ions in the initial solution and in the equilibrium.

Cu²⁺ leakage from the m-PHEMA/PEI beads was investigated with media having different pH's (4.0–11.0), and also in a medium containing 2.0 M NaCl. The bead suspensions were stirred 24 h at room temperature. Cu²⁺ ion concentration was then determined in the supernatants using an atomic absorption spectrophotometer. It should be also noted that immobilized metal containing beads were stored at 4 °C in the 10 mM Tris–HCl buffer (pH 7.4) with 0.02% sodium azide to prevent microbial contamination.

3.6. Cytochrome C Adsorption-Desorption Studies

3.6.1. Adsorption of Cytochrome C from Aqueous Solutions in Batch Mode

Adsorption of Cytochrome c on the m-PHEMA/PEI/Cu²⁺ beads was studied in batch-wise. The polymeric beads were incubated with 10 mL of for 2 h (i.e., equilibrium time), in flasks agitated magnetically at 130 rpm. Effects of initial concentration of Cytochrome c, the pH of the medium, buffer type, temperature and ionic strength on the adsorption rate and capacity were studied. To observe the influence of buffer to the adsorption capacity, the adsorption studies were carried out using 25 mM morpholinoethanesulfonic acid (MES), 25 mM morpholinopropanesulfonic acid (MOPS), 50 mM bicarbonate, 25 mM Tris-HCl, 25 mM acetate and phosphate buffers (contains 0.15 M NaCl) within their respective buffering ranges. To determine the effect of pH and temperature on the adsorption, they were changed between 5.0–11.5 and 4–37°C, respectively. To

observe the effects of the initial concentration of Cytochrome c on adsorption, it was changed between 0.05-2.0 mg/mL. To observe the effects of ionic strength, 0.01 0.1 M NaCl was added into adsorption buffer. Cytochrome c concentration was determined spectrophotometrically by UV-Vis spectrophotometer (Schimadzu UV-Vis 1601, Japan) at 409 nm wavelength. The amount of adsorbed Cytochrome c was calculated as:

$$q=(C_i-C_f)V/m \quad (3.2)$$

Here, q is the amount of Cytochrome c adsorbed onto unit mass of beads (mg/g); C_i and C_f are the concentrations of Cytochrome c in the initial solution and in the aqueous phase after treatment for certain period of time, respectively (mg/mL); V is the volume of the aqueous phase (mL); and m is the mass of the beads used (g).

3.6.2. Adsorption of Cytochrome c in Magnetically Stabilized Fluidized Bed (MSFB)

Adsorption of Cytochrome c (Sigma Cat. No: 2506) on the m-PHEMA/PEI/Cu²⁺ beads were studied in magnetically stabilized fluidized bed system (MSFB) by using BioRad economic column (Length: 5 cm, Diameter: 1 cm). Polymeric beads suspended in pure water were put into a column equipped with a water jacket for temperature control. Expanding of the beads was done conventionally. During the experiment, the magnetic beads in the column were exposed to magnetic field which surrounded the column ($B_{rms} \approx 24$ Gauss, $B_{p-p} \approx 33$ Gauss, $f = 50$ Hz). Equilibration of the column was performed by passing four column volumes of buffer before injection of Cytochrome c solution. Cytochrome c solution in the reservoir, agitated magnetically at 130 rpm. The flow of Cytochrome c solution through the column was enabled using an ALITEA (Sweden) peristaltic pump. The solution coming out of the column was gathered in a separate flask (Figure 3.2). The Cytochrome c amount in this solution was determined by UV-Vis spectrophotometer at 409 nm.

In this part of the experiment effect of flow rate on Cytochrome c adsorption capacity was investigated in optimum conditions (i.e. pH 11.0 Bicarbonate buffer, 40 mL of the solution with a Cytochrome c content of 0.2 mg/mL).

In order to determine the Cytochrome c amount going into the column and coming out of the column Equation 3.3 and Equation 3.4 were used, respectively.

$$m_i = C_o \cdot q \cdot t \quad (3.3)$$

$$m_o = C \cdot V \quad (3.4)$$

In these equations; m_i : the amount of Cytochrome c going into the column (mg); C_o : Cytochrome c initial concentration (mg/mL); q : flow rate (mL/min); t : time; m_o : the concentration of Cytochrome c coming out of the column (mg/mL); C : the concentration of Cytochrome c after adsorption (mg/mL); V : the volume of protein solution gathered in the flask (mL).

The Cytochrome c adsorption capacity of the polymeric beads was found by using Equation 3.5.

$$Q = (m_i - m_o) / m \quad (3.5)$$

m : the weight of polymeric beads in the column. The total weight of the polymer in the column is 30 mg.

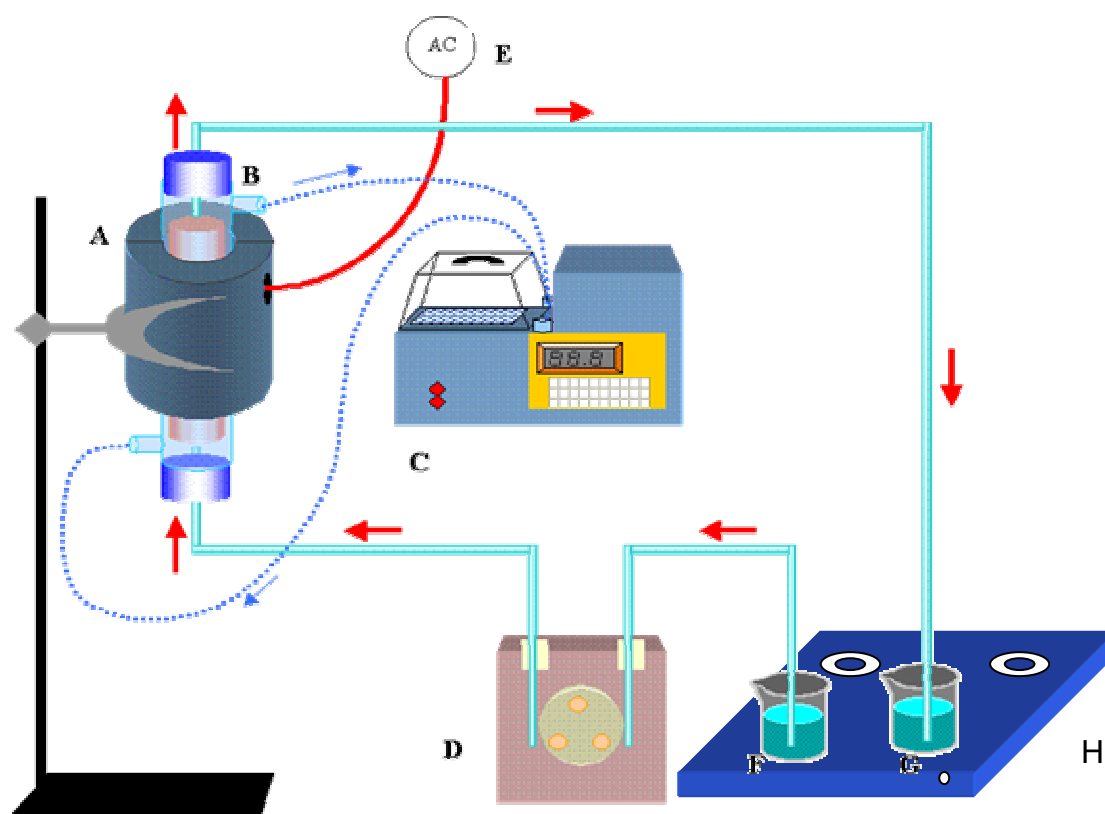


Figure 3.2. Schematic representation of magnetically stabilized fluidized bed system. A; Bobbin, B; Column with jacket, C; Water circulation system on fixed temperature, D; Peristaltic pump, E; AC Power supply, F; Sample, G; Reservoir, H; Magnetic stirrer.

3.7. Desorption and Repeated Use

Desorption of Cytochrome c was studied with 1 M NaCl solution. The m-PEMA/PEI/Cu²⁺ beads-adsorbed Cytochrome c were placed in this desorption medium and stirred continuously (at a stirring rate of 600 rpm) for 1 h at room temperature. The final Cytochrome c concentration in the desorption medium was determined spectroscopically. The desorption ratio was calculated from the amount of Cytochrome c adsorbed on the beads and the final Cytochrome c concentration in the desorption medium by the following Equation:

$$\text{Desorption ratio (\%)} = \frac{\text{Amount of Cytochrome c to the elution}}{\text{Amount of Cytochrome c adsorbed to the beads}} \quad (3.6)$$

In order to test the reusability of m-PHEMA/PEI/Cu²⁺ beads, Cytochrome c adsorption-desorption procedure was repeated ten times by using the same polymeric adsorbent. In order to regenerate and sterilize, after the desorption; the beads were washed with 50 mM NaOH solution.

4. RESULTS AND DISCUSSION

4.1. Characterization of Beads

4.1.1. PEI Immobilized onto m-PHEMA Beads

Magnetic poly(hydroxyethyl methacrylate) beads(m-PHEMA) were prepared by suspension polymerization of HEMA and EGDMA. The poly(ethylene imine)(PEI) molecules were immobilized on the m-PHEMA beads surface via reaction between hydroxyl groups of the beads and amino groups of the PEI. The presence of PEI in the m-PHEMA structure was confirmed both by the titration and by the FTIR spectra.

The maximum amount of PEI immobilized onto the m-PHEMA bead surface was found to be 102 mg PEI/g polymer from the titration. Note that this value represents available amine groups of immobilized PEI that can react with copper ions.

FTIR spectra of plain and PEI-immobilized m-PHEMA beads are presented in Figure 4.1. The broad band in the 3300-3500 cm^{-1} range indicates $-\text{OH}$ stretching vibrations in the bead structure. The vibration at 1740 cm^{-1} represents the ester configuration of HEMA. The FTIR spectra of the PEI-immobilized beads have some absorption bands different from those of the plain beads. The most important absorption bands at 1550 cm^{-1} representing N-H bending is due to the PEI immobilized to the m-PHEMA beads.

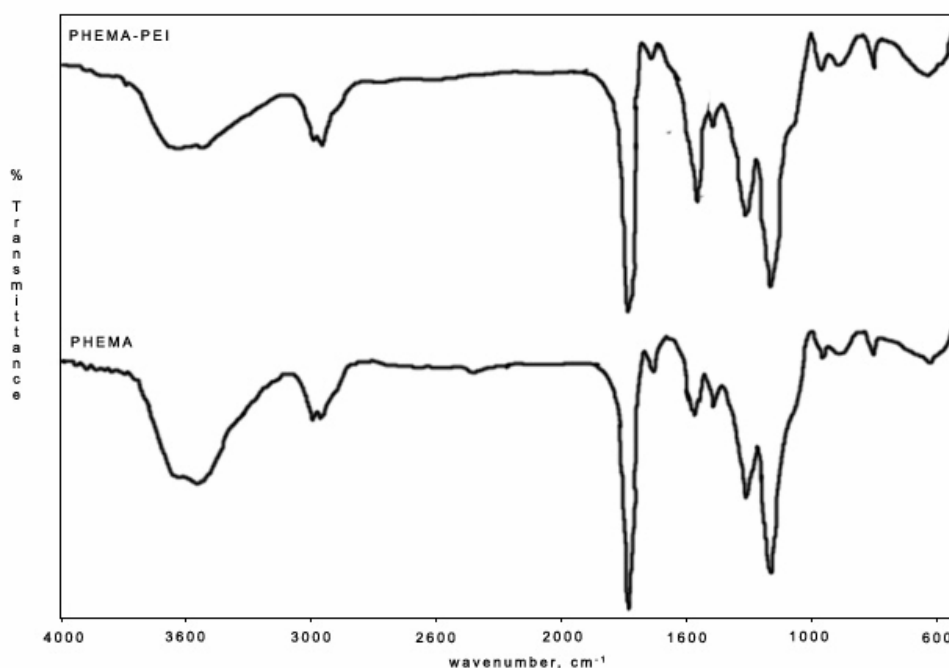


Figure 4.1. FTIR spectra of m-PHEMA and m-PHEMA/PEI beads.

4.1.2. Swelling Properties

m-PHEMA/PEI beads are crosslinked hydrogels (Figure 4.2). They do not dissolve in aqueous medium, but do swell, depending on the degree of crosslinking. The equilibrium swelling ratio of the m-PHEMA/PEI beads is 45 %. Compared with m-PHEMA (37.5 %), the water uptake ratio of the m-PHEMA/PEI beads was increased. Several possible factors may contribute to this result. First, the incorporation of PEI actually introduces more hydrophilic functional groups onto the polymer chain, which can attract more water molecules into polymer matrices. Therefore, the water molecules penetrate into the entanglement polymer structure more easily, resulting in an improvement of water uptake behavior in aqueous solutions.

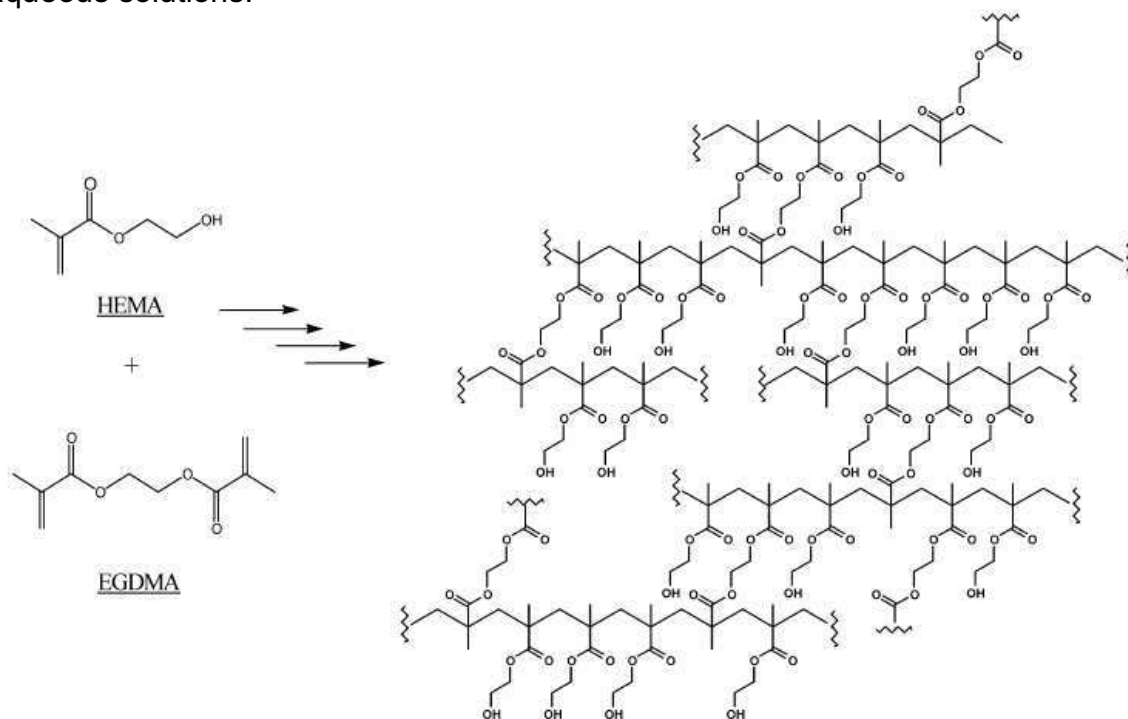


Figure 4.2. Network formation of HEMA and EGDMA monomers.

4.1.3. Surface Area and Pore Size Measurements

The radicalic suspension polymerization procedure provided crosslinked m-PHEMA beads in a spherical form mostly in the size range of 100-140 μm in diameter. According to mercury porosimetry data, the average pore size of the magnetic beads was 819 nm. The specific surface area of the mPHEMA/PEI beads was found to be 50 m^2/g . This indicated that the magnetic beads contained

mainly micropores. This pore diameter range is possibly available for diffusion of the cytochrome c molecules. The diameter of hydrated cytochrome c is 34 Å [233]. Based on this data, it was concluded that the m-PHEMA/PEI beads had effective pore structures for liquid chromatographic separation of cytochrome c.

4.1.4. Surface Morphology

The surface morphology and internal structure of m-PHEMA/PEI beads are exemplified by the electron micrographs in Figure 4.3. As clearly seen here, the magnetic beads have a spherical form and rough surface due to the pores which formed during the polymerization procedure. The presence of pores within the bead surface is clearly seen in this photograph. It can be concluded that the m-PHEMA/PEI beads have a porous interior surrounded by a reasonably rough surface, in the dry state. The roughness of the surface should be considered as a factor providing an increase in the surface area. In addition, these pores reduce diffusional resistance and facilitate mass transfer because of high internal surface area. Optical microscope photographs of the m-PHEMA/PEI beads were also shown in Figure 4.4.

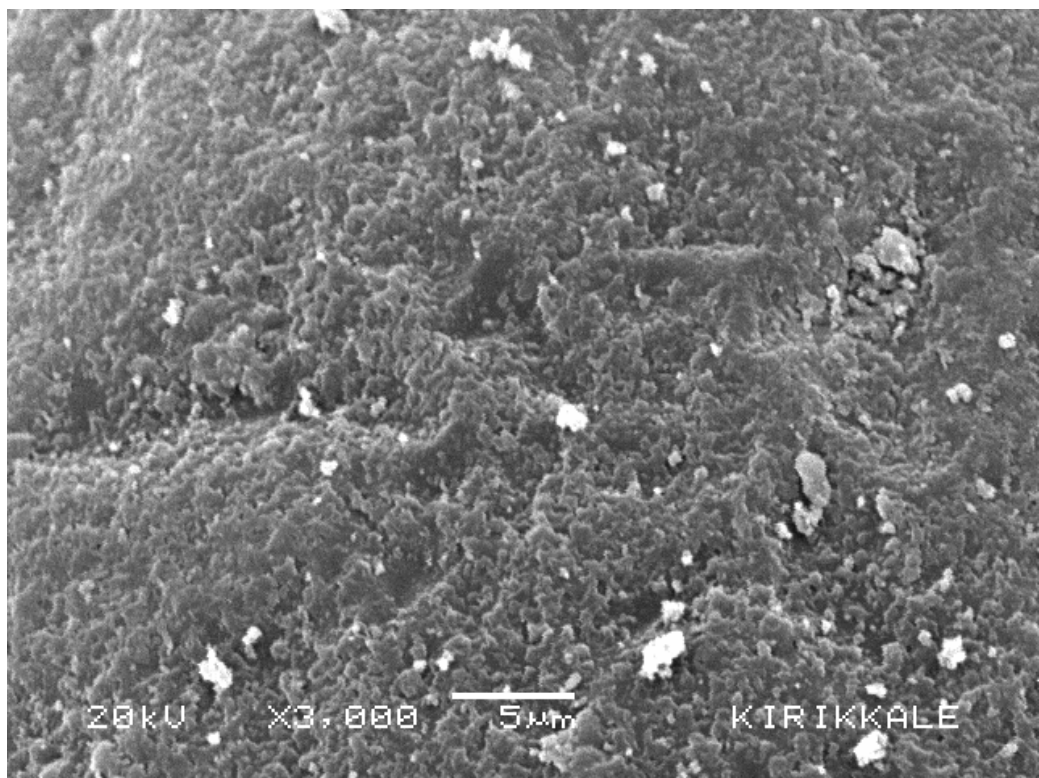
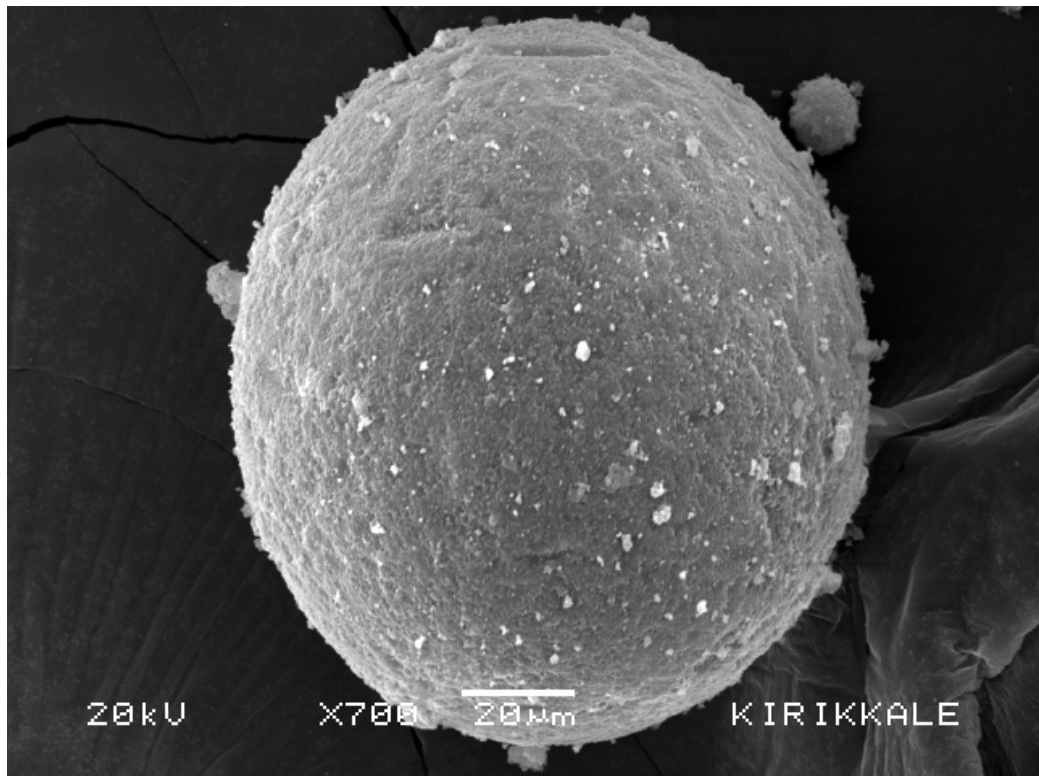


Figure 4.3. SEM micrographs of m-PHEMA/PEI beads.

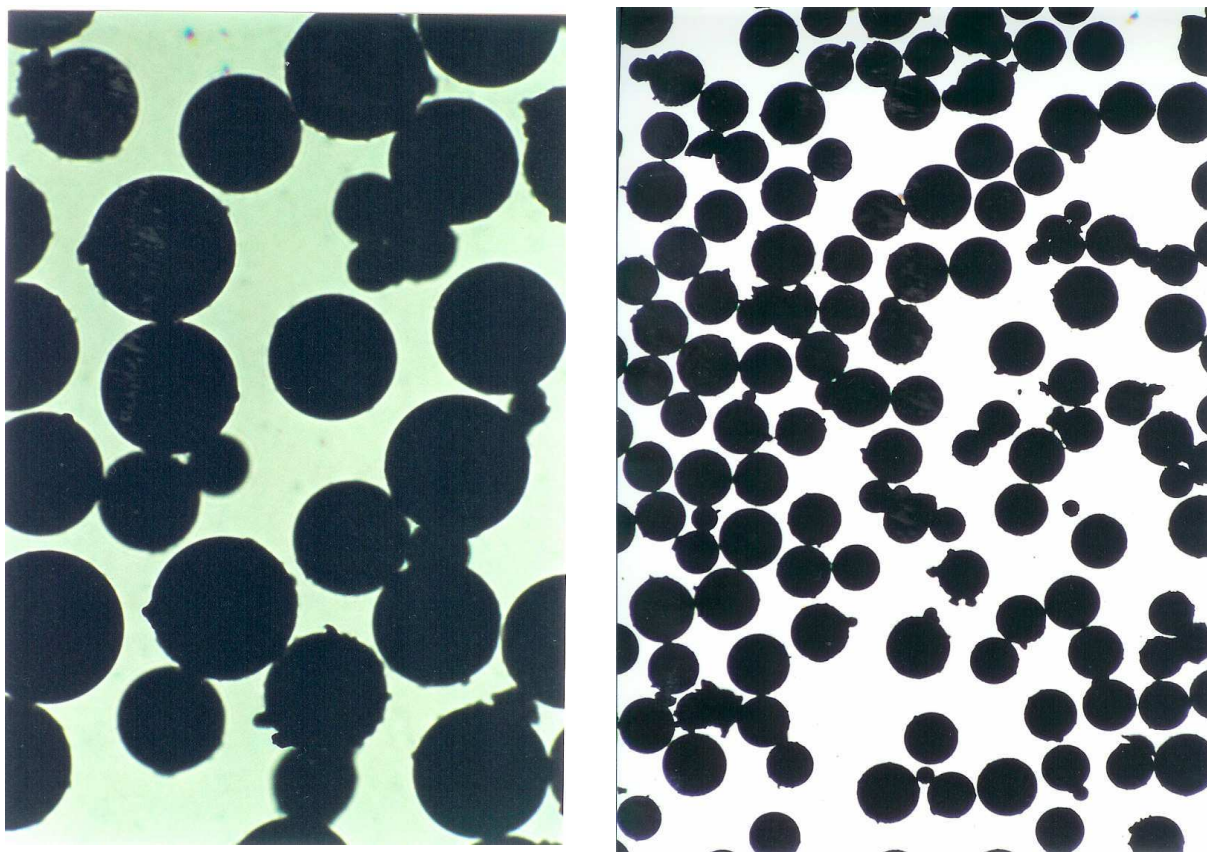


Figure 4.4. Optical microscope photographs of m-PHEMA/PEI beads.

4.1.5. Cu^{2+} Loading Onto m-PHEMA/PEI Beads

PEI immobilized m-PHEMA beads were incubated with Cu^{2+} solutions ($\text{Cu}(\text{NO}_3)_2 \cdot 2\text{H}_2\text{O}$ in deionized buffer at pH 4.0) having different Cu^{2+} initial concentrations (0-100 ppm). The amount of chelated Cu^{2+} on m-PHEMA/PEI beads was measured with atomic absorption spectrometer and it found to be 0-795 $\mu\text{mol/g}$ polymer. As seen in the Figure 4.5. copper loading onto the magnetic beads is clearly understood also by naked eye. From the mass-stoichiometry, it seems that 3 incorporated PEI molecule interact around one Cu^{2+} ions (2318.2 $\mu\text{mol/g}$ PEI/g polymer: 795 μmol Cu^{2+} /g polymer) (Figure 4.6). This 3:1 ratio is also confirmed in related literature [234]. Studies aimed at detecting leakage of Cu^{2+} from the m-PHEMA/PEI beads revealed no leakage in any of the adsorption and desorption media, and implied that the washing procedure was satisfactory for the removal of the non-specific chelated Cu^{2+} ions from the magnetic beads.



Figure 4.5. m-PHEMA/PEI beads before and after incubation with Cu^{2+} solution.

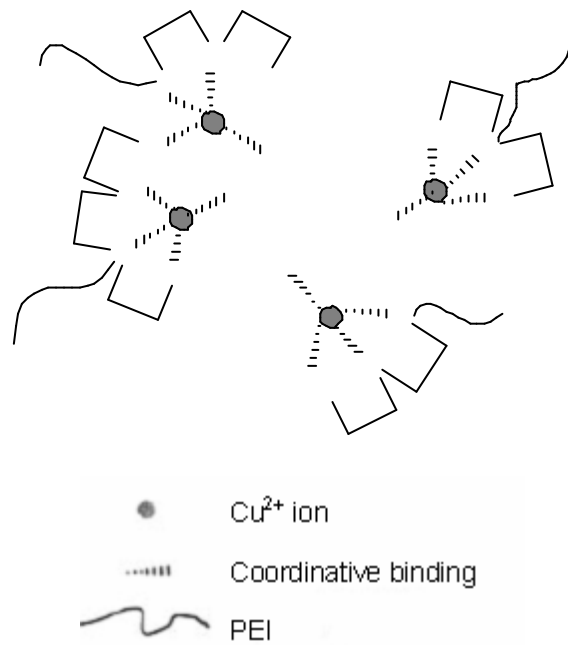


Figure 4.6. Proposed structure of m-PHEMA/PEI- Cu^{2+} complexes in aqueous solutions.

4.1.6. Analysis of Magnetism

The presence of magnetite particles in the polymeric structure was confirmed by ESR. The application of an external magnetic field may generate an internal magnetic field in the sample which will add to or subtract from the external field. The local magnetic field generated by the electronic magnetic moment will add vectorially to the external magnetic field (H_{ext}) to give an effective field (H_{eff}).

$$H_{\text{eff}} = H_{\text{ext}} + H_{\text{local}} \quad (4.1)$$

m-PHEMA/PEI beads have a relative intensity of 125. This value shows that polymeric structure has a local magnetic field because of magnetite in its structure. The g factor can be considered as quantity characteristic of the molecules in which the unpaired electrons are located, and it is calculated from Equation (4.1). The measurement of the g factor for an unknown signal can be a valuable aid in the identification of a signal's origin. In the literature the g factor for Fe^{3+} (low spin and high spin complexes) is determined between 1.4 -3.1 and 2.0-9.7, respectively [235]. In this study, the g factors were found to be 1.58 for m-PHEMA/PEI and 1.98 for m-PHEMA/PEI/ Cu^{2+} structures by using Equation 4.2.

$$g = h \cdot \nu / \beta \cdot H_r \quad (4.2)$$

Here, h is the Planck constant (6.626×10^{-34} joule/s); β is Universal constant (9.274×10^{-28} joule/G); ν is frequency (9.707×10^9 Hz) and H_r is resonance of magnetic field (G).

Magnetic properties of polymeric structure was also obtained using electron mass unit (EMU), showing the behavior of magnetic beads in a magnetic field using a vibrating magnetometer, and H_r value, is defined as the external magnetic field at resonance (Figure 4.7). In EMU spectrum and from H_r value, 4537 Gauss magnetic field was found sufficient to excite all of the dipole moments present in 1.0 g m-PHEMA/PEI sample. These values will be an important design parameter for a magnetically stabilized fluidized bed or for magnetic filtration using these magnetic beads. The value of this magnetic field is a function of the flow velocity, particle size and magnetic susceptibility of solids to be removed. In the literature,

this value was found to change from 8 kG to 20 kG for various applications, thus magnetic beads presented in this study will need less magnetic intensity in a magnetically stabilized fluidized bed or for a magnetic filter system.

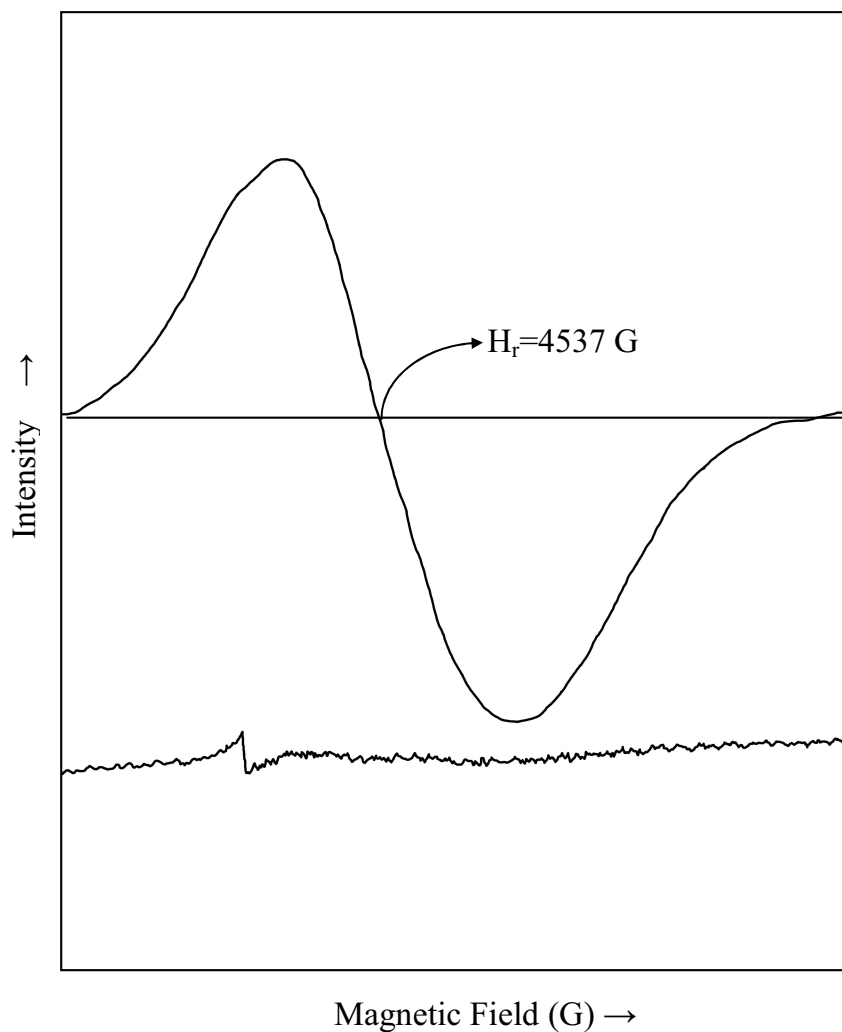


Figure 4.7. ESR spectrum of m-PHEMA beads.

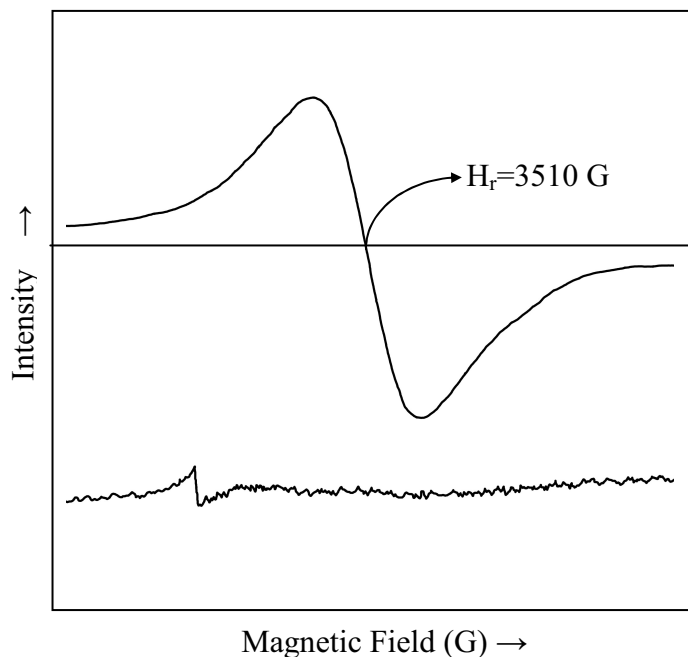


Figure 4.8. ESR spectrum of Cu(II) Loaded m-PHEMA/PEI beads.

4.2. Adsorption of Cytochrome C from Aqueous Solutions

4.2.1. Effect of pH

The amount of cytochrome c adsorbed onto the m-PHEMA/PEI and the Cu²⁺-complexed m-PHEMA/PEI beads as a function of pH was shown in Figure 4.9 (pH 5.0-6.0, 0.1 M acetate buffer; 6.5-8.0 0.1 M phosphate buffer; 9.0-11.5 carbonate buffer). The amount of cytochrome c adsorbed gradually increased with increasing pH and showed a maximum at pH 11.0, (isoelectric point of cytochrome c: 10.6). Specific interactions (electrostatic and coordination) between cytochrome c and chelated-Cu²⁺ ions at alkaline pHs may be resulted both from the ionization states of several groups on amino acid side chains in cytochrome c structure, and from the conformational state of cytochrome c molecules (more folded structure) at this pH. Note that cytochrome c is negatively charged above its isoelectric pH (10.6). More favorable electrostatic interactions can occur between Cu²⁺ loaded matrix and negatively charged proteins at these pH values. At pH values lower than pH 11.0, the adsorbed amount of cytochrome c slightly decreases. This could be created from the ionization state of cytochrome c and could be caused repulsive electrostatic forces between adsorbed cytochrome c molecules and the chelated Cu²⁺ ions. Increase in conformational size and the lateral electrostatic repulsions

between adjacent adsorbed cytochrome c molecules may also cause a decrease in adsorption efficiency. Also, the change of coordination interaction at high and low pH should have a great influence.

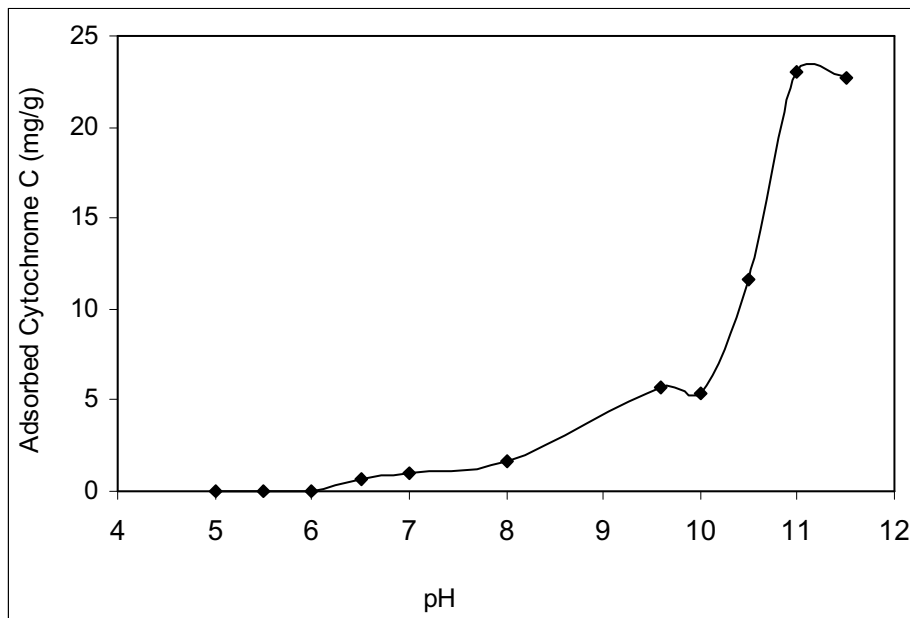


Figure 4.9. Effect of pH on cytochrome c adsorption. V: 10 ml; m_{polymer} : 30 mg; C cytochrome c: 0.2 mg/ml; T: 25 ° C; Cu^{2+} loading: 302 $\mu\text{mol/g}$ polymer

Cytochrome c adsorption onto Cu^{2+} loaded m-PHEMA/PEI beads was also investigated with organic buffer systems within their buffering regions (i.e. MES, MOPS and tris-HCl). These buffers are shown to be less effective than inorganic buffers. In MES buffer almost no adsorption was observed. In MOPS and tris-HCl buffer systems adsorption of cytochrome c was also observed above neutral pH. Cytochrome c adsorption capacities on Cu^{2+} -chelated beads were found to be 16.3 mg/g for tris-HCl, 0.2 mg/g for MES, 11.7 mg/g for MOPS and 22.7 mg/g for carbonate buffer under the same conditions (Figure 4.10). We have shown that buffer type significantly changes cytochrome c adsorption capacity of the beads. All buffer ions and the respective counterions interact with the protein molecules via charge-charge interactions. Cytochrome c adsorption capacity was demonstrated for the buffer types with the effects in the order carbonate > Tris-HCl > MOPS > MES.

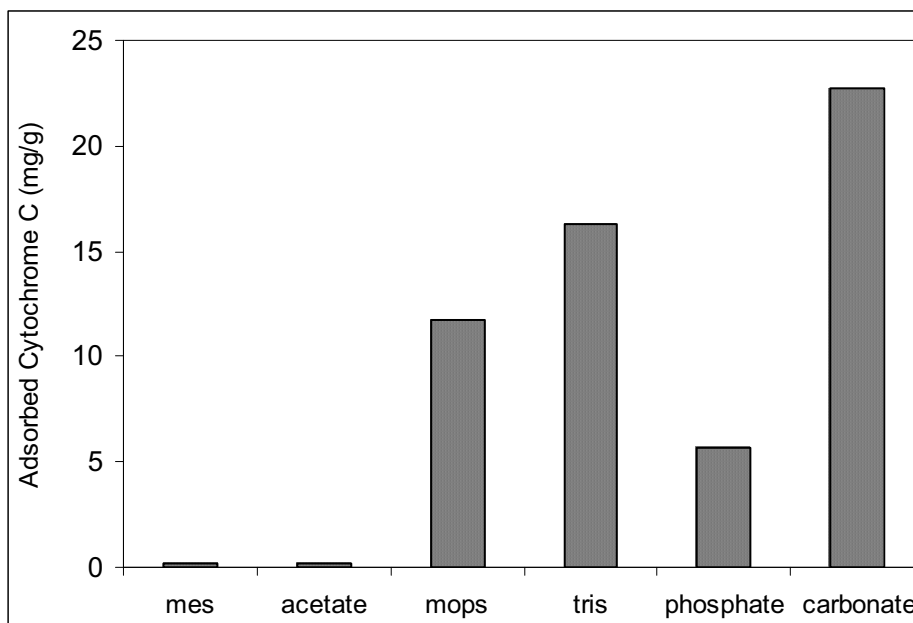


Figure 4.10. Effect of buffer type on cytochrome c adsorption. V: 10 ml; m_{polymer} : 30 mg; $C_{\text{cytochrome c}}$: 0.2 mg/ml; T: 25 ° C; Cu^{2+} loading: 302 $\mu\text{mol/g}$ polymer

4.2.2. Adsorption Time

Figure 4.11 gives the adsorption rate curves which were obtained by following the decrease of the concentration of cytochrome c within the protein solution with time. As seen here, there were relatively faster adsorption rates were observed at the beginning of adsorption process, and then adsorption equilibrium were achieved gradually in about 120 min. Note that, adsorption rates increased with increasing cytochrome c concentration. This is due to high driving force, which is the cytochrome c concentration difference between the liquid (i.e., the protein solution) and the solid (i.e., the magnetic beads) phases, in the case of high cytochrome c concentration.

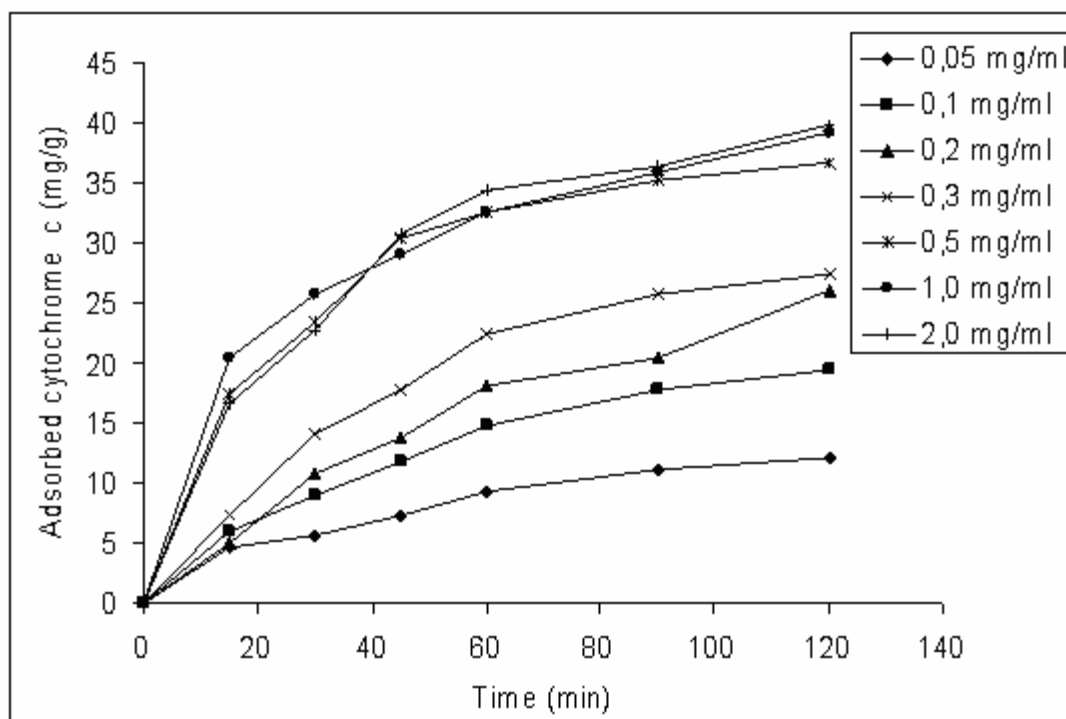


Figure 4.11. Cytochrome C adsorption rates. . pH:11.0 Carbonate buffer; V: 20 ml; m_{polymer} : 60 mg; T: 25 ° C; Cu^{2+} loading: 302 $\mu\text{mol/g}$ polymer

4.2.3. Adsorption Isotherms

Figure 4.12 shows the dependence of the adsorbed amount of cytochrome c on cytochrome c concentration. The adsorption values increased with increasing concentration of cytochrome c, and a saturation value is achieved at cytochrome c concentration of 0.5 mg/ml, which represents saturation of the active binding sites on the affinity beads. The slope of the initial part of the adsorption isotherm represents a high affinity between cytochrome c and Cu^{2+} -chelated groups. It becomes constant when the protein concentration is greater than 1.0 mg/ml. Cytochrome c molecules adsorbed on the m-PHEMA/PEI beads was about 4.6 mg/g. The adsorption capacity of cytochrome c is due to electrostatic interactions between the protein molecules and the reactive PEI groups on the magnetic beads. Cu^{2+} -chelation significantly increased the cytochrome c adsorption of the beads up to 39.8 mg/g. It is clear that this increase is due to specific interactions between chelated Cu^{2+} ions and cytochrome c molecules (especially imidazole side chains of histidine residue in cytochrome c structure). Cytochrome c has a single surface histidine at position 29 and an additional partially accessible histidine at position 33 [236]. One surface histidine is reported as sufficient for the

adsorption on a Cu^{2+} -IMAC adsorbent and proteins varying by only one histidine can be separated.

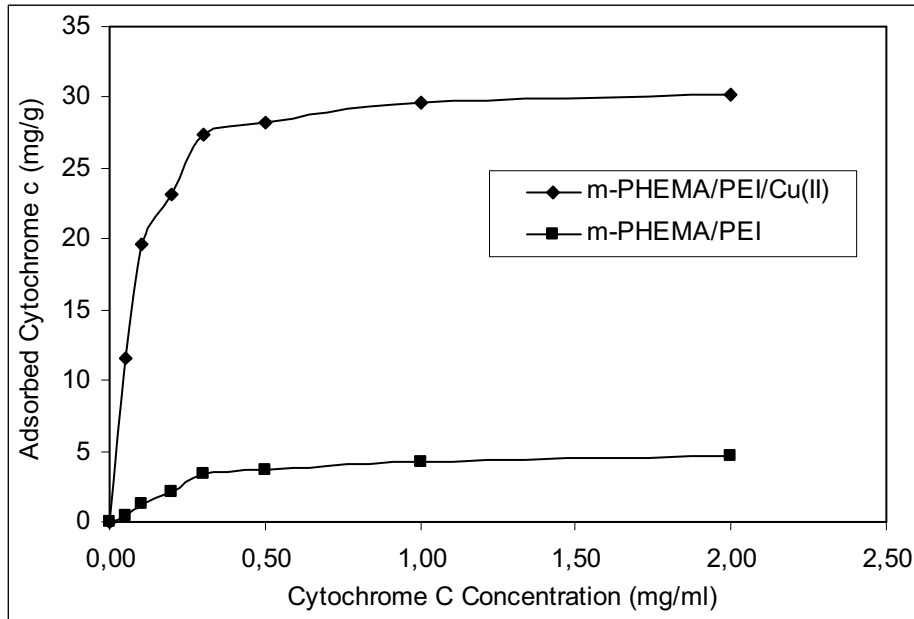


Figure 4.12. Effect of cytochrome c concentration. pH:11.0 Carbonate buffer; V: 20 ml; m_{polymer} : 60 mg; T: 25 ° C; Cu^{2+} loading: 302 $\mu\text{mol/g}$ polymer

During the batch experiments, adsorption isotherms were used to evaluate adsorption properties. For the systems considered, the Langmuir model was found to be applicable in interpreting cytochrome c adsorption by metal-complexed beads. The Langmuir adsorption isotherm is expressed by Equation 4.3. Langmuir adsorption model assumes that the molecules are adsorbed at a fixed number of well-defined sites, each of which can only hold one molecule. These sites are also assumed to be energetically equivalent and distant to each other so that there are no interactions between molecules adsorbed to adjacent sites. The corresponding transformations of the equilibrium data for cytochrome c gave rise to a linear plot, indicating that the Langmuir model could be applied in these systems and described by the Equation:

$$Q = Q_{\text{max}} \cdot b \cdot C_e / (1+bC_e) \quad (4.3)$$

Where, Q is the concentration of bound cytochrome c in the adsorbent (mg/g), C_e is the equilibrium cytochrome c concentration in solution (mg/ml), b is the

Langmuir constant (g/ml) and, Q_{\max} is the adsorption capacity (mg/g). This Equation can be linearized.

$$1/Q = [1/(Q_{\max} \cdot b)] [1/C_e] + [1/Q_{\max}] \quad (4.4)$$

The plot of $1/C_e$ versus $1/Q$ was employed to generate the intercept of $1/Q_{\max}$ and the slope of $1/Q_{\max} \cdot b$.

The maximum adsorption capacities (Q_{\max}) data for the adsorption of cytochrome c were obtained from the experimental data (Figure 4.13). The correlation coefficients (R^2) were high for both m-PHEMA/PEI and Cu^{2+} -chelated m-PHEMA/PEI beads (Table 4.1). The Langmuir adsorption model can be applied in this affinity adsorbent system.

The other well-known isotherm, which is frequently used to describe adsorption behavior, is the Freundlich isotherm. This isotherm is another form of the Langmuir approach for adsorption on a heterogeneous surface. The amount of adsorbed protein is the summation of adsorption on all binding sites. The Freundlich isotherm describes reversible adsorption and is not restricted to the formation of the monolayer. This empirical Equation takes the form:

$$Q_{\text{eq}} = K_F (C_{\text{eq}})^{1/n} \quad (4.5)$$

where, K_F and n are the Freundlich constants; C_{eq} is the equilibrium cytochrome c concentration in solution (mg/ml).

The isotherms of cytochrome c were found to be linear over the whole concentration range studies and the correlation coefficients were high (Figure 4.14). Table 4.1 shows the Freundlich adsorption isotherm constants, n and K_F and the correlation coefficients. The magnitude of K_F and n values of Freundlich model showed easy uptake of cytochrome c from aqueous medium with a high adsorption capacity of the metal-chelated affinity beads. Values of $n > 1$ for both magnetic affinity beads indicate positive cooperativity in binding and a heterogeneous nature of adsorption.

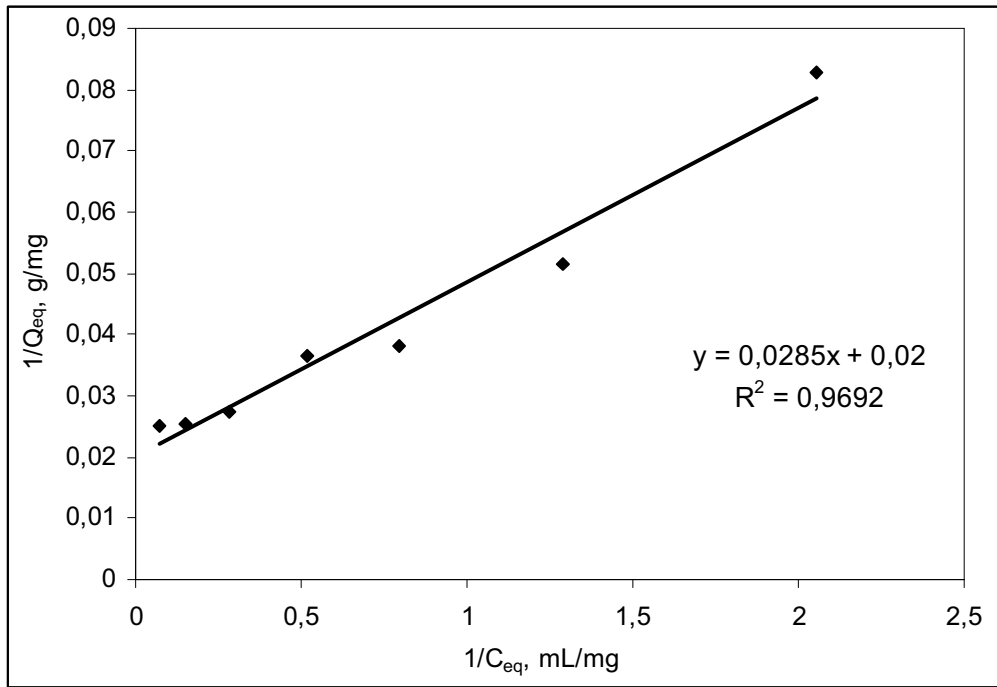


Figure 4.13. Langmuir adsorption isotherm of m-PHEMA/PEI/Cu²⁺ beads

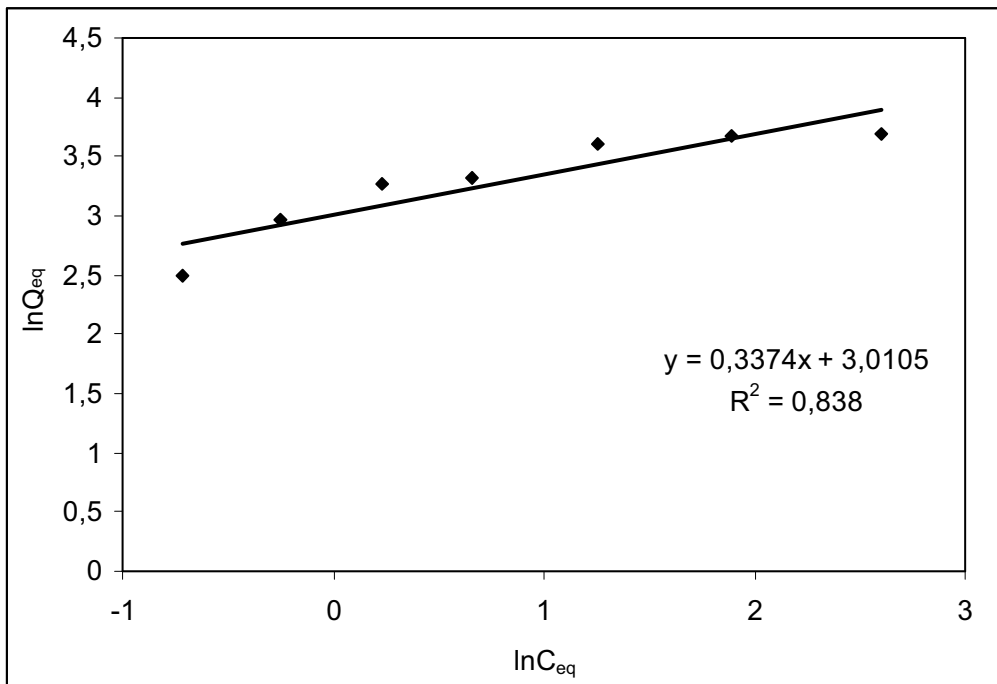


Figure 4.14. Freundlich adsorption isotherm of m-PHEMA/PEI/Cu²⁺ beads.

Table 4.1. Kinetic constants of Langmuir and Freundlich isotherms.

Langmuir Adsorption Isotherm	Freundlich Adsorption Isotherm
$Q_{\max} = 50.0 \text{ mg/g}$	$K_f = 20.30$
$b = 0.702 \text{ mL/mg}$	$n = 2.964$

4.2.4. Adsorption Kinetics Modeling

In order to examine the controlling mechanism of adsorption process such as mass transfer and chemical reaction, kinetic models were used to test experimental data. The kinetic models (Pseudo-first- and second-order equations) can be used in this case assuming that the measured concentrations are equal to adsorbent surface concentrations. The first-order rate equation of Lagergren is one of the most widely used for the adsorption of solute from a liquid solution [237]. It may be represented as follows:

$$q_t/dt=k_1(q_{eq}-q_t) \quad (4.6)$$

Where k_1 is the rate constant of pseudo-first order adsorption (1/min) and q_{eq} and q_t denote the amounts of adsorbed protein at equilibrium and at time t (mg/g), respectively. After integration by applying boundary conditions, $q_t=0$ at $t=0$ and $q_t=q_t$ at $t=t$, gives

$$\log[q_{eq}/(q_{eq}-q_t)]= (k_1t)/2.303 \quad (4.7)$$

Equation 4.7 can be rearranged to obtain a linear form

$$\log(q_{eq}-q_t)= \log(q_{eq}) - (k_1t)/2.303 \quad (4.8)$$

a plot of $\log(q_{eq}-q_t)$ versus t should give a straight line to confirm the applicability of the kinetic model. In a true first-order process $\log q_{eq}$ should be equal to the interception point of a plot of $\log(q_{eq}-q_t)$ via t .

In addition, a pseudo-second order equation based on equilibrium adsorption capacity may be expressed in the form

$$q_t/dt = k_2 (q_{eq}-q_t)^2 \quad (4.9)$$

Where k_2 (g/mg·min) is the rate constant of pseudo-second order adsorption process. Integrating Equation 4.10 and applying the boundary conditions, $q_t=0$ at $t=0$ and $q_t=q_t$ at $t=t$, leads to

$$[1/(q_{eq}-q_t)] = (1/q_{eq}) + k_2 t \quad (4.10)$$

or equivalently for linear form

$$(t/q_t) = (1/k_2 q_{eq}^2) + (1/q_{eq}) t \quad (4.11)$$

a plot of t/q_t versus t should give a linear relationship for the applicability of the second-order kinetics. The rate constant (k_2) and adsorption at equilibrium (q_{eq}) can be obtained from the intercept and slope, respectively. A comparison of the experimental adsorption capacity and the theoretical values are presented in Table 4.2. The theoretical q_e value estimated from pseudo-first and second order kinetic models were very close to the experimental values and the correlation coefficients were high. Results indicate that this metal-chelated adsorbent system was described both by the first and second order kinetic models.

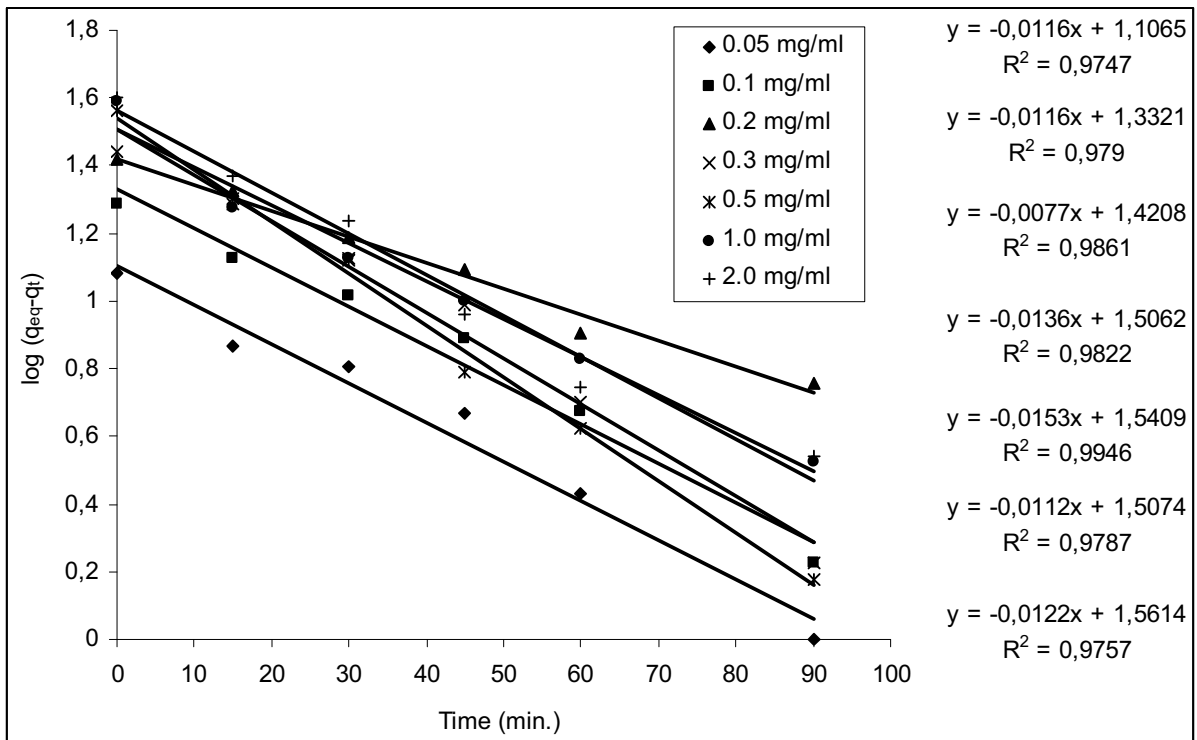


Figure 4.15. First order kinetics of cytochrome c adsorption onto m-PHEMA/PEI/Cu²⁺ beads.

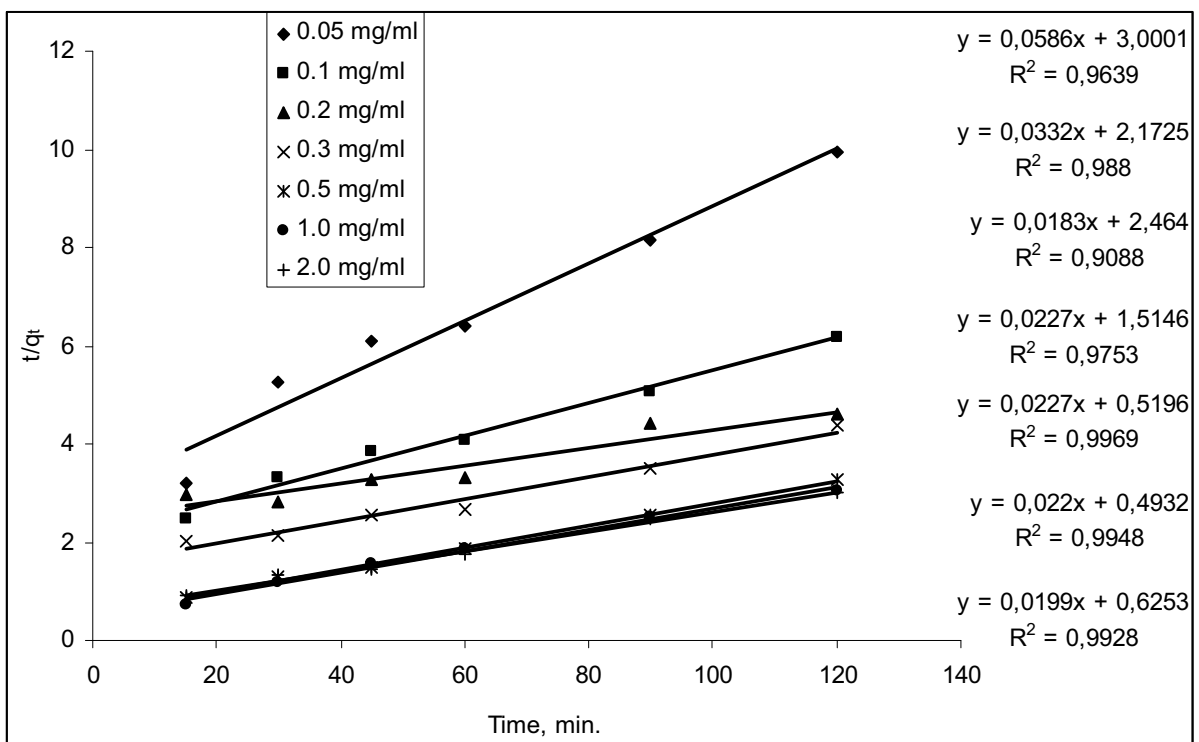


Figure 4.16. Second order kinetics of cytochrome c adsorption onto m-PHEMA/PEI/Cu²⁺ beads.

Table 4.2. First and second order kinetic constants.

Initial cytochrome-c concentration (mg mL ⁻¹)	Experimental $q_{eq\ ex}$ (mg g ⁻¹)	First-order kinetic			Second-order kinetic		
		k_1 (min ⁻¹)	q_{eq} (mg g ⁻¹)	R^2	k_2 (x10 ⁻⁴ g mg ⁻¹ min ⁻¹)	q_{eq} (mg g ⁻¹)	R^2
0.05	12.05	0.0267	12.78	0.9747	11.45	17.06	0.9639
0.1	19.42	0.0267	21.48	0.9790	5.07	30.12	0.9880
0.2	26.11	0.0177	26.35	0.9861	1.36	54.64	0.9088
0.3	27.45	0.0313	32.08	0.9822	3.40	44.05	0.9753
0.5	36.66	0.0352	34.75	0.9946	9.92	44.05	0.9969
1.0	39.17	0.0258	32.17	0.9787	9.82	45.45	0.9948
2.0	39.89	0.0281	36.42	0.9757	6.33	50.25	0.9928

4.2.5. Effect of Temperature

The effect of temperature on cytochrome c adsorption was studied in the range of 4-37°C. At all temperatures, adsorption of cytochrome c on the m-PHEMA/PEI was lower than the Cu²⁺-chelated m-PHEMA/PEI beads. No significant effect of the temperature was observed on the physical adsorption of the cytochrome c onto the m-PHEMA. However, the equilibrium adsorption of cytochrome c onto the m-PHEMA/PEI and m-PHEMA/PEI/Cu²⁺ significantly decreased with increasing temperature and the maximum adsorption was achieved at 4°C (Figure 4.17). From 4°C to 37°C, the adsorption capacity of the magnetic beads decreased for about 35% for m-PHEMA/PEI/Cu²⁺ beads. A possible explanation for this behavior is the exothermic nature of the adsorption process.

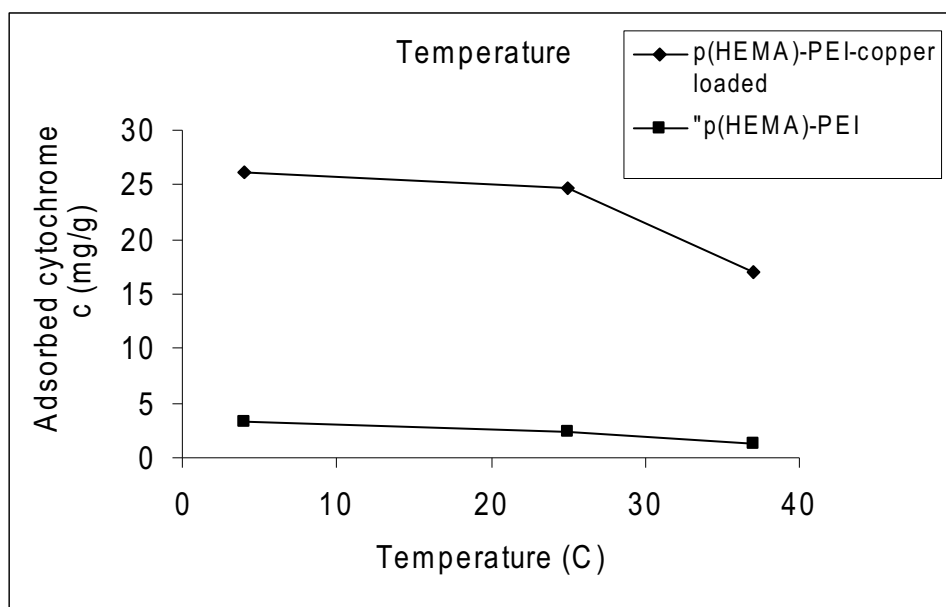


Figure 4.17. Effect of temperature on cytochrome c adsorption. pH:11.0
 Carbonate buffer; V: 10 ml; m_{polymer} : 30 mg; $C_{\text{cytochrome c}}$: 0.2 mg/ml; Cu^{2+} loading:
 302 $\mu\text{mol/g}$ polymer

4.2.6. Effect of Salt Concentration

The effect of NaCl concentration on the cytochrome c adsorption is shown in Figure 4.18. The adsorption capacity of Cu^{2+} chelated m-PHEMA/PEI beads slightly increased with increasing NaCl concentration from 0 to 0.05 and then decreased with increasing NaCl concentration of the binding buffer. The adsorption of cytochrome c decreases by about 47% as the NaCl concentration changes from 0.05 to 0.1 M. The decrease in the adsorption capacity as the NaCl concentration increases can be attributed to the repulsive electrostatic interactions between the Cu^{2+} -chelated m-PHEMA/PEI beads and protein molecules.

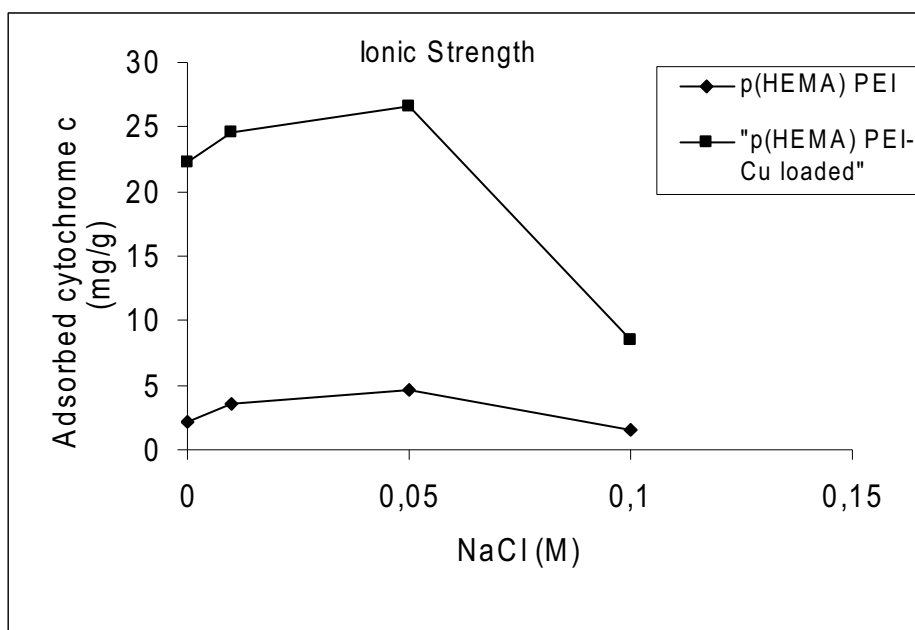


Figure 4.18. Effect of temperature on cytochrome c adsorption. pH:11.0
 Carbonate buffer; V: 10 ml; m_{polymer} : 30 mg; $C_{\text{cytochrome c}}$: 0.2 mg/ml; T: 25 ° C;
 Cu^{2+} loading: 302 $\mu\text{mol/g}$ polymer

4.2.7. Effect of Cu^{2+} Loading

Figure 4.19 shows the effects of the amount of Cu^{2+} incorporated on the m-PHEMA/PEI beads on cytochrome c adsorption. Theoretically one expects that three active imine groups on PEI graft coordinated at least one copper ions, giving different geometrical structures such as planar, tetrahedral, or octahedral arrangements around the metal ion (coordination number of copper ion is four). Other free coordination valences of the copper ions are occupied by water molecules. As expected, adsorption increased with Cu^{2+} loading and then reached a saturation value. This is due to the preferential interaction between cytochrome c molecules (especially imidazole side chains of histidine residue in cytochrome c structure) and chelated Cu^{2+} ions. Above the 320 $\mu\text{mol/g}$ Cu^{2+} loading, this effect becomes less pronounced because of the molecular size of cytochrome c occupies certain area on the polymer surface.

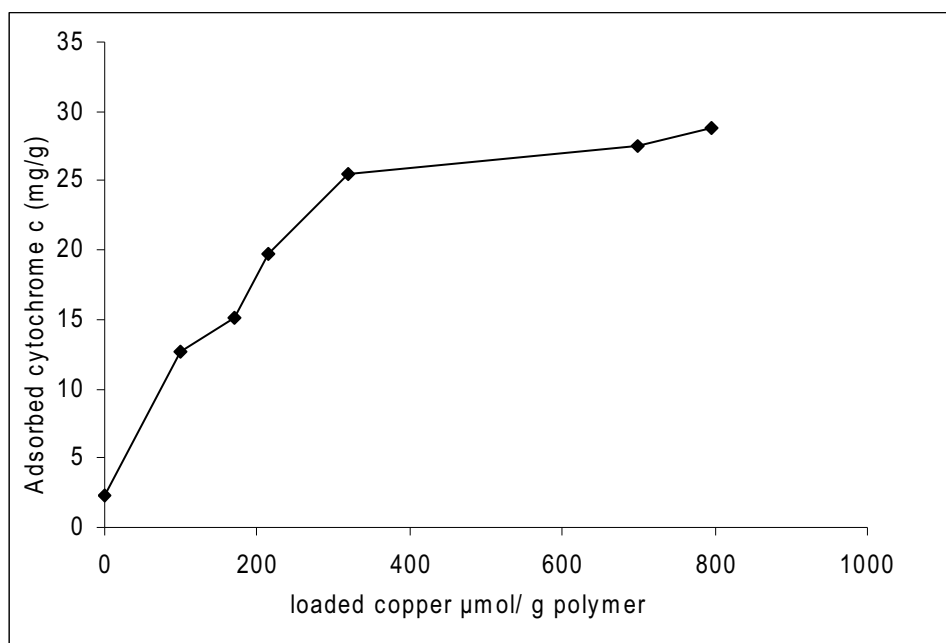


Figure 4.19. Effect of Cu^{2+} loading onto cytochrome c adsorption. pH:11.0 Carbonate buffer; V: 10 ml; m_{polymer} : 30 mg; $C_{\text{cytochrome c}}$: 0.2 mg/ml; T: 25 ° C

4.2.8. Cytochrome C adsorption in continuous MSFB system

Optimum conditions for the adsorption of cytochrome c molecules onto the Cu^{2+} chelated m-PHEMA/PEI beads were determined in the batch experiments which their results were given above (i.e. pH, buffer type, initial concentration, temperature and ionic strength). MSFB experiments were performed at these conditions. The adsorption capacity at different flow-rates at MSFB was investigated and the results are as shown in Figure 4.20. The adsorption capacity decreased significantly from 26.78 mg/g to 5.36 mg/g polymer with the increase of the flow-rate from 0.5 ml/min to 4.0 ml/min. One of the explanations for such phenomenon would be a faster ligand-adsorbate dissociation rate compared to the association rate. Hence, the adsorbate (i.e. cytochrome c molecules) would pass through the magnetically stabilized column without adsorption at high flow-rate. Second explanation could be that the increased nonideal flow hydrodynamics of liquid phase and the solid phase for magnetically stabilized fluidized bed. These phenomena can be summarized by the increase of the axial dispersion coefficient in the axial dispersion model.

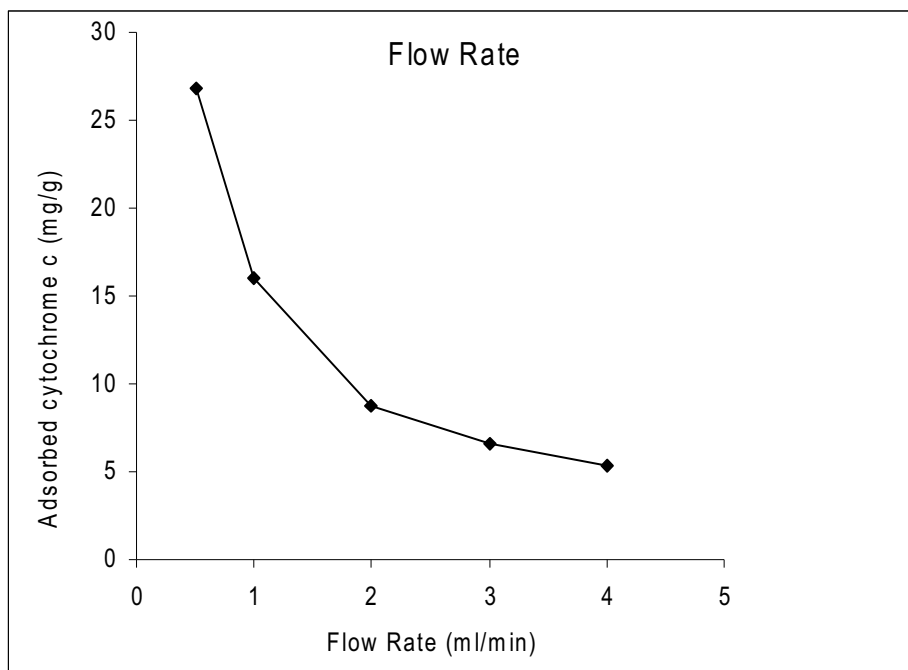


Figure 4.20. Effect of flow rate on cytochrome c adsorption. pH:11.0 Carbonate buffer; V: 40 ml; m_{polymer} : 30 mg; $C_{\text{cytochrome c}}$: 0.2 mg/ml; T: 25 ° C; Cu^{2+} loading: 302 $\mu\text{mol/g}$ polymer

4.3. Comparison with Related Literature

Our results were compared with the results obtained with commercial materials used in immobilized metal affinity column chromatography and other adsorbents in literature for cytochrome c adsorption. O'Brien et al reported 170 mg Cytochrome c/g polymer maximum adsorption capacity with micron sized non-porous superparamagnetic aminoalkyltrimethoxysilane treated chelator supports carrying iminodiacetic acid/ Cu^{2+} [238]. Abudiab and Beitle used magnetic agarose as the carrier matrix, and immobilized iminodiacetic acid/ Cu^{2+} as a metal-chelate bioligand. They reported Cytochrome c adsorption capacities around 6 mg/g [226]. O'Brien et al used polyglutaraldehyde coated BioMag[®] superparamagnetic iron oxide particles carrying Cu^{2+} and they obtained 8.4 mg per gram polymer for Cytochrome c [238]. Serafica et al used different supports including commercial chelating sepharose 6B metal-chelate affinity matrix and chemically modified glass carrying IDA [239]. They presented adsorption capacities in the range of 2-38.2 mg Cytochrome c/g polymer for IDA/ Cu^{2+} modified glass adsorbents. They achieved 48 mg/g maximum adsorption capacity for commercial chelating sepharose 6B. Zeng and Ruckenstein used cross-linked macroporous chitosan

anion exchange membranes with controlled pore sizes and good mechanical properties [240]. Their Cytochrome c adsorption value was 15.5 mg per milliliter sorbent. Lewus and Carta used polyacrylamide functionalized highly porous polystyrene coated silica cation-exchange material and they achieved maximum adsorption capacity up to 105 mg bovine heart cytochrome c per gram polymer [241]. Todd et al studied cytochrome c adsorption on TSK Guardgel Chelate-5PW macroporous beads and they reported the adsorption capacities in the range of 3.4-12.3 mg/ml gel [242]. Emir et al used Cu^{2+} chelated poly(2-hydroxyethyl methacrylate-N-methacryloyl-(L)-histidine methyl ester) beads [243] for cytochrome c. The maximum cytochrome c adsorption capacity was found to be 31.7 mg/g. The Cytochrome c adsorption capacity obtained in this study (up to 39.8 mg/g) would seem to be sufficient to propose the m-PHEMA/PEI metal-chelated affinity beads as IMAC supports.

4.4. Regeneration of the Beads

In the last step of the affinity separation, the main concern was to desorb the adsorbed protein in the shortest time and at the highest amount possible. It was thus necessary to evaluate the regeneration efficiency of the affinity adsorbents after each cycle. In this study, more than 95% of the adsorbed cytochrome c molecules was removed easily from the chelating beads during the 30 min in all cases when NaCl was used as desorption agent. With the desorption data given above, we concluded that NaCl is a suitable desorption agent for the Cu^{2+} -chelated beads. In order to show the reusability of the Cu^{2+} -chelated m-PHEMA/PEI beads, the adsorption-desorption cycle was repeated ten times using the same modified beads from aqueous cytochrome c solution (Figure 4.21). There was no significant loss in the adsorption capacity of the beads. After 10 cycles, the capacity had decreased by ca. 10%. Moreover, no obvious changes of the morphology of the magnetic beads were found in the recycling process when examined visually. These results demonstrated the stability of the present solid support as a metal-chelate affinity adsorbent.

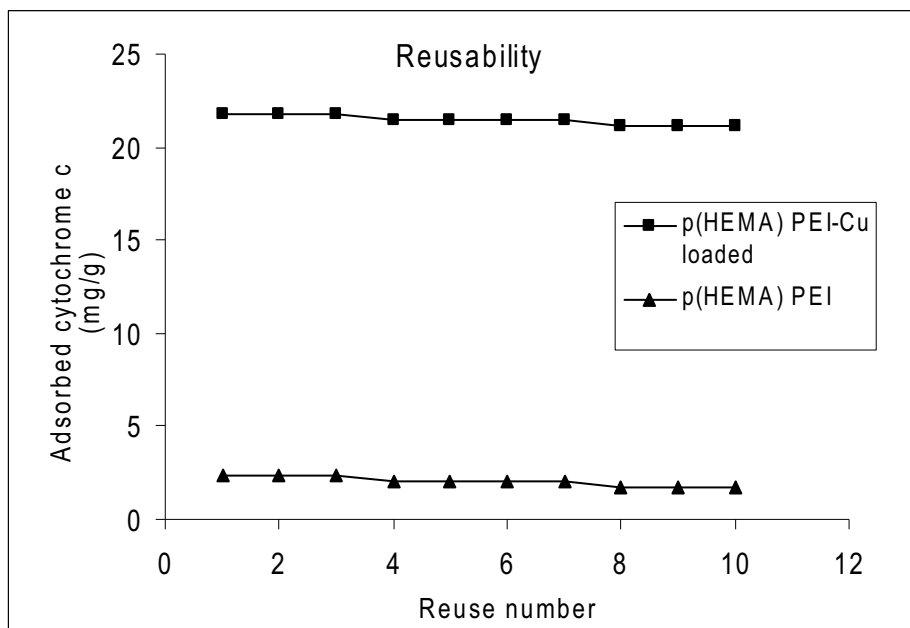


Figure 4.21. Reusability of m-PHEMA/PEI/Cu²⁺ beads. pH:11.0 Carbonate buffer; V: 10 ml; m_{polymer}: 30 mg; m_{cytochrome c}: 0.2 mg/ml; T: 25 ° C; Cu²⁺ loading: 302 μmol/ g polymer

5. CONCLUSION

- Magnetic poly(hydroxyethyl methacrylate) beads(m-PHEMA) were prepared by suspension polymerization of HEMA and EGDMA. The poly(ethylene imine)(PEI) molecules were immobilized on the m-PHEMA beads surface via reaction between hydroxyl groups of the beads and amino groups of the PEI. The maximum amount of PEI immobilized onto the m-PHEMA bead surface was found to be 102 mg PEI/g polymer from the titration.
- The equilibrium swelling ratio of the m-PHEMA/PEI beads is 45 %. Compared with m-PHEMA (37.5 %), the water uptake ratio of the m-PHEMA/PEI beads was increased.
- The radicalic suspension polymerization procedure provided crosslinked m-PHEMA beads in a spherical form mostly in the size range of 100-140 μm in diameter.
- According to mercury porosimetry data, the average pore size of the magnetic beads was 819 nm. The specific surface area of the mPHEMA/PEI beads was found to be 50 m^2/g .
- The magnetic beads have a spherical form and rough surface due to the pores which formed during the polymerization procedure. The presence of pores within the bead surface is clearly seen in SEM photographs. It can be concluded that the m-PHEMA/PEI beads have a porous interior surrounded by a reasonably rough surface, in the dry state.
- The amount of chelated Cu^{2+} on m-PHEMA/PEI beads was measured with atomic absorption spectrometer and it found to be 0-795 $\mu\text{mol/g}$ polymer. From the mass-stoichiometry, it seems that 3 incorporated PEI molecule interact around one Cu^{2+} ions (2318.2 $\mu\text{mol/g}$ PEI/g polymer: 795 μmol Cu^{2+}/g polymer)
- Studies aimed at detecting leakage of Cu^{2+} from the m-PHEMA/PEI beads revealed no leakage in any of the adsorption and desorption media, and implied that the washing procedure was satisfactory for the removal of the non-specific chelated Cu^{2+} ions from the magnetic beads.
- m-PHEMA/PEI beads have a relative intensity of 125. This value shows that polymeric structure has a local magnetic field because of magnetite in its

structure. The g factors were found to be 1.58 for m-PHEMA/PEI and 1.98 for m-PHEMA/PEI/Cu²⁺ structures

- In EMU spectrum and from H_r value, 2400 Gauss magnetic field was found sufficient to excite all of the dipole moments present in 1.0 g m-PHEMA/PEI sample.
- The amount of cytochrome c adsorbed gradually increased with increasing pH and showed a maximum at pH 11.0, (isoelectric point of cytochrome c: 10.6).
- Organic buffers are shown to be less effective than inorganic buffers. In MES buffer almost no adsorption was observed. In MOPS and tris-HCl buffer systems adsorption of cytochrome c was also observed above neutral pH. Cytochrome c adsorption capacities on Cu²⁺-chelated beads were found to be 16.3 mg/g for tris-HCl, 0.2 mg/g for MES, 11.7 mg/g for MOPS and 22.7 mg/g for carbonate buffer under the same conditions.
- Relatively faster adsorption rates were observed at the beginning of adsorption process, and then adsorption equilibrium were achieved gradually in about 120 min.
- The adsorption values increased with increasing concentration of cytochrome c, and a saturation value is achieved at cytochrome c concentration of 0.5 mg/ml, which represents saturation of the active binding sites on the affinity beads.
- Cytochrome c molecules adsorbed on the m-PHEMA/PEI beads was about 4.6 mg/g. Cu²⁺-chelation significantly increased the cytochrome c adsorption of the beads up to 39.8 mg/g. It is clear that this increase is due to specific interactions between chelated Cu²⁺ ions and cytochrome c molecules.
- The isotherms of cytochrome c were found to be linear over the whole concentration range studies and the correlation coefficients were high.
- The theoretical q_e value estimated from pseudo-first and second order kinetic models were very close to the experimental values and the correlation coefficients were high. Results indicate that this metal-chelated adsorbent system was described both by the first and second order kinetic models.

- No significant effect of the temperature was observed on the physical adsorption of the cytochrome c onto the m-PHEMA. However, the equilibrium adsorption of cytochrome c onto the m-PHEMA/PEI and m-PHEMA/PEI/Cu²⁺ significantly decreased with increasing temperature and the maximum adsorption was achieved at 4°C.
- The adsorption capacity of Cu²⁺ chelated m-PHEMA/PEI beads slightly increased with increasing NaCl concentration from 0 to 0.05 and then decreased with increasing NaCl concentration of the binding buffer. The adsorption of cytochrome c decreases by about 47% as the NaCl concentration changes from 0.05 to 0.1 M.
- Cytochrome c adsorption increased with Cu²⁺ loading and then reached a saturation value. This is due to the preferential interaction between cytochrome c molecules (especially imidazole side chains of histidine residue in cytochrome c structure) and chelated Cu²⁺ ions. Above the 320 µmol/g Cu²⁺ loading, this effect becomes less pronounced because of the molecular size of cytochrome c occupies certain area on the polymer surface.
- The adsorption capacity at different flow-rates at MSFB was investigated. The adsorption capacity decreased significantly from 26.78 mg/g to 5.36 mg/g polymer with the increase of the flow-rate from 0.5 ml/min to 4.0 ml/min. One of the explanations for such phenomenon would be a faster ligand-adsorbate dissociation rate compared to the association rate.
- In this study, more than 95% of the adsorbed cytochrome c molecules was removed easily from the chelating beads during the 30 min in all cases when NaCl was used as desorption agent. With the desorption data given above, we concluded that NaCl is a suitable desorption agent for the Cu²⁺-chelated beads.

REFERENCES

- [1] Gupta, M. N.; Jain, S.; Roy., *Biotechnol. Prog.* 2002, 18, 78-81.
- [2] Hochuli, E.; Do'beli, H.; Schacher, J. *Chromatogr.* 1987, 411, 174-184.
- [3] Kronina, V. V.; Wirth, H. J.; Hearn, M. T. W., *J. Chromatogr. A* 1999, 852, 261-272.
- [4] Hansen, P.; Lindeberg, G., *J. Chromatogr. A* 1995, 690, 155-159.
- [5] Denizli, A.; Salih, B.; Piskin, E., *J. Chromatogr. A* 1996, 731, 57-63.
- [6] Tishchenko, G.; Dybal, J.; Meszarova, K.; Sedlakova, Z.; Bleha, M. J., *Chromatogr. A* 2002, 954, 115-126.
- [7] Arica, M. Y.; Testereci, H.; Denizli, A., *J. Chromatogr. A* 1998, 799, 83-91.
- [8] Denizli, F.; Denizli, A.; Arica, M. Y., *Polym. Int.* 1999, 48, 360-366.
- [9] Hemdan, E. S.; Zhao, Y. J.; Sulkowski, E.; Porath., *Proc. Natl. Acad. Sci. U.S.A.* 1989, 86, 1811-1815.
- [10] Porath, J., *Protein Expression Purif.* 1992, 3, 263-281.
- [11] Reif, O. W.; Nier, V.; Bahr, U.; Freitag, R., *J. Chromatogr. A* 1994, 664, 13-25.
- [12] Denizli, A.; Yavuz, H.; Garipcan, B.; Arica, M. Y., *J. Appl. Polym. Sci.* 2000, 76, 115-124.
- [13] Gaberc-Porekar, V., Menart, V., *J. Biochem. Biophys. Methods* 2001, 49, 335-360.
- [14] Chaga, G. S., *J. Biochem. Biophys. Methods* 2001, 49, 313-334.
- [15] Denizli, A.; Denizli, F.; Piskin, E., *J. Biomater. Sci., Polym. Ed.* 1999, 10, 305-318.
- [16] Wu, C. Y.; Suen, S. Y.; Chen, S. C.; Tzeng, J. H. 2003.
- [17] Yip, T. T.; Hutchens, T. W., *Mol. Biotechnol.* 1994, 1, 151-164.
- [18] Teramoto, M., Nishibue, H., Okuhara, K., Ogawa, H., Kozono, H., Matsuyama, H., *Applied Microbiology and Biotechnology* 1992, 38 (2) , 203-208.
- [19] Xue B, Sun Y., *J Chromatogr A* 2001, 921:109-119.
- [20] Burns MA, Kvesitadze GI, Graves DJ., *Biotechnol Bioeng* 1985, 27:137-145.
- [21] Bilkova Z, Slovakova M, Lycka A, Horak D, Lenfeld J, Turkova J, Churacek J., *J Chromatogr B* 2002, 770:25-34.
- [22] O'Brien SM, Thomas ORT, Dunnill P., *J Biotechnol* 1996, 50:13-25.
- [23] Rad AY, Yavuz H, Denizli A., *Macromol Biosci* 2003, 3:471-476.
- [24] Martin C, Cuellar J., *Ind Eng Chem Res* 2004, 43:475-485.
- [25] Tong XD, Xue B, Sun Y., *Biotechnol Prog* 2001, 17:134-139.
- [26] Cocker TM, Fee CJ, Evans RA., *Biotechnol Bioeng* 1997, 53:79-87.
- [27] Chetty AS, Gabis DH, Burns MA., *Powder Technol* 1991, 64:165-174.
- [28] Arica Y, Yavuz H, Patir S, Denizli A., *J Mol Catal B* 2000, 11:127-138.
- [29] Akgöl S, Denizli A., *J Mol Catal B* 2004, 28:7-14.
- [30] Scopes R.K., 1982, *Protein Purification; Principles and Practise*, New York: Springer Verlag.

- [31] Wilchek, M., Miron, T., Kohn, J., 1984, *Methods in Enzymol.*, 104, W.B.Jacoby, Ed., Academic Press, New York, USA, 3.
- [32] Scouten, W.H., Affinity chromatography; bioselective adsorption an inert matrices. *Chemical Analysis Series*, vol.9. Canada; Wiley; 1981, 7-9
- [33] Jonson, J.C., Ryden, L., 1998, *Protein Purification*, John Wiley & Sons, 2nd Edi., New York, USA, 375-442.
- [34] Porath, J., Sundberg, L., Fornstedt, N., Olson, I., 1973, *Nature*, 245, 465.
- [35] Wilchek, M., Miron, T., 1999, *React. and Func. Polymers*, 41, 263-268.
- [36] Keller, G. E., *AIChE Monogr. Ser.*, 1983, 17, 83, 3-4.
- [37] Jones, D. T., *Process, Biochem.*, 1974, 9, 12, 17-19.
- [38] Mc Naughton, G. S., Robins, J. C., Zwaaneveld, C. H., *Sep. Purif. Methods*, 1978, 7, 1, 31-54.
- [39] Pungor, E., Jr, Afeyan, N. B., Gordon, N. F., Cooney, C. L., *Biotechnology*, 1987, 5, 604-607.
- [40] Sussman, M. V., *Chem. Tech.*, April, 1976, 260-264.
- [41] Broughton, D. B., Gembicki, S. A., *AIChE Symp. Ser.*, 1984, 80, 233, 62-67.
- [42] Burns, M. A., Graves, D. J., *Reactive Polym.*, 1987, 6, 45-60.
- [43] Chetty, A. S., Gabis, D. H., Burns, M. A., *Powder Technol.*, 1991, 64, 1-2.
- [44] Lee, W. K., *AIChE Symp. Ser.*, 1983, 222, 79, 87-96.
- [45] Rosenweig, R. E., *Science*, 1979, 204, 57-60.
- [46] Rosenweig, R. E., *Ind. Eng. Chem. Fundam.*, 1979, 18, 260-269.
- [47] Rosenweig, R. E., Siegel, J. H., Lee, W. K., Mikus, T., *AIChE Symp. Ser.*, 1981, 77, 205, 8-16.
- [48] Siegel, J. H., *Ind. Eng. Chem. Process. Des. Dev.*, 1982, 21, 135-141.
- [49] Siegel, J. H., *Powder Technol.*, 1988, 52, 139-148.
- [50] J. Porath, J. Carlsson, I. Olsson and G. Belfrage *Nature* 258 (1975), p. 598.
- [51] F. Hellferich *Nature* 189 (1961), p. 1001.
- [52] L. Kågedal In: J.-C. Janson and L. Rydén, Editors, *Protein Purification: Principles, High-Resolution Methods, and Applications* (2nd ed ed.), Wiley-VCH, New York (1998), p. 311 Chapter 8 .
- [53] B. Nilsson, G. Forsberg, T. Moks, M. Hartmanis and M. Uhlén *Curr. Opin. Struct. Biol.* 2 (1992), p. 569.
- [54] A. Seidler *Protein Eng.* 7 (1994), p. 1277.
- [55] T. Hopp, K.S. Pricket, V.L. Price, R.T. Libby, C.J. March, D.P. Cerretti, D.L. Urdal and P.J. Conlon *Biotechnology* 6 (1988), p. 1204.
- [56] J.-S. Kim and R.T. Raines *Protein Sci.* 2 (1993), p. 348.
- [57] T.G. Schmidt and A. Skerra *Protein Eng.* 6 (1993), p. 109.

- [58] D.B. Smith and K.S. Johnson *Gene* 67 (1988), p. 31.
- [59] C. Lauritzen, E. Tüchsen, P.E. Hansen and O. Skovgaard *Protein Expr. Purif.* 2 (1991), p. 372.
- [60] E.R. LaVallie, E.A. DiBlasio, S. Kovacic, K.L. Grant, P.F. Schendel and J.M. McCoy *Biotechnology* 11 (1993), p. 187.
- [61] E. Hochuli, H. Döbeli and A. Schacher *J. Chromatogr.* 411 (1987), p. 177.
- [62] R.C. Hockney *Trends Biotechnol.* 12 (1994), p. 456.
- [63] E. Flaschel and K. Friehs *Biotechnol. Adv.* 11 (1993), p. 31.
- [64] E. Hochuli *Genet. Eng. (NY)* 12 (1990), p. 87.
- [65] D.B. Evans, A.F. Vosters, J.B. Carter and S.K. Sharma *J. Immunol. Methods* 156 (1992), p. 231.
- [66] Wulfing, J. Lombardero and A. Plückthun *J. Biol. Chem.* 269 (1994), p. 2895
- [67] T.W. Hutchens, R.W. Nelson, C.M. Li and T.T. Yip *J. Chromatogr.* 604 (1992), p. 125.
- [68] T.W. Hutchens and T.T. Yip *J. Chromatogr.* 604 (1992), p. 133.
- [69] R.R. Begum, R.J. Newbold and D. Whitford *J. Chromatogr. B* 737 (2000), p. 119.
- [70] T. Oswald, W. Wende, A. Pingound and U. Rinas *Appl. Microbiol. Biotechnol.* 42 (1994), p. 73.
- [71] M.M. Enzelberger, S. Minning and R.D. Schmid *J. Chromatogr. A* 898 (2000), p. 83.
- [72] G. Chaga, M. Widersten, L. Andersson, J. Porath, U.H. Danielson and B. Mannervik *Protein Eng.* 7 (1994), p. 1115.
- [73] H. Chaouk and M.T. Hearn *J. Biochem. Biophys. Methods* 39 (1999), p. 161.
- [74] L. Drake and T. Barnett *Biotechniques* 12 (1992), p. 645.
- [75] S. Sharma and G.P. Agarwal *Anal. Biochem.* 288 (2001), p. 126.
- [76] C. Fiore, V. Trezeguet, P. Roux, A. Lê Saux, F. Noel, C. Schwimmer, D. Arlot, A.C. Dianoux, G.J. Lauquin and G. Brandolin *Protein Expr. Purif.* 19 (2000), p. 57.
- [77] J. Wu and M. Filutowicz *Acta Biochim. Pol.* 46 (1999), p. 591.
- [78] J.C. Dalton, D.F. Bruley, K.A. Kang and W.N. Drohan *Adv. Exp. Med. Biol.* 411 (1997), p. 419.
- [79] W. He, D.F. Bruley and W.N. Drohan *Adv. Exp. Med. Biol.* 454 (1998), p. 689.
- [80] N.T. Mrabet *Biochemistry* 31 (1992), p. 2690.
- [81] H. Yeomans-Reina, A. Ruiz-Manriquez, B.R. Wong and A.T. Mansir *Biotechnol. Prog.* 17 (2001), p. 729.
- [82] F.H. Arnold *Biotechnology* 9 (1991), p. 151.
- [83] J. Porath *Trends Anal. Chem.* 7 (1988), p. 254.
- [84] T.T. Yip and T.W. Hutchens *Mol. Biotechnol.* 1 (1994), p. 151.
- [85] S.A. Lopatin and V.P. Varlamov *Prikl. Biokhim. Mikrobiol.* 31 (1995), p. 259.
- [86] J. Zouhar *Chem. Listy* 93 (1999), p. 683.

- [87] J.W. Wong, R.L. Albright and N.-H. Wang *Sep. Purif. Methods* 20 (1991), p. 49.
- [88] V. Gaberc-Porekar and V. Menart *J. Biochem. Biophys. Methods* 49 (2001), p. 335.
- [89] G.S. Chaga *J. Biochem. Biophys. Methods* 49 (2001), p. 313.
- [90] N.T. Mrabet and M.A. Vijayalakshmi In: M.A. Vijayalakshmi, Editor, *Biochromatography*, Taylor and Francis, London (2002), p. 272.
- [91] Z. Zhang, K.-T. Tong, M. Belew, T. Pettersson and J.-C. Janson *J. Chromatogr.* 604 (1992), p. 143.
- [92] D. Sinha, M. Bakhshi and R. Vora *Biotechniques* 17 (1994), p. 509.
- [93] L. Nieba, S.E. Nieba-Axmann, A. Persson, M. Hämäläinen, F. Edebratt, A. Hansson, J. Lidholm, K. Magnusson, Å.F. Karlsson and A. Plückthun *Anal. Biochem.* 252 (1997), p. 217.
- [94] L. Schmitt, M. Ludwig, H.E. Gaub and R. Tampé *Biophys. J.* 78 (2000), p. 3275.
- [95] C. Min and G.L. Verdine *Nucleic Acids Res.* 24 (1996), p. 3806.
- [96] P.L. Roberts, C.P. Walker and P.A. Feldman *Vox Sang.* 67 Suppl. 1 (1994), p. 69.
- [97] K.L. Franken, H.S. Hiemstra, K.E. van Meijgaarden, Y. Subronto, J. den Hartigh, T.H. Ottenhoff and J.W. Drijfhout *Protein Expr. Purif.* 18 (2000), p. 95.
- [98] R.G. Pearson *J. Chem. Educ.* 45 (1968), p. 581.
- [99] T.-T. Yip, Y. Nakagawa and J. Porath *Anal. Biochem.* 183 (1989), p. 159.
- [100] G. Chaga, L. Andersson, B. Ersson and J. Porath *Biotechnol. Appl. Biochem.* 11 (1989), p. 424.
- [101] E.S. Hemdan, Y.J. Zhao, E. Sulkowski and J. Porath *Proc. Natl. Acad. Sci. USA* 86 (1989), p. 1811.
- [102] R.J. Todd, M.E. Van Dam, D. Casimiro, B.L. Haymore and F.H. Arnold *Proteins* 10 (1991), p. 156.
- [103] S.-S. Suh, B.L. Haymore and F.H. Arnold *Protein Eng.* 4 (1991), p. 301.
- [104] E. Leporati *J. Chem. Soc. Dalton Trans.* (1986), p. 199.
- [105] E.S. Hemdan and J. Porath *J. Chromatogr.* 323 (1985), p. 247.
- [106] Z. El Rassi and C. Horvath *J. Chromatogr.* 359 (1986), p. 241.
- [107] M. Sawadogo and M.W. Van Dyke *Genet. Eng.* 17 (1995), p. 53.
- [108] P. Hansen, L. Andersson and G. Lindeberg *J. Chromatogr. A* 723 (1996), p. 51.
- [109] P. Hansen and G. Lindeberg *J. Chromatogr. A* 690 (1995), p. 155.
- [110] D.R. Williams *The Metals of Life: The Solution Chemistry of Metal Ions in Biological Systems*, Van Nostrand Reinhold, London (1971).
- [111] M. Zachariou and M.T. Hearn *J. Protein Chem.* 14 (1995), p. 419.
- [112] M. DiDonato, S. Narindrasorasak, J.R. Forbes, D.W. Cox and B. Sarkar *J. Biol. Chem.* 272 (1997), p. 33279.

- [113] P.E. Dykema, P.R. Sipes, A. Marie, B.J. Biermann, D. N Crowell and S.K. Randall *Plant Mol. Biol.* 41 (1999), p. 139.
- [114] J.M. Berg and Y. Shi *Science* 271 (1996), p. 1081.
- [115] S. Kinet, S. Bernichtein, P.A. Kelly, J.A. Martial and V. Goffin *J. Biol. Chem.* 274 (1999), p. 26033.
- [116] M.Y. Lorensen, T. Patel, J.-W. Liu and A.M. Walker *Endocrinology* 137 (1996), p. 809.
- [117] H.B. Lowman, B.C. Cunningham and J.A. wells *J. Biol. Chem.* 266 (1991), p. 10982.
- [118] E.A. Permyakov, D.B. Veprintsev, G.Y. Deikus, S.E. Permyakov, L.P. Kalinichenko, V.M. Grishchenko and C.L. Brooks *FEBS Lett.* 405 (1997), p. 273.
- [119] Z. Sun, M.S. Lee, H.K. Rhee, J.M. Arrandale and P.S. Dannies *Mol. Endocrinol.* 11 (1997), p. 1544.
- [120] B.C. Cunningham, M.G. Mulkerrin and J.A. Wells *Science* 253 (1991), p. 545.
- [121] B.C. Cunningham, D.J. Henner and J.A. Wells *Science* 247 (1990), p. 1461.
- [122] B.C. Cunningham, S. Bass, G. Fuh and J.A. Wells *Science* 250 (1990), p. 1709.
- [123] J. Porath *Protein Expr. Purif* 3 (1992), p. 263.
- [124] G.E. Lindgren *Am. Biotechnol. Lab.* 12 (1994), p. 36.
- [125] E. Hochuli, W. Bannwarth, H. Dobeli, R. Gentz and D. Stuber *Biotechnology* (1988), p. 1321.
- [126] M. Zaveckas, B. Baskeviciute, V. Luksa, G. Zvirblis, V. Chmieliauskaite, V. Bumelis and H. Pesliakas *J. Chromatogr. A* 904 (2000), p. 145.
- [127] M. Zachariou and M.T. Hearn *J. Chromatogr. A* 890 (2000), p. 95.
- [128] R.V. Lehr, L.C. Elefante, K.K. Kikly, S.P. O'Brien and R.B. Kirkpatrick *Protein Expr. Purif.* 19 (2000), p. 362.
- [129] D. Leibler, A. Rabinkov and M. Wilchek *J. Mol. Recogn.* 9 (1996), p. 375.
- [130] C. Mateo, G. Fernandez-Lorente, B.C. Pessela, A. Vian, A.V. Carrascosa, J.L. Garcia, R. Fernandez-Lafuente and J.M. Guisan *J. Chromatogr. A* 915 (2001), p. 97.
- [131] Q. Zeng, J. Xu, R. Fu and Q. Ye *J. Chromatogr. A* 921 (2001), p. 197.
- [132] R.J. Todd, R.D. Johnson and F.H. Arnold *J. Chromatogr. A* 662 (1994), p. 13.
- [133] M. Belew and J. Porath *J. Chromatogr.* 516 (1990), p. 333.
- [134] F. Maisano, S.A. Testori and G. Grandi *J. Chromatogr.* 472 (1989), p. 422.
- [135] E. Sulkowski *J. Mol. Recogn.* 9 (1996), p. 389.
- [136] E. Sulkowski *J. Mol. Recogn.* 9 (1996), p. 498.
- [137] J. Porath *Trends Anal. Chem.* 7 (1992), p. 254.
- [138] K.D. Bush and J.A. Lumpkin *Biotechnol. Prog.* 14 (1998), p. 943.
- [139] E. Sulkowski *Bioessays* 10 (1989), p. 170.
- [140] D. Beyersmann *Toxicol. Lett.* 127 (2002), p. 63.

- [141] G. Muszynska, Y.-J. Zhao and J. Porta *J. Immunoreact. Biochem.* 26 (1986), p. 127.
- [142] J.R. Requena, D. Groth, G. Legname, E.R. Stadtman, S.B. Prusiner and R.L. Levine *Proc. Natl. Acad. Sci. USA* 98 (2001), p. 7170.
- [143] W. Wang *Int. J. Pharm.* 185 (1999), p. 129.
- [144] H.R. Constantino, R. Langer and A.M. Klibanov *Pharm. Res.* 11 (1994), p. 21.
- [145] B. Chen, H.R. Constantino, J. Liu, C.C. Hsu and S.J. Shire *J. Pharm. Sci.* 88 (1999), p. 477.
- [146] M.S. Kamat, G.L. Tolman and J.M. Brown *Pharm. Biotechnol.* 9 (1996), p. 343.
- [147] T. Oswald, G. Hornbostel, U. Rinas and F.B. Anspach *Biotechnol. Appl. Biochem.* 25 (1997), p. 109.
- [148] J. Xiao, C.E. Kibbey, D.E. Coutant, G.B. Martin and M.E. Meyerhoff *J. Liq. Chromatogr.* 19 (1996), p. 2901.
- [149] I.M. Rosenberg *Protein Analysis and Purification: Benchtop Techniques*, Birkhäuser, Boston (1996) Chapter 10, p. 345 .
- [150] G. Chaga, J. Hopp and P. Nelson *Biotechnol. Appl. Biochem.* 29 (1999), p. 19.
- [151] J. Pedersen, C. Lauritzen, M.T. Madsen and S. Weis Dahl *Protein Expr. Purif.* 15 (1999), p. 389.
- [152] J. Crowe, H. Dobeli, R. Gentz, E. Hochuli, D. Stuber and K. Henco *Methods Mol. Biol.* 31 (1994), p. 371.
- [153] H.J. Cha, N.G. Dalal, M.Q. Pham and W.E. Bentley *Biotechnol. Prog.* 15 (1999), p. 283.
- [154] B. Tallet, T. Astier-Gin, M. Castroviejo and X. Santarelli *J. Chromatogr. B* 753 (2001), p. 17.
- [155] M. Chang, J.L. Bolton and S.Y. Blond *Protein Expr. Purif.* 17 (1999), p. 443.
- [156] F.H. Arnold and B.L. Haymore *Science* 252 (1991), p. 1796.
- [157] H.W. Hellings *Curr. Opin. Biotechnol.* 7 (1996), p. 437.
- [158] R.S. Pasquinelli, R.E. Shepherd, R.R. Koepsel, A. Zhao and M.M. Ataai *Biotechnol. Prog.* 16 (2000), p. 86.
- [159] V. Gaberc-Porekar, V. Menart, S. Jevsevar, A. Vidensek and A. Stalc *J. Chromatogr. A* 852 (1999), p. 117.
- [160] A.M. Schmidt, H.N. Muller and A. Skerra *Chem. Biol.* 3 (1996), p. 645.
- [161] V.V. Kronina, H.-J. Wirth and M.T. Hearn *J. Chromatogr. A* 852 (1999), p. 261.
- [162] J. Liesiené, K. Raciulyte, M. Morkeviciene, P. Valancius and V. Bumelis *J. Chromatogr. A* 764 (1997), p. 27.
- [163] S.A. Lopatin, A.V. Il'ina, A.A. Shul'ga, O.S. Grinchenko, V.P. Varlamov, K.G. Skriabin and M.P. Kirpichnikov *Biokhimiia* 59 (1994), p. 226.

- [164] T.M. McNerney, S.K. Watson, J.-H. Sim and R.L. Bridenbaugh *J. Chromatogr. A* 744 (1996), p. 223.
- [165] E.K. Ueda, P.W. Gout and L. Morganti *J. Chromatogr. A* 922 (2001), p. 165.
- [166] R. Anguenot, S. Yelle and B. Nguyen-Quoc *Arch. Biochem. Biophys.* 365 (1999), p. 163.
- [167] V. Boden, J.J. Winzerling, M. Vijayalakshmi and J. Porath *J. Immunol. Methods* 181 (1995), p. 225.
- [168] G.S. Chaga, B. Ersson and J.O. Porath *J. Chromatogr. A* 732 (1996), p. 261.
- [169] U. Winkler, T.M. Pickett and D. Hudig *J. Immunol. Methods* 191 (1996), p. 11
- [170] D.K. McCormick *Biotechnology* 11 (1993), p. 1059.
- [171] B.C. Batt, V.M. Yabannavar and V. Singh *Bioseparation* 5 (1995), p. 41
- [172] F.P. Gailliot, C. Gleason, J.J. Wilson and J. Zwarick *Biotechnol. Prog.* 6 (1990), p. 370.
- [173] H.J. Johansson, C. Jägersten and J. Shiloach *J. Biotechnol.* 48 (1996), p. 9.
- [174] A.-K. Barnfield Frej, H.J. Johansson, S. Johansson and P. Leijon *Bioprocess Eng.* 16 (1997), p. 57.
- [175] R. Hjorth *Trends Biotechnol.* 15 (1997), p. 230.
- [176] N. Ameskamp, C. Priesner, J. Lehmann and D. Lütkemeyer *Bioseparation* 8 (1999), p. 169.
- [177] R.H. Clemmitt and H.A. Chase *Biotechnol. Bioeng.* 67 (2000), p. 206.
- [178] R.H. Clemmitt, L.J. Bruce and H.A. Chase *Bioseparation* 8 (1999), p. 53.
- [179] S. Noronha, J. Kaufman and J. Shiloach *Bioseparation* 8 (1999), p. 145.
- [180] N.A. Willoughby, T. Kirschner, M.P. Smith, R. Hjorth and N.J. Titchener-Hooker *J. Chromatogr. A* 840 (1999), p. 195.
- [181] S. Plunket and F.H. Arnold *Biotechnol. Biotech.* 4 (1990), p. 45.
- [182] A. Otto and G. Birkenmeier *J. Chromatogr.* 644 (1993), p. 25.
- [183] U. Sivars, J. Abramson, S. Iwata and F. Tjerneld *J. Chromatogr. B* 743 (2000), p. 307.
- [184] H. Pesliakas, V. Zutautas and B. Baskeviciute *J. Chromatogr. A* 678 (1994), p. 25.
- [185] S.M. O'Brien, R.P. Sloane, O.R. Thomas and P. Dunnill *J. Biotechnol.* 54 (1997), p. 53.
- [186] J. Porath *J. Protein Chem.* 16 (1997), p. 463.
- [187] K.M. Müller, K.M. Arndt, K. Bauer and A. Plückthun *Anal. Biochem.* 259 (1998), p. 54.
- [188] T.G. Consler, B.L. Persson, H. Jung, K.H. Zen, K. Jung, G.G. Prive, G.E. Verner and H.R. Kaback *Proc. Natl. Acad. Sci. USA* 90 (1993), p. 6934.

- [189] C. Jones, A. Patel, S. Griffin, J. Martin, P. Young, K. O'Donnell, C. Silverman, T. Porter and I. Chaiken *J. Chromatogr. A* 707 (1995), p. 3.
- [190] S.A. McMahan and R.R. Burgess *Anal. Biochem.* 236 (1996), p. 101.
- [191] H. Wernéus, J. Lehtiö, T. Teeri, P.-A. Nygren and S. Ståhl *Appl. Environ. Microbiol.* 67 (2001), p. 4678.
- [192] C. Buchel, E. Morris, E. Orlova and J. Barber *J. Mol. Biol.* 312 (2001), p. 371.
- [193] M. Saleemuddin *Adv. Biochem. Eng. Biotechnol.* 64 (1999), p. 203.
- [194] J. Turková *J. Chromatogr. B* 722 (1999), p. 11.
- [195] D.A. Butterfield, D. Bhattacharyya, S. Daunert and L. Bachas *J. Membr. Sci.* 181 (2001), p. 29.
- [196] C.F. Ford, I. Suominen and C.E. Glatz *Protein Expr. Purif.* 2 (1991), p. 95.
- [197] S. Supattapone, H.O. Nguyen, T. Muramoto, F.E. Cohen, S.J. DeArmond, S.B. Prusiner and M. Scott *J. Virol.* 74 (2000), p. 11928.
- [198] A. Varshavsky *Cell* 69 (1992), p. 725.
- [199] J. Nilsson, S. Ståhl, J. Lundeberg, M. Uhlén and P.A. Nygren *Protein Expr. Purif.* 11 (1997), p. 1.
- [200] L. Morganti, M. Huyer, P.W. Gout and P. Bartolini *Biotechnol. Appl. Biochem.* 23 (1996), p. 67.
- [201] Z. Li and E. Crooke *Protein Expr. Purif.* 17 (1999), p. 41.
- [202] J.P. Jin, A. Chen, O. Ogut and Q.Q. Huang *Am. J. Physiol. Cell Physiol.* 279 (2000), p. C1067.
- [203] R. Janknecht, G. de Martynoff, J. Lou, R.A. Hipskind, A. Nordheim and H.G. Stunnenberg *Proc. Natl. Acad. Sci. USA* 88 (1991), p. 8972.
- [204] C.M. Halliwell, G. Morgan, C.-P. Ou and A.E. Cass *Anal. Biochem.* 295 (2001), p. 257.
- [205] A. Goel, D. Colcher, J.-S. Koo, B.J. Booth, G. Pavlinkova and S.K. Batra *Biochem. Biophys. Acta* 1523 (2000), p. 13.
- [206] H. Büning, U. Gärtner, D. von Schack, P.A. Baeuerle and H. Zorbas *Anal. Biochem.* 234 (1996), p. 227.
- [207] J.L. Rosales and K.Y. Lee *Biochem. Biophys. Res. Commun.* 273 (2000), p. 1058.
- [208] H. Tang and P.R. Chitnis *Indian J. Biochem. Biophys.* 37 (2000), p. 433.
- [209] T. Sprules, N. Green, M. Featherstone and K. Gehring *Biotechniques* 25 (1998), p. 20.
- [210] G. Georgiou and P. Valax *Curr. Opin. Biotechnol.* 7 (1996), p. 190.
- [211] D.R. Thatcher and A. Hitchcock In: R.H. Pain, Editor, *Mechanisms of Protein Folding*, Oxford University Press, New York (1996), p. 232 Chapter 9 .
- [212] R. Zahn, C. von Schroetter and K. Wuthrich *FEBS Lett.* 417 (1997), p. 400.

- [213] M. Itoh, K. Masuda, Y. Ito, T. Akizawa, M. Yoshioka, K. Imai, Y. Okada, H. Sato and M. Seiki *J. Biochem.* 119 (1996), p. 667.
- [214] S.F. Beresten, R. Stan, A.J. van Brabant, T. Ye, S. Naureckiene and N.A. Ellis *Protein Expr. Purif.* 17 (1999), p. 239.
- [215] J. Zouhar, E. Nanak and B. Brzobohatý *Protein Expr. Purif.* 17 (1999), p. 153.
- [216] A. Holzinger, K.S. Phillips and T.E. Weaver *Biotechniques* 20 (1996), p. 804.
- [217] P.-Y. Shi, N. Maizels and A.M. Weiner *Biotechniques* 23 (1997), p. 1036.
- [218] Suh, Y.J., Hager, L.P.(1991)., *Journal of Biological Chemistry* 266 (33) , 22102-22109
- [219] Burgess, R.R.(1991)., *Methods in Enzymology* 208 , 3-10
- [220] Nayak, S.S., Ramani, A., Kamath, S.S., Kundaje, G.N., Aroor, A.R.(1988)., *Biochemical Medicine and Metabolic Biology* 40 (3) , 299-304
- [221] Senthuran, A., Senthuran, V., Mattiasson, B., Kaul, R.(1997)., *Biotechnology and Bioengineering* 55 (6) , 841-853
- [222] Helander, I.M., Alakomi, H.-L., Latva-Kala, K., Koski, P.(1997)., *Microbiology* 143 (10) , 3193-3199
- [223] Pettigrew, G.W. and Moore, G.R. (1987) *Cytochromes c. Biological Aspects.*
- [224] Moore, G.R. and Pettigrew, G.W. (1990) *Cytochromes c. Evolutionary, Structural, and Physicochemical Aspects.*
- [225] Ambler, R.P. (1991). *Biochim. Biophys. Acta* 1058, 42-47.
- [226] Moore, G.R. (1991). *Biochim. Biophys. Acta* 1058, 38-41.
- [227] Coutinho, I.B. and Xavier, A.V. (1994). *Methods Enzymol.* 243, 119-140.
- [228] Bowden, E.F.; Hawkridge, F.M.; Blount, H.N. *J. Electroanal. Chem.* 1984, 161, 355-376
- [229] Dickerson, R.E.; Timkovich, R. *The Enzymes.* (P. Boyer Ed.) New York: Academic Press, 1975.
- [230] Margaret Dayhoff (1979) *Atlas of Protein Sequence and Structure.*
- [231] Odabasi, M., Denizli, A., (2001)., *Journal of Chromatography B.*,(760) 137-148
- [232] Duru E, Bektas S, Genç O, Patir S., Denizli A, (2001)., *Journal of Applied Polymer Science* 81 (1) , 197-205
- [233] G.V. Louie, G.D. Brayer, *J. Mol. Biol.* 1990, 214, 527.
- [234] Ping-L. K, Wu-J. L, Fu-Y. W., (2003), *Journal of Polymer Science: Part A: Polymer Chemistry*, Vol. 41, 1360–1370
- [235] H.M. Swartz, J.R. Bolton, D.C. Borg, *Biological Applications of Electron Spin Resonance*, Wiley, New York, 1972.
- [236] T. Abudiab, R.R. Beitle, *J. Chromatogr.* 1998, 795, 211.
- [237] Y.S. Ho, G. McKay, *Proc. Biochem.* 1999, 34, 451.

- [238] S.M. O'Brien, O.R.T. Thomas, P. Dunnill, *J. Biotechnol.* 1996, 50, 13.
- [239] G.C. Serafica, J. Pimbley, G. Belfort, *Biotechnol. Bioeng.* 1994, 43, 21.
- [240] X. Zeng, E. Ruckenstein, *J. Membr. Sci.* 1998, 148, 195.
- [241] R.K. Lewus, G. Carta, *AIChE J.* 1999, 45, 512.
- [242] R.J. Todd, R.D. Johnson, F.H. Arnold, *J. Chromatogr. A.* 1994, 662, 13.
- [243] S. Emir, R. Say, H. Yavuz, A. Denizli, *Biotechnol. Prog.* 2004, 20, 223.

CIRRUCULUM VITAE

Name : Deniz
Surname : Türkmen
Date of Birth : 11.09.1979
Place of Birth : Kartal, İstanbul-Turkiye
Gender : Male
Nationality : Turkish
Marital Status : Single
Foreign Language : English
Mail Address : Hacettepe University, Chemistry Department, Beytepe,
06532 Ankara, TURKEY
Telephone : (+90 312) 297 79 63
Fax : (+90 312) 299 21 63
e-mail : denizturkmen06@yahoo.com

EDUCATION

BSc Chemistry Department, Hacettepe University, Ankara, 1998-2003
MSc Chemistry Department, Biochemistry Div., Hacettepe University, Ankara,
2003-